PL ISSN 0028-3894

STOWARZYSZENIE
NEUROPATOLOGÓW POLSKICH

NEUROPATOLOGIA POLSKA

TOM 28 1990 ZESZYT 3–4

WROCŁAW · WARSZAWA · KRAKÓW
ZAKŁAD NARODOWY IM. OSSOLIŃSKICH
WYDAWNICTWO POLSKIEJ AKADEMII NAUK

NEUROPATOLOGIA POLSKA

KWARTALNIK

TOM 28 1990 ZESZYT 3–4

ADRES REDAKCJI

Centrum Medycyny Doświadczalnej i Klinicznej Polskiej Akademii Nauk
ul. Dworkowa 3, 00-784 Warszawa, tel. 49-54-10

Wydano z pomocą finansową Polskiej Akademii Nauk

Maszynopis niniejszego zeszytu przekazano Wydawcy 19.12.1989 r.

Zakład Narodowy im. Ossolińskich – Wydawnictwo. Wrocław 1991.
Objętość: ark. wyd. 9,10; ark. druk. 8,50+0,25 wkł.; ark. A_1-11,3.
Wrocławska Drukarnia Naukowa 290/90.

NEUROPAT. POL. 1990, 28, 3-4
PL ISSN 0028-3894

MIROSŁAW J. MOSSAKOWSKI, IRMINA B. ZELMAN

DYNAMICS OF PATHOMORPHOLOGICAL CHANGES IN THE BRAIN OF RATS AFTER CLINICAL DEATH

Department of Neuropathology, Medical Research Centre,
Polish Academy of Sciences, Warsaw, Poland

Progress in studies on functional, metabolic and structural aspects of cerebral ischemia turned the attention of numerous authors to the late sequelae of the ischemic incident. The milestones on this way have been marked by observations concerning metabolic abnormalities resulting from temporary ischemia which may play the role of both compensatory and secondarily damaging factors (Siesjö 1981), by description of the maturation phenomenon (Ito et al. 1975; Klatzo 1975; Yamagushi, Klatzo 1984) and of the feature, known under the name of the delayed neuronal death (Suzuki et al. 1983 a, b; 1985), with its implication concerning the possibility of a neurotransmitter-induced excitotoxic mechanism of neuronal lesions (Pulsinelli 1985 a, b). Two opposite phenomena underlay studies on late sequelae of cerebral ischemia — the first of which is the question of reversibility of tissue damage due to ischemia, the second — the progressive nature of ischemic encephalopathy stressed by reanimatologists.

Studies of those problems require an appropriate experimental model, preferentially of global cerebral ischemia. In searching for such one we decided to apply the model of experimental clinical death in rats, described by Korpachev and his collegues in 1982. The main advantage of the model consists in the possibility of long survival of animal after the resuscitation procedure, related with relatively little experimental trauma. In addition it does not require deep anesthesia and pharmacological treatment. Its disadvantages consist in high mortality during and immediately after the experimental procedure, connected to a great extend with the duration of cardiac arrest and above all in the fact that it is not a model of isolated cerebral ischemia, but of experimental clinical death with all consequences resulting from generalized ischemia of all body organs (Safar 1986).

Paper presented at Symposium on Neurobiology of Cerebral Ischemia and Hypoxia. Poznań, June 29-July 1, 1989.

MATERIAL AND METHODS

The experiments were performed on adult albino rats of both sexes, weighing ca 180 g in which clinical death was induced according to the method described by Korpachev et al. (1982). Compression of the heart vascular bundle by a special hook inserted into the thorax led in the course of 1.5-2 min to complete cardiac arrest and cessation of the respiratory function lasting till resuscitatory management was undertaken. In the case of our experiments this was done either after 10 or 15 min of complete cessation of brain bioelectric activity. Following resuscitation, which included external heart massage and controlled respiration, the experimental animals survived for 3, 6 and 24 hrs, 3, 7, 14 and 28 days as well as 6, 9 and 12 months. Their age mates not subjected to any experimental procedures formed the control group.

The brains of control and experimental animals were examined histologically and immunomorphologically. Histology was done on paraffin sections stained with hematoxylin-eosin and according to the Klüver--Barrera's method. Immunomorphology included immunostaining of glial fibrillary acidic protein (GFAP). Detailed description of methods applied is presented in previously published papers of Mossakowski et al. (1986), Mossakowski and Krajewski (1988) and Zelman and Mossakowski (1988).

As detailed physiopathological characteristics of the experimental model are given elsewhere (Mossakowski et al. 1986; Kapuściński 1987; Majkowska 1989), only basic data concerning cerebral bioelectric activity and cerebral blood flow are presented here.

Control electrocorticographic activity preceding compression of the heart vascular bundle was typical for anesthetized animals with waves of 6-8 Hz and amplitude to 300 mvolts. Efficient vascular compression resulted in appearance of slow waves with decreasing amplitude and frequency. The isoelectric line was usually observed after 15-20 seconds of compression. The first burst of bioelectric activity in case of 10 and 15 min cardiac arrest appeared 26.8 $\pm$3.9 and 39.0 $\pm$2.8 min respectively from the beginning of vascular compression. Continuous ECG activity with numerous slow waves and spikes usually appeared 40.0 $\pm$5.2 min after beginning of resuscitation.

Cerebral blood flow, measured by the 133-Xenon clearance method showed a total stop at the time of cardiac arrest followed by an increase to 161.6 $\pm$38.5% in 35 min after resuscitation and average drop to 85% two hours after resuscitation.

RESULTS

Brain light microscopy revealed structural abnormalities in all examined animals, although their extent and intensity showed wide individual differences. A characteristic feature of the cerebral pathology

consisted in the involvement of practically all the brain structures and differences in their nature and intensity depending on the survival time after experimentally induced cardiac arrest. Less striking were differences between animals surviving 10 or 15 min cardiac arrest. This was even more obvious in the light of the above mentioned individual variances of the extensiveness of pathological changes.

The early changes, appearing during the first postresuscitation day consisted in moderate widespread neuronal degeneration involving various structures of the central nervous system, prevailing specially in the cerebral and cerebellar cortex and basal ganglia. However, they were also present in areas relatively resistant to ischemic damage, such for instance as substantia nigra, some nuclei of the reticular formation and cranial nerves. The degenerative changes involved usually single neurons or their groups lying against a backround of otherwise unchanged neuronal population.

The earliest neuronal degeneration took the form of microvacuolization localized either intracytoplasmically or pericellularly (Fig. 1). As known from electron microscopic study, the former corresponds to swelling of cytoplasmatic structures, mostly mitochondria, the latter to swelling of perineuronal astrocytic processes. The other forms of neuronal abnormalities consisted in chromatolysis leading to pictures described in classical neuropathology as acute neuronal swelling (Fig. 2) and central or peripheral chromatolysis, respectively. At the same time typical ischemic neuronal changes appeared (Fig. 3). Purkinje cells showed characteristic homogenous degeneration. Some slight focal tissue spongiosis was present in the cerebral cortex and basal ganglia. In the white matter some loosening of tissue texture with acute swelling of oligodendrocytes were seen.

Features of neuronal loss appeared starting from the third postresuscitation day. At first they were superimposed on the above mentioned degenerative changes of the nerve cells, which at that time became even more intense and diffuse (Fig. 4). In later stages the number of neurons with degenerative changes became steadily reduced, being replaced by neuronal loss. The latter was localized mostly in typical selectively vulnerable areas such as hippocampus, mostly CA_1 sector, ganglion cell layer of the cerebellar cortex, IIIrd neocortical layer and striatum, with particular involvement of larger nerve cells. Degenerative changes, if present, at that time were mostly localized in the same brain structures. Borderline zones of the cerebral cortex were also the site of severe changes.

In the 6th postresuscitation month in addition to localized neuronal loss, different types of degenerative changes involving nerve cells were present. Several groups of them could be distinguished. The first one, taking the form of chronic nerve cell degeneration and their calcification

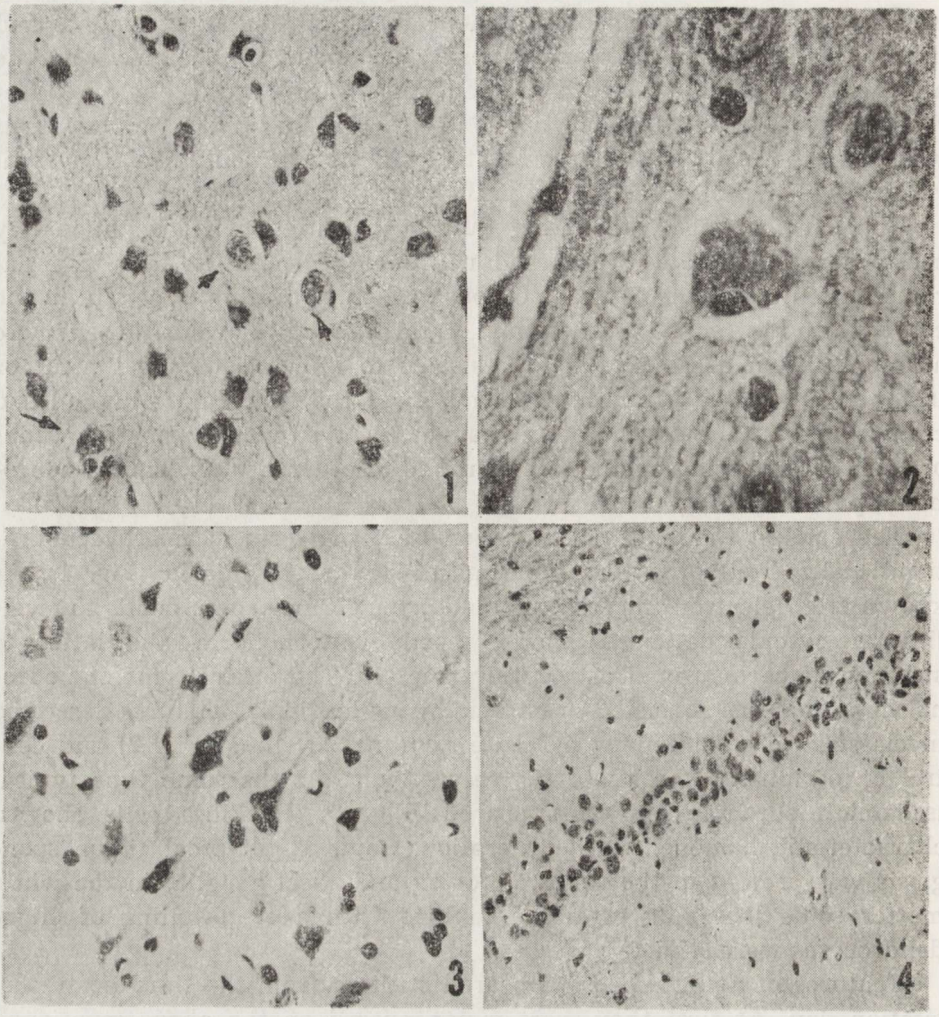

Fig. 1. Perineuronal vacuolization of neuropil (arrows) in early postischemic stage. Experimental animal, survival 72 hours after ischemia. HE. × 200

Ryc. 1. Okołoneuronalna wakuolizacja neuropilu (strzałki) we wczesnym okresie po niedokrwieniu. Zwierzę doświadczalne. 72-godzinne przeżycie po niedokrwieniu. HE. Pow. 200 ×

Fig. 2. Cortical neuron with features of acute swelling of cytoplasm. Experimental animal, survival 24 hours after ischemia. HE. × 1000

Ryc. 2. Neuron piramidowy kory mózgu z cechami ostrego obrzmienia cytoplazmy. Zwierzę doświadczalne, czas przeżycia 24 godz. po niedokrwieniu. HE. Pow. 1000 ×

Fig. 3. Typical ischemic neurons in the IIIrd cortical layer. Experimental animal, survival 24 hours after ischemia. HE. × 400

Ryc. 3. Neurony III warstwy korowej z typowymi zmianami niedokrwiennymi. Zwierzę doświadczalne, czas przeżycia 24 godz. po niedokrwieniu. HE. Pow. 400 ×

Fig. 4. Neuronal loss and degeneration of Ammon's horn pyramidal neurons. Experimental animal, survival 7 days after ischemia. HE. × 200

Ryc. 4. Ubytki neuronalne i zwyrodnienie w warstwie piramidowej rogu Amona. Zwierzę doświadczalne, czas przeżycia po niedokrwieniu 7 dni. HE. Pow. 200 ×

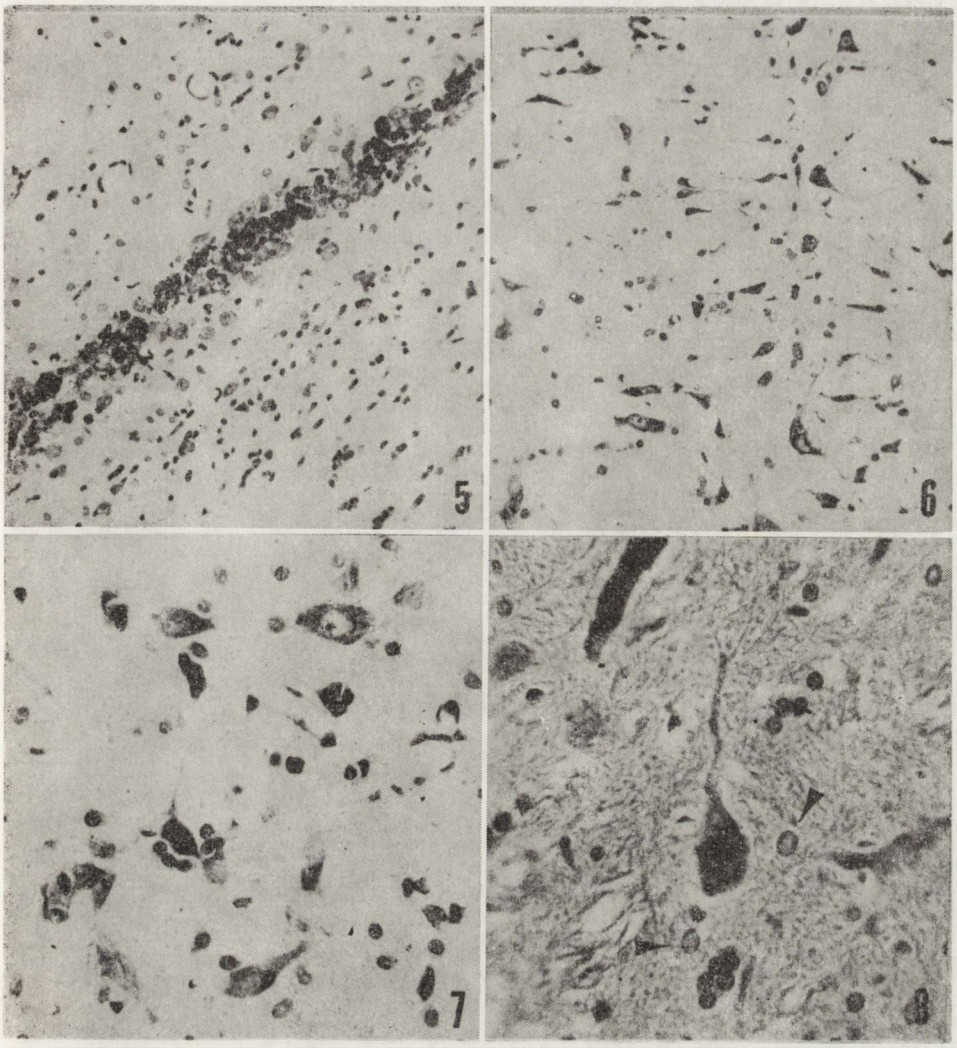

Fig. 5. Dense calcifications in the pyramidal cell layer of Ammon's horn. Experimental animal, survival time 6 months after ischemia. HE. × 100

Ryc. 5. Obfite zwapnienia w warstwie piramidowej rogu Amona. Zwierzę doświadczalne, czas przeżycia 6 miesięcy po niedokrwieniu. HE. Pow. 100 ×

Fig. 6. Shrunken dark neurons in pontine nucleus raphe centralis. Experimental animal, survival 6 months after ischemia. Cresyl violet. × 200

Ryc. 6. Obkurczone ciemne neurony w mostowym jądrze szwu. Zwierzę doświadczalne, czas przeżycia 6 miesięcy po niedokrwieniu. Fiolet krezylu. Pow. 200 ×

Fig. 7. Degenerating neurons from brain stem reticular formation. Note increased perineuronal glial satelitosis. Experimental animal, survival 6 months after ischemia. Cresyl violet. × 400

Ryc. 7. Wyrodniejące neurony z tworu siatkowatego pnia mózgu. Uwagę zwraca wzmożona okołoneuronalna satelitoza glejowa. Zwierzę doświadczalne, czas przeżycia 6 miesięcy po niedokrwieniu. Fiolet krezylu. Pow. 400 ×

Fig. 8. Nodular glial proliferation replacing broken down neurons. Two astrocytic nuclei resembling Alzheimer cells type II (arrows). Experimental animal, survival 6 months after ischemia. HE. × 900

Ryc. 8. Grudkowa proliferacja gleju w miejscach ubytków neuronalnych. Dwa jądra astrocytarne, przypominające komórki Alzheimera typu II (strzałki). Zwierzę doświadczalne, czas przeżycia 6 miesięcy po niedokrwieniu. HE. Pow. 900 ×

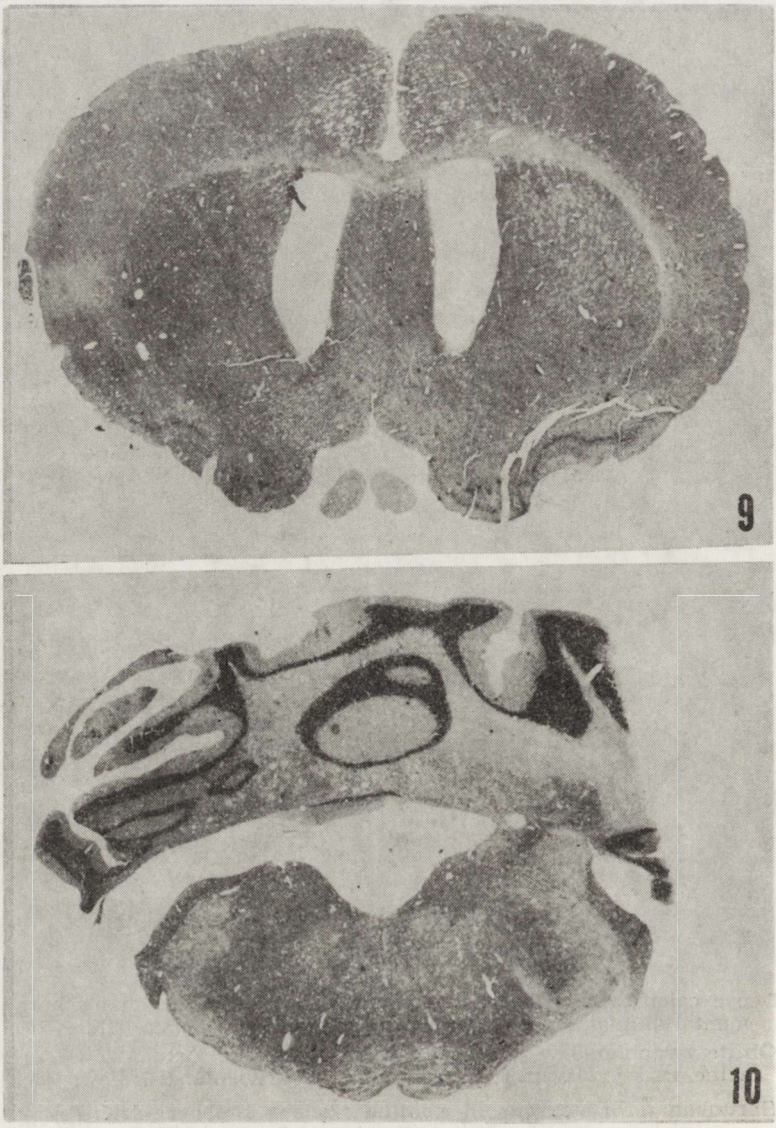

Fig. 9. Enlarged lateral ventricles in an experimental animal with 9 months survival after ischemia. HE. × 9

Ryc. 9. Poszerzone komory boczne mózgu zwierzęcia doświadczalnego z 9-miesięcznym przeżyciem po niedokrwieniu. HE. Pow. 9 ×

Fig. 10. Dilated IV ventricle in an experimental animal with 12 months survival after ischemia. HE. × 9

Ryc. 10. Poszerzona komora IV u zwierzęcia doświadczalnego z 12-miesięcznym przeżyciem po niedokrwieniu. HE. Pow. 9 ×

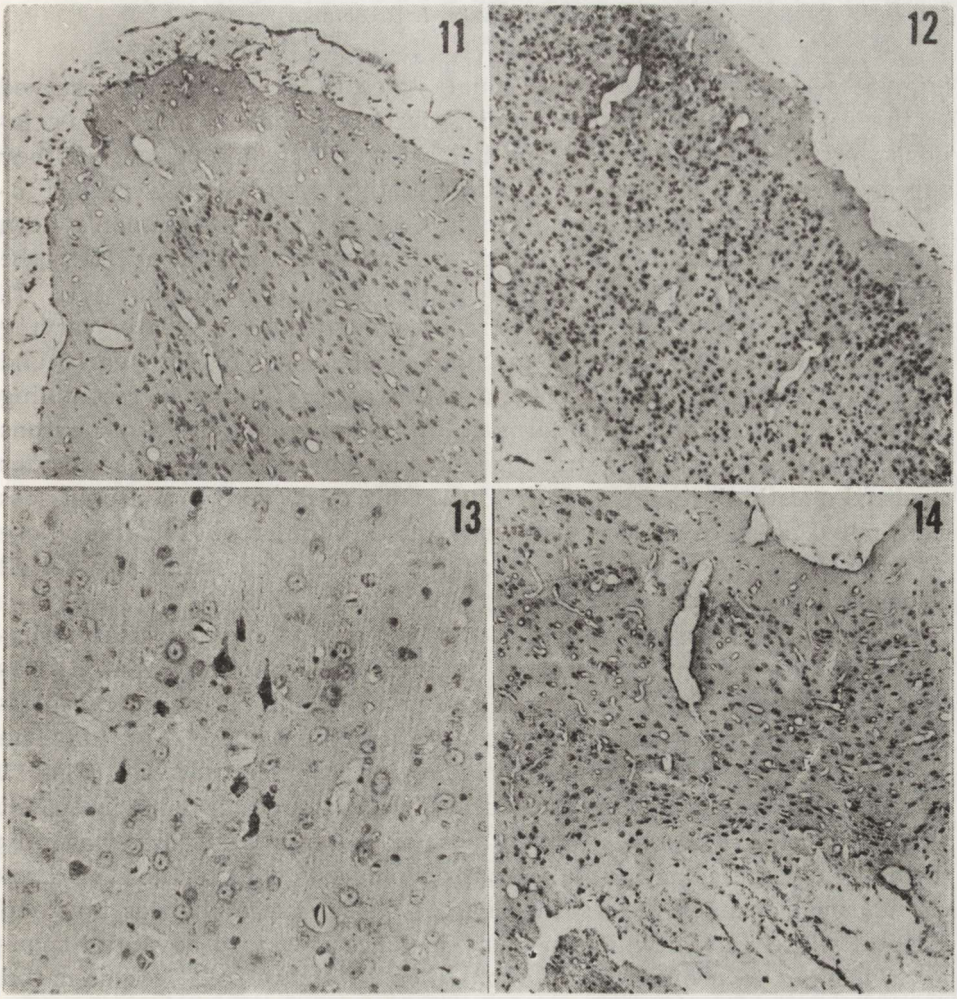

Fig. 11. Considerable dilatation of subarachnoid space with uneven outlines of the cerebral cortex. Experimental animal, survival 12 months after ischemia. HE. × 60

Ryc. 11. Znaczne poszerzenie przestrzeni podpajęczynówkowej z nierównym obrysem powierzchni kory mózgu. Zwierzę doświadczalne z 12 miesięcznym przeżyciem po niedokrwieniu. HE. Pow. 60 ×

Fig. 12. Thinned densely populated cerebral cortex with uneven outlines and total disintegration of subcortical white matter. Experimental animal, survival 12 months after ischemia. HE. × 200

Ryc. 12. Zcieńczała, bogatokomórkowa kora mózgu z nierównymi obrysami powierzchni i całkowitym rozpadem istoty białej podkorowej. Zwierzę doświadczalne, czas przeżycia 12 miesięcy po niedokrwieniu. HE. Pow. 60 ×

Fig. 13. Group of shrunken dark neurons in the IIIrd cortical layer, surrounded by otherwise normal neuronal population. Experimental animal, survival 9 months after ischemia. HE. × 200

Ryc. 13. Grupa ciemnych, obkurczonych neuronów w otoczeniu niezmienionej populacji komórek nerwowych. Zwierzę doświadczalne, czas przeżycia 9 miesięcy po niedokrwieniu. HE. Pow. 200 ×

Fig. 14. Cavernous disintegration of subcortical white matter in an experimental animal with 9 months survival after ischemia. HE. × 100

Ryc. 14. Jamisty rozpad podkorowej istoty białej u zwierzęcia doświadczalnego z 9-miesięcznym przeżyciem po niedokrwieniu. HE. Pow. 100 ×

(Fig. 5) seemed to represent residual states of abnormalities observed in the early postresuscitation period. Curiously enough some other lesions were of a nature typical for the early postischemic period but they appeared in those areas and structures of the brain which were not involved previously, for instance sector CA_2 and CA_4 of Ammon's horn and some specific brain stem nuclei, such as serotoninergic nuclei raphe (Fig. 6) or gigantocellular nucleus of the reticular formation (Fig. 7). Neuronal loss and degeneration were accompanied by a greatly varying glial reaction, taking different morphological forms. In both early and relatively late stages after ischemia naked astrocytic nuclei, resembling Alzheimer type II cells and glial nodules replacing broken down neurons appeared (Fig. 8). Intensive proliferation and hypertrophy of astrocytes localized mostly but not exclusively, in areas of severe neuronal loss were noted later. In some cases mixed astrocytic-microglial nodules were present. Hematogenous cellular reaction was not a feature at any period of postischemic pathology.

Morphological observations performed 9 and 12 months after resuscitation following both 10 and 15 min cardiac arrest revealed hydrocephalic features. They were expressed by widening of both the ventricular system (Figs 9 and 10) and the subarachnoid space (Fig. 11). The brain surface outlines were uneven indicating atrophic processes (Figs 11 and 12). Cerebral cortex in most areas was narrow, showing increased cellular density (Fig. 12), although most of the neurons were apparently normal. Only occasionally small groups of neurons with features of chronic neuronal changes were seen (Fig. 13). More severe changes involved cerebral white matter which in many instances revealed advanced spongiosis leading to profound cavitation (Figs 13 and 14). In less damaged areas features of glial proliferation were noted. Diffuse astrocytic proliferation was seen also in grey matter formations.

DISCUSSION

The results of our studies indicate clearly that global cerebral ischemia resulting from experimentally induced 10 or 15 min cardiac arrest in rats is followed by widespread neuronal damage, involving practically all brain structures, belonging or not to selectively vulnerable areas of the central nervous system. In general the intensity of changes, revealing marked individual variability, was moderate as compared with similar conditions in other mammalians; this being probably the result of a relatively high resistance of the rat central nervous system to ischemia. It seems worth mentioning that the extent and intensity of structural brain abnormalities, as well as their nature, depended more on the survival time after the ischemic incident than on the duration of the latter. Due to the above mentioned individual differences in res-

ponse to cerebral ischemia, it was not exceptional to find more severe tissue alterations in animals with 10 min clinical death than in those in which total cerebral blood flow stop lasted 15 min.

The postresuscitation encephalopathy observed represents a gradually progressing process extended over a long period after ischemic incident. This nature of the process is indicated by the pathological changes in the brain occurring during the whole observation period, including one year. They revealed characteristics of not only residual features resulting from early tissue damage, but of an active pathological process even in very late postischemic stage.

The pathological process is characterized by specific dynamics consisting of early widespread neurodegenerative changes followed by localized neuronal loss, confined mostly to selectively vulnerable areas of the central nervous system. The longer period of the postischemic stage displays non-specific degeneration of the nerve cells, accentuated specially in the brain stem formations. After one year the process ended in generalized cerebral atrophy, expressed by features of internal and external hydrocephalus and narrowing of the cerebral cortex, showing exponents of increased cellular density. Brain antrophy occurring only in the experimental animals, in contrast to their age-mates not subjected to any experimental procedure, permits to reject an age-dependent origin of the atrophic process. In addition, one more element of late cerebral pathology is worth pointing out. This is diffuse and severe cerebral white matter damage, taking the form of breakdown and cavitation. This type of changes in a rather rare phenomenon in postischemic rat pathology. Neither does it appear frequently in human pathology (Brucher 1962). This type of the white matter alteration is usually considered as the result of severe and prolonged vasogenic brain edema, which was not the case, at least to such a degree, in the experimental conditions under study (Mossakowski et al. 1986; Kapuściński 1988; Zelman, Mossakowski 1988).

The mechanism of postresuscitation encephalopathy, leading to generalized cerebral atrophy requires elucidation. The question arises as to whether the pathological process initiated by acute global cerebral ischemia and progressing for one year can be considered as an exponent of the maturation phenomenon in the sense described by Klatzo (1975), and, if so, what is the factor or factors responsible for its appearance and course. As one of the possibilities, the autoimmune reaction, evoked by massive neuronal breakdown with accompanying damage of the blood-brain system occurring in the early period of postresuscitation, should be taken into consideration (Mossakowski, Krajewski 1988). The appearance and increase in the content of antineuronal antibodies in the sera of experimental animals found in the course of the postresuscitation period may suggest a mechanism of neuronal loss similar to that sug-

gested by Nandy (1975, 1983) in the case of aging processes. In part of the experimental animals appearance of antimyelin antibodies complementing antineuronal ones was revealed. In such a case autoimmune mechanism may also concern white matter damage.

DYNAMIKA ZMIAN PATOMORFOLOGICZNYCH W MÓZGU SZCZURÓW PO DOŚWIADCZALNEJ ŚMIERCI KLINICZNEJ

Streszczenie

Przeprowadzono ocenę obrazu patomorfologicznego mózgu szczurów poddanych doświadczalnej śmierci klinicznej trwającej 10-15 minut. Okres przeżycia po incydencie niedokrwiennym zawierał się w granicach od 3 godzin do 1 roku.

Wykazano postępujący charakter zmian rozwijających się w następstwie przebytego incydentu niedokrwiennego, cechujących się typową i powtarzalną dynamiką. Wczesne nieprawidłowości wyrażały się uogólnionymi zmianami zwyrodnieniowymi, na które w dalszym okresie nakładały się ubytki neuronalne zlokalizowane przede wszystkim, choć nie wyłącznie, w obszarach wybiórczej wrażliwości na niedokrwienie. W dalszej ewolucji procesu obserwowano narastanie zwyrodnienia neuronów w obszarach nie zajętych we wczesnej fazie procesu, w tym przede wszystkim w strukturach pnia mózgu. W końcowym stadium obserwacji stwierdzono cechy uogólnionego zaniku mózgu, wyrażające się wodogłowiem zewnętrznym i wewnętrznym oraz znacznym zcieńczeniem kory mózgu. W znacznej części przypadków towarzyszyło temu uszkodzenie istoty białej prowadzące do jej rozpadu. Wysunięto hipotezę, opartą na wcześniejszym spostrzeżeniu, że postępujący proces encefalopatyczny, kończący się uogólnionym zanikiem mózgu i rozpadem jego istoty białej, może mieć charakter procesu autoimmunologicznego, związanego z pojawianiem się we krwi przeciwciał przeciw neuronalnych i przeciw mielinowych.

REFERENCES

1. Brucher J. M.: Neuropathological problems posed by carbon monoxide poisoning and anoxia. Prog Brain Res, 1962, 24, 96-100.
2. Ito U., Spatz M., Walker J. T. Jr., Klatzo I.: Experimental cerebral ischemia in Mongolian gerbil. I. Light microscopic observations. Acta Neuropathol (Berl), 1975, 32, 209-223.
3. Kapuściński A.: Mózgowy przepływ krwi w doświadczalnym modelu śmierci klinicznej. Neuropatol Pol, 1987, 25, 287-298.
4. Kapuściński A.: Bariera krew-mózg w modelu śmierci klinicznej u szczurów. Neuropatol Pol, 1988, 26, 175-183.
5. Klatzo I.: Pathophysiological aspects of cerebral ischemia. In: Nervous system. Vol. 1. The basic neuroscience. Ed.: Tower B. Raven Press, New York, 1975, pp. 313-322.
6. Korpachev V. G., Lysenkov S. P., Tiel L. Z.: Modelirowanije kliniczeskoj smierti i postreanimationnoj bolesni u krys. J Patol Fiziol Exp Ter, 1982, 3, 78-80.
7. Majkowska-Wierzbicka J.: Pathophysiological characteristics of clinical death in rats. Neuropatol Pol, 1989, 27, 83-96.
8. Mossakowski M. J., Hilgier W., Januszewski S.: Ocena zmian morfologicznych

w ośrodkowym układzie nerwowym w doświadczalnym zespole poreanimacyjnym. Neuropatol Pol, 1986, 24, 471-489.
9. Mossakowski M. J., Krajewski S.: Antineuronal antibodies in blood sera of rats subjected to global cerebral ischemia. Neuropatol Pol, 1988, 26, 37-48.
10. Nandy K.: Significance of brain reactive antibodies in serum of aged mice. J Gerontol, 1975, 30, 412-416.
11. Nandy K.: Neuroimmunology and the ageing brain. Exp Brain Res, 1982 (Suppl. 5), 123-127.
12. Pulsinelli W. A.: Selective neuronal vulnerability: morphological and molecular characteristics. Prog Brain Res, 1985a, 63, 29-31.
13. Pulsinelli W. A.: Deafferentation of the hippocampus protects CA1 pyramidal cells against ischemic injury. Stroke, 1985b, 16, 144-146.
14. Siesjö B. K.: Cell damage in the brain. A speculative synthesis. J Cereb Blood Flow Metab, 1981, 1, 155-185.
15. Suzuki R., Yamaguchi T., Kirino T., Orzi F., Klatzo I.: The effect of 5-minute ischemia in Mongolian gerbils. I. Blood-brain barrier, cerebral blood flow and local glucose utilization changes. Acta Neuropathol (Berl), 1983, 60, 207-216.
16. Suzuki R., Yamaguchi T., Li C. L., Klatzo I.: The effects of 5-minut ischemia in Mongolian gerbils. II. Changes of spontaneous neuronal activity in cerebral cortex and CA_1 sector of hippocampus. Acta Neuropathol (Berl), 1983, 60, 217-222.
17. Suzuki R., Yamaguchi T., Inaba V., Wagner H. G.: Microphysiology of selectively vulnerable neurons. Prog Brain Res, 1985, 63, 59-68.
18. Yamaguchi T., Klatzo I.: Maturation of cell damage fallowing transient ischemia in Mongolian gerbils. In: Cerebral ischemia. Eds.: A. Bes, P. Braquet, R. Paoletti, B. K. Siesjö. Elsevier, Amsterdam, New York, Oxford, 1984, pp. 13-24.
19. Zelman I. B., Mossakowski M. J.: Remote pathological brain changes in rats following experimentally induced clinical death. Neuropatol Pol, 1988, 26, 151-162.

Authors' address: Department of Neuropathology, Medical Research Centre, Polish Academy of Sciences, 3, Dworkowa Str., 00-784 Warsaw, Poland.

NEUROPAT. POL. 1990, 28, 3-4
PL ISSN 0028-3894

ALEXANDER M. GURVITCH

SOME NEW TRENDS IN STUDIES OF POSTRESUSCITATION BRAIN PATHOLOGY

Institute of General Reanimatology, USSR Academy of Medical Sciences, Moscow, USSR

In recent years great progress has been made in studies of the nature of CNS postresuscitation pathology (Niegovsky et al. 1983). However, further progress will encounter serious difficulties, since tissue changes have to be studied over a long period of time simultaneously in all brain regions. It will also be necessary to determine the nature of neurophysiological behavioural alterations observed during the postresuscitation period.

This paper presents some results of research trends which previously have been used insufficiently or not used at all in brain postresuscitation pathology studies. The results were obtained in a rat model of clinical death designed by Korpachev et al. (1982) (intrathoracic clamp of the aorta and caval vein) with 5, 10, and 15 min circulatory arrest. Clinical death of such duration in rats is compatible with an apparently complete restoration of the neurological status.

A physiological phenomenon, such as spreading depression (SD) was used to detect inapparent lesions in the rat brain after comparatively short-lasting (10-min) clinical death followed by complete restoration of the neurological status and conditioned-reflex performance. The main changes of the SD wave observed in the postresuscitation period in rats were as follows (Kuznecova et al. 1982): changes in duration (generally 2-3 to 5-10-fold increase), in the shape of anterior and posterior wave-fronts, in the propagation rate in the brain (slowing down), in refractoriness (a 2-3-fold increase), in the variability of the shape and amplitude after repeated KCl injections, as well as in some other parameters. It should be emphasized that these changes vary in extent from region to region of the cortex, that is this test reveals a medley picture of cortical pathology and allows to differentiate between different cortical regions *in vivo*. Because the astroglia is also involved in the development of some characteristics of the SD wave, this phenomenon seems to be

Paper presented at Symposium on Neurobiology of Cerebral Ischemia and Hypoxia. Poznań, June 29-July 1, 1989.

a unique tool for the study of functional astroglial changes in postresuscitation states.

Another non-invasive method of study of functional cortical tissue changes in resuscitated animals is quantitative thermography and investigation of its parameters under functional loads. This method helps locate the regions with gross pathology of this parameter and study the changes of this parameter in response to a variety of experimental influences. As well as by SD, these changes can be further studied by means of rational biochemical, morphological and neuropharmacological analyses.

Another important problem of postresuscitation brain pathology is the nature and functional significance of neurophysiological disturbances. It seems appropriate to concentrate on the following data.

The significant acceleration of formation of the food-conditioned reflex (learning period about 1.5 month) after 5, and 10 min clinical death as compared with the control is noteworthy. Unexpected results were obtained after neurotization of resuscitated animals (2 or 3 months after resuscitation) with long-lasting (7 hrs daily for 3 weeks) noise. Thus, in animals after 10 or 15 min clinical death the neurotization was associated with restoration of time characteristics (duration of performance) of conditioned reflex disturbed at the onset of neurotization, whereas in control animals a delayed deterioration of reflex behavior was observed, followed by a loss of reflex performance in some animals.

Resuscitated rats exposed to hypodymic stress showed an AP rise only at the onset of stress; AP then returned to normal values within 2 hrs. In control rats, however, a delayed rise of AP was observed. A combination of prior noise stress with hypodynamia made this difference still more pronounced. The complex of these facts calls for explanation, since they do not comply with the standard knowledge of the mechanisms of neurotic response development in postresuscitation conditions.

The data of memory pathology observed after resuscitation are also discordant with common ideas of the character of postresuscitation cerebral disorders, for example, in the studies of conditioned passive avoidance of electric shock in rats. It has been shown that the normally learned reaction at the early postresuscitation stage (1 to 3 days) cannot be reproduced even as early as after 24 hours. The same reflex, however, learned 2 weeks after resuscitation, left a more stable memory trace than in normal animals, and the difference between resuscitated and intact animals remained significant over more than 1 month after passive avoidance reflex learning.

The question of drug employment in postresuscitation brain pathology studies deserves special attention. It seems essential to establish the stage pattern of drug effect, and its dependence on the time after

resuscitation. This concerns both CNS stimulants, and tranquilizers. Thus, for instance, phenazepam administered in therapeutic doses (2 mg/kg) the next day after resuscitation when neurological status appeared to be completely restored (rats, 10 min clinical death) produced a dramatic depression of both emotional-behavioural and locomotor functions, and even had a fatal outcome in 50% of animals. Seven days later the depressing effect of the drug subsides and, in some parameters, is close to the norm. Its action on emotional responsiveness, aggressiveness, motor activity, however, remains dramatically enhanced and similar to its effect on the next day after resuscitation. This is essential not only for the selection of adequate therapeutic doses; it also calls for elucidation of the nature of the increased action of the drug.

It has been previously pointed out that the memory trace of electric shock in the passive avoidance reflex learned within one to three days after resuscitation seems to be lost after 24 hours and the reflex is no longer reproducible. It turned out, however, that if after 24 hrs the animal is reminded of the learned skill and this reminding is reinforced by a subsequent nootropic treatment, the memory trace is preserved for a long time. This indicates that the trace does not dissapear even in the early stage of postresuscitation period, but it is the reproduction processes that are damaged and lays special emphasis on the fundamental problem of the studies of postresuscitation structural memory disorders.

The use of a complex of different approaches seems to be the most important prerequisite for gaining essentially new data. The optimal proportion of physiological, biochemical, neuromorphological and other methods in the integral study would thus be a determining factor in the solution of particular tasks.

The data presented were obtained in our Institute (E. Mutuskina) in cooperation with the Institute of Higher Nervous Activity and Neurophysiology of the USSR Academy of Sciences (G. Kuznetzova, N. Nezlina, A. Podolets) and the Institute of Pharmacology of the USSR Academy of Medical Sciences (T. Voronina, J. Garibova).

NIEKTÓRE NOWE KIERUNKI W BADANIACH POREANIMACYJNEJ PATOLOGII MÓZGU

Streszczenie

Postęp w zakresie poresuscytacyjnej patologii mózgu jest możliwy jedynie dzięki kompleksowo dobranym metodom badawczym. Badania te muszą obejmować wszystkie tkanki i struktury mózgu, a także wiele procesów fizjologicznych i behawioralnych. Takie badania jak „spreading depression", ilościowa termografia czy farmakologiczne badania zmian behawioralnych i zaburzeń pamięci mogą w tym wypadku stanowić efektywne metody alternatywne.

REFERENCES

1. Korpachev V. G., Lysenkov S. P., Tell L. Z.: Model of clinical death and post-resuscitation disease in rats (in Russian). Patol Fiziol Eksp Ter, 1982, 3, 78-80.
2. Kuznetzova G. D., Nezlina N. Y., Mutuskina E. A., Podolets A., Gurvitch A. M.: Changes of spreading depression wave during postresuscitation period in rats (in Russian). Fiziol Zh SSSR, 1989 (in press).
3. Negovsky V. A., Gurvitch A. M., Zolotokrylina E. S.: Postresuscitation disease. Elsevier, Amsterdam, 1983, p. 383.

Author's address: Institute of General Reanimatology, USSR Academy of Medical Sciences, Moscow, USSR.

NEUROPAT. POL. 1990, 28, 3-4
PL ISSN 0028-3894

TOSHIHIKO KUROIWA, PETRA BONNEKOH,
KONSTANTIN A. HOSSMANN

POSTISCHEMIC HALOTHANE ANESTHESIA AND MOTOR HYPERACTIVITY IN GERBIL

Department of Experimental Neurology, Max-Planck-Institute for Neurological Research, Cologne, FRG

It has been shown that postischemic treatment with certain substances protects hippocampal CA_1 neurons against delayed neuronal injury. Recently, we reported that post-ischemic prolonged halothane inhalation is also able to prevent CA_1 injury in the gerbil (Kuroiwa et al. 1989a). In this study, we examined the therapeutic window of postischemic halothane anesthesia and correlated it with the postischemic motor hyperactivity which is reportedly linked with the severity of CA_1 injury (Gerhardt, Boast 1988). Details of this experiment will be published elsewhere (Kuroiwa et al. 1989b).

Transient forebrain ischemia was induced by occluding the bilateral common carotid artery for 5 min under 1% halothane anesthesia. Gerbils were separated into the following groups: grup 1 without postischemic halothane anesthesia, groups 2, 3 and 4 with postischemic 1% halothane anesthesia during 0-100 min, 100-200 min and 200-300 min of recirculation, respectively. In each group motor activity was measured by counting the number of infrared beams interrupted by gerbil movement every 100 min for 1 day before and 2 days after ischemia. The animal was sacrificed after 7 days of recirculation for the morphometry of CA_1 injury.

In the control group in which the gerbil was sham-operated under halothane anesthesia for 15 to 115 min, a non-significant decrease of motor activity was observed during the first day after sham operation. In group 1, significant motor hyperactivity was observed during 100--400 min of recirculation. Only 15% of CA_1 neurons survived in this group. In group 2, motor hyperactivity was less than 25% of that in

Paper presented at Symposium on Neurobiology of Cerebral Ischemia and Hypoxia. Poznań, June 29-July 1, 1989.

group 1 and limited to 100-200 min of recirculation. No motor hyperactivity was observed during later periods of recirculation. More than 80% of the CA_1 neurons in this group were preserved. In groups 3 and 4, postischemic motor hyperactivity was observed during the initial 100--400 min of recirculation except for the period of anesthesia. In these groups less than 25% of the CA_1 neurons were preserved.

The presented results show that:

1. The gerbil subjected to a 5 min of forebrain ischemia develops motor hyperactivity during 100-400 min of recirculation.

2. Postischemic halothane anesthesia during the initial 100 min of recirculation significantly reduces the subsequent motor hyperactivity and protects CA_1 neurons against delayed neuronal injury.

3. Postischemic halothane anesthesia either during 100-200 or 200--300 min of recirculation did not reduce motor hyperactivity and did not protect CA_1 neurons from delayed neuronal injury.

Thus, the therapeutic window of postischemic halothane anesthesia for protection against CA_1 injury precedes the phase of increased motor activity, indicating that post-ischemic neuronal hyperexcitability follows rather than precedes CA_1 injury.

PONIEDOKRWIENNA ANESTEZJA HALOTANOWA A ZWIĘKSZENIE AKTYWNOŚCI RUCHOWEJ U CHOMIKA MONGOLSKIEGO

Streszczenie

Badano wpływ anestezji halotanowej, zastosowanej w różnym czasie recyrkulacji, na aktywność ruchową i rozwój uszkodzeń neuronalnych u gerbili, u których wywołano 5-minutowe niedokrwienie przodomózgowia. Zwierzęta nie poddane po niedokrwieniu działaniu halotanu wykazywały nadmierną aktywność ruchową przez okres 100-400 minut recyrkulacji, a w sektorze CA_1 hipokampa obserwowano tylko 17% zachowanych neuronów. Poniedokrwienna anestezja w trakcie pierwszych 100 minut recyrkulacji prawie całkowicie znosiła nadmierną aktywność ruchową zwierząt i działała ochronnie na neurony sektora CA_1 (84% zachowanych komórek). Podawanie halotanu przez okres 100 minut w późniejszych okresach po niedokrwieniu nie zmniejszało natomiast nadmiernej aktywności ruchowej zwierząt i wykazywało znacznie słabsze działanie cytoprotekcyjne z zachowaniem mniej niż 24% neuronów sektora CA_1. Ochronne działanie anestezji halotanowej wobec poischemicznych uszkodzeń sektora CA_1 wyprzedza fazę nadmiernej aktywności ruchowej po niedokrwieniu, co wskazuje, że nadpobudliwość neuronów stanowi raczej następstwo niż wyprzedza uszkodzenie sektora CA_1.

REFERENCES

1. Gerhardt S. C., Boast C. A.: Motor activity changes following cerebral ischemia in gerbils are correlated with the degree of neuronal degeneration in hippocampus. Behav Neurosci, 1988, 102, 301-303.

2. Kuroiwa T., Bonnekoh P., Hossmann K. A.: Postischemic halothane anesthesia prevents delayed neuronal death of CA_1 neurons in gerbil. J Cereb Blood Flow Metab, 1989a, 9 (Suppl. 1), 756.
3. Kuroiwa T., Bonnekoh P., Hossmann K.-A.: Therapeutic window of halothane anesthesia to reverse delayed neuronal injury: Relationship to postischemic motor hyperactivity in gerbil. Submitted for publication, 1989b.

Authors' address: Department of Experimental Neurology, Max-Planck-Institute for Neurological Research, Gleueler Str. 50, D-5000 Cologne 41, FRG.

NEUROPAT. POL. 1990, 28, 3-4
PL ISSN 0028-3894

PETRA BONNEKOH, ANKA BARBIER, KONSTANTIN A. HOSSMANN

ULTRASTRUCTURAL FINDINGS IN THE GERBIL HIPPOCAMPUS AFTER BRIEF GLOBAL ISCHEMIA AND LONG SURVIVAL TIMES

Max-Planck-Institute for Neurological Research,
Department of Experimental Neurology, Cologne, RFN

After a brief period of global forebrain ischemia the CA_1 sector of the hippocampus may exhibit selective neuronal injury (Kirino 1982). The number of injured neurons depends on the duration of ischemia, but even after a 20 min circulatory arrest a small population of neurons is able to survive (Johansen et al. 1983). It has not been established if survival of these neurons is permanent or if they succumb to ischemic injury after prolonged recirculation times. For this reason we studied the ultrastructural morphology of the hippocampal CA_1 sector after recirculation times up to 10 months, following a period of 5 min forebrain ischemia in gerbils.

MATERIAL AND METHODS

Bilateral common carotid artery occlusion was produced in adult gerbils for 5 min under halothane anesthesia. After survival times of 3 weeks, 6 months and 10 months ($n = 4$ animals in each group) the brains were fixed by transcardiac perfusion. The hippocampus was dissected and processed for ultrastructural examination. Three non-ischemic animals served as controls.

RESULTS

Controls

In non-ischemic animals the number of pyramidal cells in 1 μm semithin sections of the CA_1 sector of the hippocampus amounted to 96.3

Paper presented at Symposium on Neurobiology of Cerebral Ischemia and Hypoxia. Poznań, June 29-July 1, 1989.

±6.2 neurons per 1 mm (mean ±SD). Electron microscopy of the control CA_1 *stratum pyramidale* revealed closely packed neurons with rounded nuclei and a scanty perikaryon. Cisternae of the endoplasmic reticulum and polyribosomes were randomly distributed in the cytoplasm. Astrocytes were rare in this layer. *Stratum radiatum* was composed of presynaptic boutons and dendritic endings forming synapses (Fig. 1A). The CA_3 sector contained pyramidal neurons the cell bodies of which were generally larger than those of CA_1 neurons. The cytoplasm of granular cells in the dentate gyrus contained sparsely distributed cisternae of granular endoplasmic reticulum.

Ischemic animals

Three weeks survival

The number of pyramidal cells of the CA_1 sector amounted to 5.6 ±2.3 neurons per 1 mm. Glial cells and phagocytic cells filled with numerous lipid droplets were present in the *stratum pyramidale* and the neighbouring strata. The striation of *stratum radiatum* had disappeared. Hippocampal CA_1 layers showed a minor reduction in thickness in comparison with the control. The CA_3 sector and dentate gyrus were not different from that of controls.

Ultrastructurally 3 types of surviving neurons could be distinguished. A few neurons appeared morphologically intact and did not differ from control ones. A more frequent "pale" type of neurons exhibited organelles clustered around the crenated nucleus, leaving thereby the periphery of the cytoplasm relatively electron lucent. Finally, some "dark" neurons showed condensation of chromatin and cytoplasm. In the *stratum radiatum* the number of vesicles contained in the presynaptic terminals was increased. The dendrites of CA_1 pyramidal neurons were destroyed, leaving clear spaces between the presynaptic sites. Enlargement of axonal cytoplasm by inclusion of dense bodies and tubular structures was obvious after this recirculation time. The astrocytic population of CA_1 *stratum pyramidale* after 3 weeks survival was characterized by sparse glial filaments and abundant cytoplasmic vacuoles.

Six months survival

The pyramidal layer of the CA_1 sector exhibited 11.1 ±7.9 neurons per 1 mm and numerous glial cells. The number of neurons was higher than after 3 weeks survival, because the thickness of the CA_1 sector was dramatically reduced. This was due to the shrinkage of all CA_1 layers. The CA_3 sector and gyrus dentatus showed a normal morphological structure.

The electron-microscopic investigation showed several surviving neurons in the CA_1 sector with a normal ultrastructure and some deposits of lipofuscin. Other neurons were of the "pale" type. In these neurons

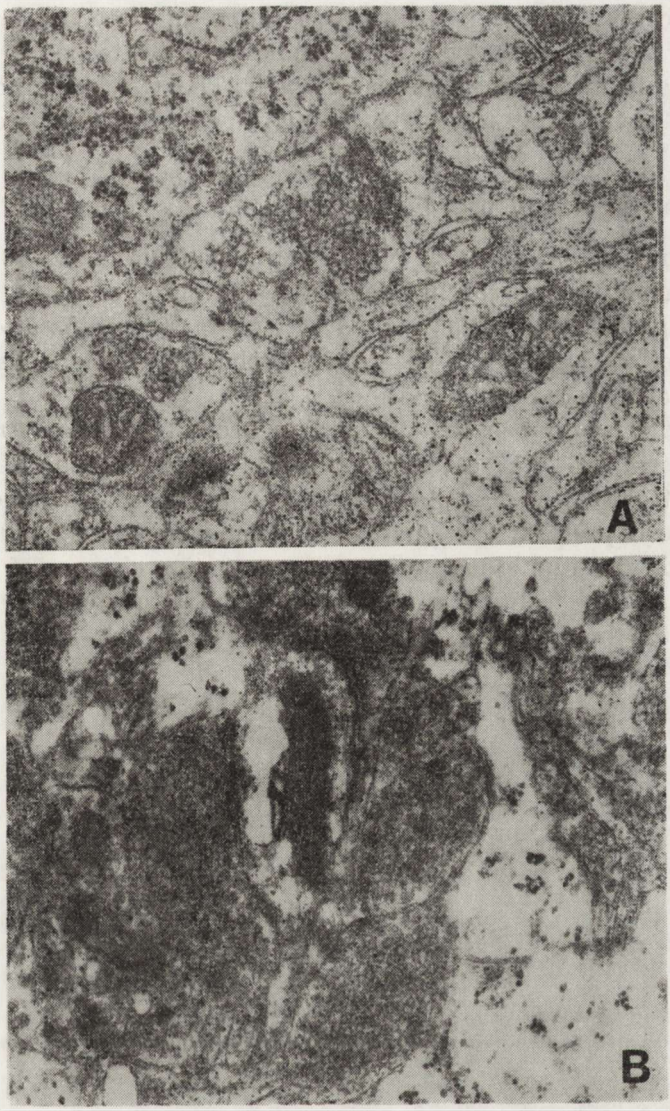

Fig. 1. Stratum radiatum of a control animal (A) and six months (B) after 5 min of ischemia. After six months of recirculation presynaptic boutons are filled with numerous clear vesicles

Ryc. 1. Stratum radiatum kontrolnego zwierzęcia (A) i zwierzęcia z 6-miesięcznym przeżyciem po 5-min niedokrwieniu (B). Po 6 miesiącach recyrkulacji zakończenia presynaptyczne wypełniają liczne jasne pęcherzyki

the peripheral rim of the cytoplasm contained few organelles. The "dark" type of neurons was not observed at this recirculation time. In *stratum radiatum* axosomatic and axodendritic synapses were found. The astrocytes presented a profusion of glial fibrils in their cytoplasm. Fibers traversing the CA_1 sector showed partial demyelination. The pre-

synaptic terminals of the CA_1 *stratum radiatum* were filled with numerous clear vesicles (Fig. 1B). The terminals were attached to each other, but rarely formed axodendritic synapses. The CA_3 sector and dentate gyrus did not exhibit ultrastructural changes when compared with the controls.

Ten months recirculation

The number of surviving CA_1 neurons amounted to 13.5 $\pm$7.6 per 1 mm. There was no further reduction in thickness of the CA_1 sector when compared with the animals surviving for 6 months after an ischemic period of 5 min but occasionally phagocytic-like cells were still visible in all CA_1 layers.

The ultrastructure of the surviving neurons in the CA_1 *stratum pyramidale* resembled that after 6 months of recirculation. Neurons with normal ultrastructure and neurons with peripheral "pallor" of the perikaryon were present. Presynaptic terminals of CA_1 *stratum radiatum* were filled with numerous vesicles. Degenerative changes of axons were still present. The content of glial fibrils in astrocytes had further increased after this long recirculation time (Fig. 2).

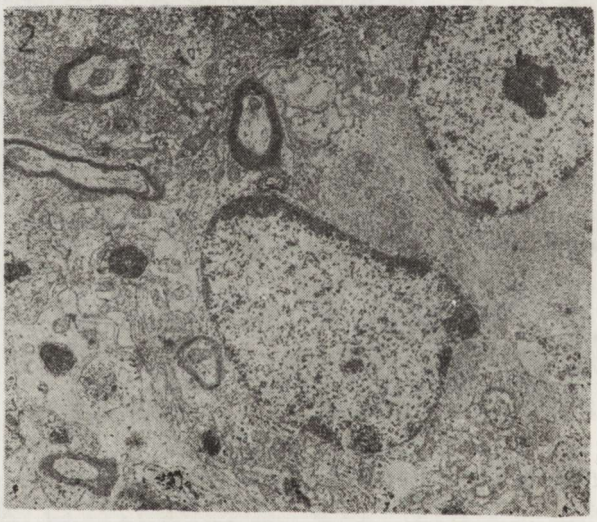

Fig. 2. Astrocytes in CA_1 *stratum pyramidale* 10 months after an ischemic period of 5 min. The cytoplasm is filled with densely packed glial fibrils

Ryc. 2. Stratum pyramidale odcinka CA_1 u zwierzęcia z 10-miesięcznym przeżyciem po 5-min niedokrwieniu. Cytoplazmę astrocytów wypełniają gęsto ułożone włókienka glejowe

DISCUSSION

The present study shows that after an ischemic period of 5 min morphological signs of ongoing processes of neuronal destruction, myelin

breakdown and a massive glial reaction persist for as long as 10 months. Since the *stratum radiatum* contains intact presynaptic terminals after the long survival time, there might be a source of neurotransmitters excitotoxic to the remaining neuronal population. Petito and Pulsinelli (1984) showed in the rat ischemic model altered CA_1 neurons after 36 hours of recirculation, which resembled those observed after long recirculation times in the present study. The distribution of the organelles around the nucleus with the electron lucent rim at the periphery of the cytoplasm is similar to that seen after up to 10 months of recirculation in this study. This suggests that these neurons survive in a morphologically altered condition for very long times. Further evidence for this assumption is provided by a study of Nishikawa et al. (1989) who investigated the gerbil model of unilateral transient cerebral ischemia. They observed in the cortical layer II of animals surviving for up to 5 weeks neurons with a characteristic peripheral pallor of the cytoplasm. The neuronal change of the "pale" type, therefore, seems to indicate the capacity of a neuron to survive permanently the ischemic insult.

BADANIA ULTRASTRUKTURALNE HIPOKAMPA PO KRÓTKOTRWAŁYM NIEDOKRWIENIU MÓZGU I DŁUGIM OKRESIE PRZEŻYCIA U GERBILA

Streszczenie

Badano morfologię hipokampa u gerbila po 5-minutowym niedokrwieniu przodomózgowia, w okresie do 10 miesięcy recyrkulacji. U zwierząt z 3 tygodniowym przeżyciem stwierdzono zanik 84,6% neuronów sektora CA_1. Po 6 i 10 miesiącach wykazano dodatkowo znaczne zwężenie wszystkich warstw sektora CA_1, przy czym nie zaobserwowano zwiększenia ubytku neuronów CA_1. W obrazie mikroskopowo-elektronowym stwierdzono zmiany dotyczące ciał komórkowych neuronów CA_1 i wypustek nerwowych w obrębie tego sektora. Poszerzenia aksonalne i rozpad mieliny obserwowano we wszystkich grupach czasowych, aż do 10 miesiąca recyrkulacji. Astrocyty sektora CA_1 charakteryzowała obfita ilość włókienek glejowych, zwiększająca się wraz z czasem przeżycia po incydencie niedokrwiennym. Zakończenia presynaptyczne w *stratum radiatum* były niezmienione i zawierały liczne jasne pęcherzyki. U zwierząt z 3-tygodniowym przeżyciem, struktury postsynaptyczne wykazywały cechy uszkodzenia, ale po dłuższym okresie recyrkulacji obserwowano prawidłowe połączenia dendrytów, odchodzących od zachowanych neuronów CA_1. Sektor CA_3 i *gyrus dentatus* nie wykazywały zmian histologicznych i ultrastrukturalnych, niezależnie od czasu przeżycia zwierząt po niedokrwieniu.

REFERENCES

1. Ito U., Spatz M., Walker J. T., Klatzo I.: Experimental cerebral ischemia in Mongolian gerbils. I. Light microscopic observations. Acta Neuropathol (Berl), 1975, 32, 209-223.

2. Johansen F. F., Jorgensen M. B., Diemer N. H.: Resistance of hippocampal CA-1 interneurons to 20 min of transient cerebral ischemia in the rat. Acta Neuropathol (Berl), 1983, 61, 135-140.
3. Kirino T.: Delayed neuronal death in the gerbil hippocampus following ischemia. Brain Res, 1982, 239, 57-69.
4. Nishikawa Y., Takahashi T., Shimada A.: Morphological studies on cerebral cortical lesions induced by transient ischemia in Mongolian gerbil. Diffuse and peripheral pallor of the neuronal perikarya. Acta Neuropathol (Berl), 1989, 78, 1-8.
5. Petito C. K., Pulsinelli W. A.: Sequential development of reversible and irreversible neuronal damage following cerebral ischemia. J Neuropathol Exp Neurol, 1984, 43, 141-153.

Authors' address: Max-Planck-Institute for Neurological Research, Department of Experimental Neurology, Gleueler Str. 50, D-5000 Cologne 41, FRG.

NEUROPAT. POL. 1990, 28, 3-4
PL ISSN 0028-3894

IRINA V. GANNUSHKINA, MARINA V. BARANCHIKOVA,
LILI A. SIBELDINA, NATALIA A. SEMENOVA*,
SIERGIEJ ST. LICHODY*, ALEXANDER A. KONRADOV*

SOME INDIVIDUAL PECULIARITIES OF BRAIN ENERGY METABOLISM AND THEIR CHANGES IN THE CONDITION OF BRAIN ISCHEMIA. AN *IN VIVO* ^{31}P NUCLEAR MAGNETIC RESONANCE STUDY

Institute of Neurology, Academy of Medical Sciences of USSR,
*Chemico-physical Institute, Academy of Sciences of USSR, Moscow, USSR

It is well known that identical brain artery occlusion or cerebral trauma may result in damage of the central nervous system varying both in intensity and extensiveness. The same artery occlusion may be followed by either mild or severe tissue alterations. Those variabilities were explained by differences in the collateral circulation systems and inequal organism reactivity, including different immune sensitivity to particular brain antigens, occurring in patients and in experimental animals.

The well documented changes in brain energy metabolism in patients and in experimental animals with cerebral blood flow disorders have been studied in many investigations with a wide spectrum of techniques, including ^{31}P nuclear magnetic resonance spectroscopy (NMR--spect), which is one of the most informative and noninvasive methods.

The purpose of the present study was an attempt:

1. to find any peculiarities of brain energy metabolism under control conditions prior to experimental brain ischemia, and
2. to study the changes of brain energy metabolism during the development of both severe and mild brain ischemia.

MATERIAL AND METHODS

The experiments were performed on 44 white laboratory rats (body weight 140-170 g), anesthetized with 50 mg/kg i.p. of sodium penta-

Paper presented at Symposium on Neurobiology of Cerebral Ischemia and Hypoxia. Poznań, June 29-July 1, 1989.

barbital for measuring ^{31}P NMR-spectra and performing bilateral occlusion of the common carotid arteries. Nine rats, which developed mild cerebral ischemia without neurological deficit or with it, but not more severe than 3 units in the 10-unit McGrow scale were included in the first experimental group. The 35 rats, which died within 24 h after application of the same model of cerebral ischemia, constituted the second experimental group.

^{31}P NMR-spectra measurements were performed in the initial stage before artery occlusion, then 3-4 times during the first hour after occlusion and in the animals, which survived the ischemic incident 24 hours later. ^{31}P NMR-spectra were registered with the use of a Fourier transform spectrophotometer — AM-400 (Bruker, FRG) with a vertical wide bore magnet, operating at 162 MH_z — 9,4 T for phosphorus, equipped with a special home-built probehead with surface coil of a special geometry (Lekhody et al. 1987), securing its close contact with the animal's head. The homogeneity of the magnetic field (BO) was promoted by optimizing the currents of shimming coils for the registration on the tissue water proton resonance signal. ^{31}P NMR-spectra were obtained from the Fourier transformation of 120 signals of the free induction decrease, accumulated in the course of 2 min (a coherent sum of 120 signals was required to receive sufficiently high signal-to-noise ratio). Duration of the observation pulse (30 μs) and relaxation delay (3 s) were optimized in the model conditions in order to reduce to negligible values the contribution of the signals originating from the tissue surrounding the brain in the registered spectra. One K time domain points and 7 KHz spectral width were used. The broad signals derived from bone phosphates and brain phospholipids were removed by the "convolution difference method" (Campbell et al. 1973).

Thereafter the integral intensities of spectral lines (areas) were mathematically analyzed. In our analysis all integral areas and all ratios of brain phosphorus metabolites signals within the ^{31}P NMR-spectra (10 parameters) were used. The standard statistical calculations of averaged values often do not allow to detect small, but coordinated changes of the complex multicomponent systems. In this case multidimensional mathematic analysis is a useful means for detecting fine differences. However, those differences, for example, the structural changes of the statistically significant correlation component bonds, are often not only difficult to interpret, but also to measure. It is necessary to characterize these quality changes quantitatively in the first degree of approximation, i.e. introduce a measure that reflects the integral correlation bond force in the system and its variability. In order to ensure a universal nature and to give the possibility to compare the results of different experiments, this value should not to depend either on the number of measurements or the correlation matrix dimension.

Besides, this value should permit analysis of the obtained data with

the use of statistical comparrative criteria, i.e. to have calculative dispersion. For this reason Fisher's transformation, which translates the excerpt correlation coefficient r to the value z was applied. Averaged on the correlation matrix value z characterizes the force correlation bond measure. Variability (Var) was evaluated from the excerption dispersion of value z within the corresponding correlation matrix.

By means of ^{31}P NMR spectroscopy *in vivo* 5 groups of signals were obtained in the brain. Averaged values of signal areas, all possible ratios of these areas, the correlation matrix, the measure of correlation force bond z and its variability (Var) were calculated. Differences of the averaged values were estimated by Student's t-test.

RESULTS

We failed to find any visual differences in the initial spectra taken from rat brains before carotid artery occlusion (Fig. 1). But mathematical

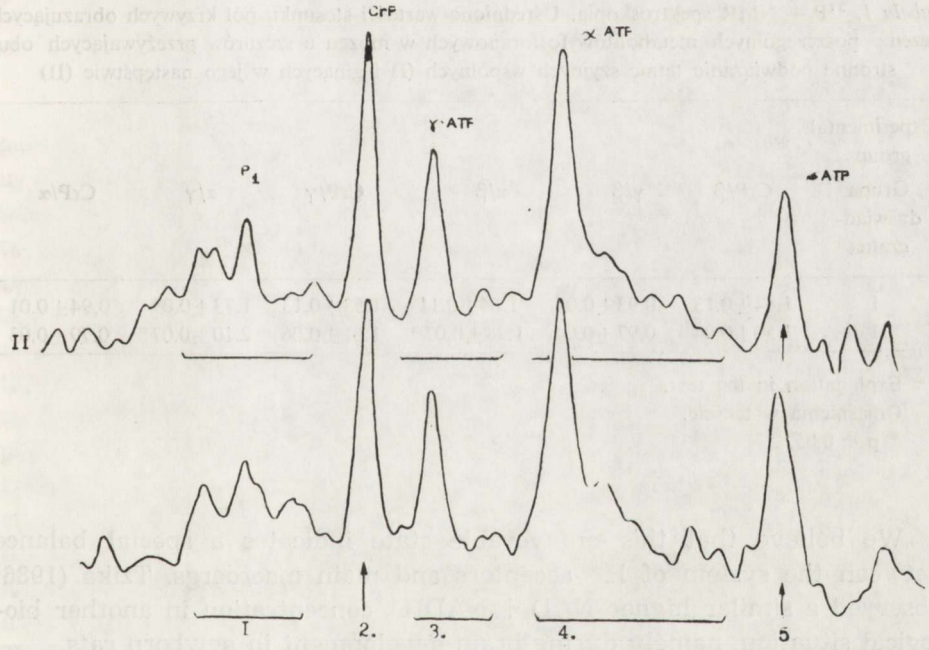

Fig. 1. Initial ^{31}P NMR spectra obtained *in vivo* from the brain before artery occlusion in surviving (I) and subsequently dying (II) rats after induction of brain ischemia. 1 peak — phosphomonoethers, inorganic phosphate (P_i), phosphodiethers; 2 peak — creatine phosphate (CrP); 3 peak — γ ATP + β ADP; 4 peak — α ATP + α ADP + NAD + $NADH^+$ + uridindiphosphoglucose (UDFG); 5 peak — β ATP

Ryc. 1. Wyjściowe krzywe ^{31}P NMR spektrometrii uzyskane przyżyciowo z mózgów przed obustronnym podwiązaniem tętnicy szyjnej wspólnej u szczurów przeżywających incydent niedokrwienny (I) i ginących w jego następstwie (II). 1 wierzchołek — fosfomonoestry, fosfodwuestry, fosfór nieorganiczny (P_i); 2 wierzchołek — fosfokreatyna (CrP); 3 wierzchołek — γ ATP + β ADP; 4 wierzchołek — α ATP + α ADP + NAD + $NADH^+$ + urydyno-dwufosfo-glukoza (UDFG); 5 wierzchołek — β ATP

analysis indicated that in normal conditions the brain energy metabolism of the animals belonging to the first experimental group significantly differed from that of the second group only as far as the square of the αATP peak was concerned. The most pronounced difference was observed at square ratios of αATP to γATP and creatine phosphate (CrP) to αATP (Ttable 1). As known, ratio αATP/γATP originally meaning NAD + $NADH^+$ + ADP + ATP + UDFG to ADP + ATP can be simplified according to Kopp et al. (1984) as NAD + $NADH^+$/ATP + 1. The ratio CrP to α ATP = CrP/NAD + $NADH^+$ + ADP + ATP + UDFG can also be simplified as CrP/NAD + $NADH^+$. Thus, considering this data, a somewhat higher initial level of the NAD + $NADH^+$/ATP ratio, as well as lower initial ratio of CrP to NAD + $NADH^+$ indicate a worse prognosis of tolerance to cerebral ischemia and its metabolic parameters.

Table 1. Averaged ratios of ^{31}P — NMR spectra peaks areas reflecting the concentrations of phosphate metabolites obtained *in vivo* before arteries occlusion in surviving (I) and subsequently dying animals (II), after development of brain ischemia

Tabela 1. ^{31}P — NMR spektroskopia. Uśrednione wartości stosunku pól krzywych obrazujących stężenie poszczególnych metabolitów fosforanowych w mózgu u szczurów przeżywających obustronne podwiązanie tętnic szyjnych wspólnych (I) i ginących w jego następstwie (II)

Experimental groups / Grupa doświadczalna	CrP/β	γ/β	α/β	CrP/γ	α/γ	CrP/α
I	1.44±0.13	0.93±0.04	1.64±0.11	1.53±0.13	1.73±0.09	0.94±0.01
II	1.50±0.04	0.97±0.04	1.98±0.07*	1.61±0.06	2.10±0.07*	0.79±0.03

Explanation in the text.
Objaśnienia w tekście.
* $p \leq 0.05$.

We believe that this unfavorable state indicates a special balance between the system of H^+ acceptors and main macroergs. Tzika (1986) observed a similar higher NAD + $NADH^+$ concentration in another biological situation, namely during brain development in newborn rats.

Apart from above mentioned differences between the spike squares and their ratios, correlation analysis allowed us to find other parameters which are initially different in rats which then survived or died after bilateral common carotid artery occlusion. Figure 2 shows that initial brain energy metabolism depends not only of the ratio of macroergs to hydrogen acceptors, but also on the correlation coefficient in Fisher's modification (*z*), which was 10 times higher in the second group as com-

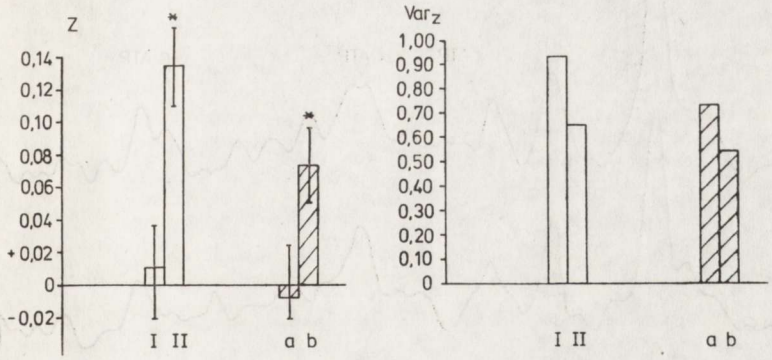

Fig. 2. Correlations forces of ^{31}P NMR spectral parameters (z) and variability (Var_z) of elements in each correlation matrix: I — initial spectra in surviving rats; II — initial spectra of subsequently dying rats; a — initial spectra of surviving rats; b — spectra 24 h after development of mild cerebral ischemia

Ryc. 2. Moce korelacyjne parametrów ^{31}P NMR spektrometrii (z) oraz zmienność (Var_z) elementów w poszczególnych układach korelacyjnych: I — krzywe wyjściowe u zwierząt przeżywających incydent niedokrwienny; II — krzywe wyjściowe u zwierząt ginących w przebiegu incydentu niedokrwiennego; a — krzywe wyjściowe u zwierząt przeżywających incydent niedokrwienny; b — krzywe uzyskane u zwierząt po 24 godz. umiarkowanego niedokrwienia mózgu

pared to the first surviving one. Peculiarities of the energy metabolism in the second group were accompanied by an almost double low dispersion (Var_z) of the parameters in each correlation matrix. This may indicate that the brain of animals less resistant to ischemia has a more regulated or less flexible initial energy metabolism from the point of view of balance between production and utilization of macroergic molecules.

The development of severe brain ischemia in rats which died during the first 24 hours after artery occlusion induced well known marked changes in spectral parameters (Fig. 3) with an increase of inorganic phosphate and decrease of CrP, ATP and pH (Gernabi et al. 1988; Horikowa et al. 1985; Likhody et al. 1987; Naritomi et al. 1988; Thulborn et al. 1982; Welch et al. 1987). Similarly to other authors we failed to find significant visual changes of spectral parameters during the development of mild brain ischemia after bilateral carotid artery occlusion in animals without any or only with mild neurological deficit (Fig. 4). The results obtained in the initial differences in spectral parameters in animals highly and low sensitive to brain ischemia inclined us to perform analysis of spectral parameters obtained in rats during development of mild brain ischemia in the same algorithm. Thus, we found an increase of the ratio between NAD + $NADH^+$ to ADP + ATP, but not to CrP (Table 2). The second feature was also the same: an increase of correlation forces between spectral parameters (z) and decrease of dispersion of value (z) inside corresponding correlation matrix (Fig. 2).

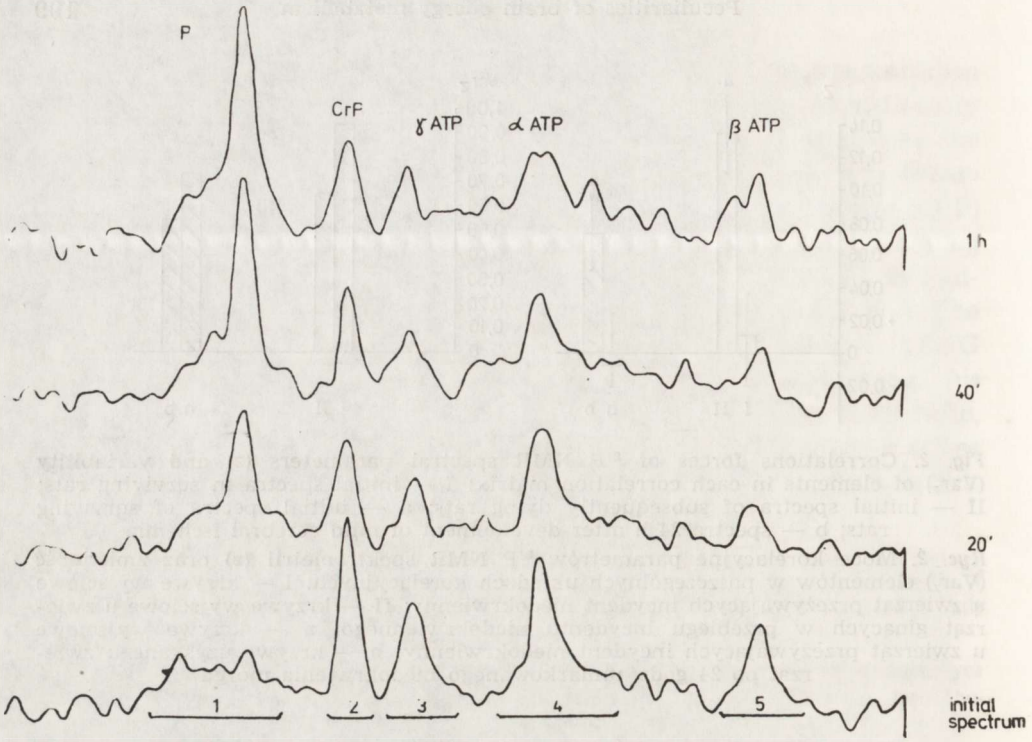

Fig. 3. Changes in phosphate metabolites during the development of severe brain ischemia with death of rat (from initial state in low spectrum to 20 min, 40 min and 1 h after bilateral common carotid artery occlusion)

Ryc. 3. Zmiany obrazu metabolitów fosforanowych w przebiegu ciężkiego niedokrwienia mózgu u zwierząt ginących w jego następstwie (poczynając od krzywej wyjściowej do obrazów w 20, 40 i 60 min po obustronnym podwiązaniu tętnic szyjnych wspólnych)

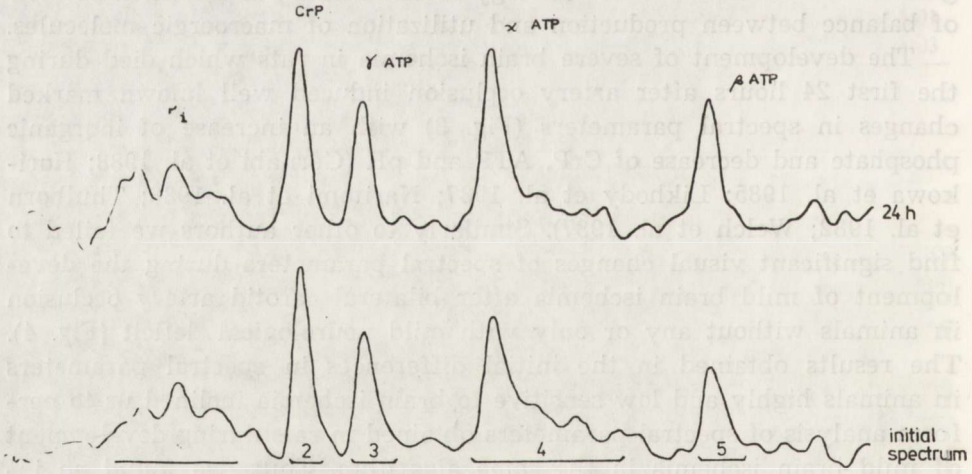

Fig. 4. No marked visual changes from initial state in phosphate metabolites concentration (low spectrum) to 24 h after artery occlusion and development of mild brain ischemia (upper spectrum)

Ryc. 4. Brak znacznych uchwytnych zmian w stężeniu metabolitów fosforanowych u szczurów w umiarkowanym niedokrwieniu mózgu (zestawienie krzywej wyjściowej i zapisu w okresie 24 godz. po podwiązaniu tętnic szyjnych)

Table 2. Averaged ratios of ^{31}P — NMR spectra peaks areas reflecting the concentrations of phosphate metabolites obtained *in vivo* during the development of mild brain ischemia

Tabela 2. ^{31}P — NMR spektroskopia. Uśrednione wartości stosunku pól krzywych obrazujących stężenie poszczególnych metabolitów fosforanowych w mózgu szczurów w przebiegu umiarkowanego niedokrwienia

Experimental group Grupa doświadczalna	CrP/β	γ/β	α/β	CrP/γ	α/γ	CrP/α
a — before artery occlusion przed podwiązaniem tętnic	1.37±0.07	1.02±0.04	1.60±0.10	1.36±0.07	1.55±0.08	0.91±0.08
b — 24 h after artery occlusion 24 godz. po podwiązaniu tętnic	1.49±0.14	1.06±0.12	1.72±0.16	1.45±0.09	1.76±0.08*	0.89±0.07

Explanation in the text.
Objaśnienia w tekście.
* $p < 0.05$.

DISCUSSION

In biological terms such a strained state of brain energy metabolism under ischemic conditions means increased vulnerability of the animals to ischemia or to other types of brain injury. The differences between the energetic states of the various parts of the brain could not be studied owing to the limitations of sensitivity when using NMR-spectroscope, however, we suggest that the energetic state in various parts of the brain could determine their different vulnerability. Only with NMR-spectroscopy did have we a tool for individual recording of the different parameters of brain energy metabolism prior to the induction of experimental cerebral ischemia, providing individual self-control data before and after experimental procedure as compared with the routine biochemical studies confronting control and treated groups separately. Literature data indicate that various species including humans exhibit a different sensitivity to hypoxia (Lakjanova, Korobkov 1981). These findings allow to search for new methods of prophylaxy and treatment of hypoxia with different antihypoxants.

We firstly indicate the compounds of brain energy metabolism as their predicative value of the ischemic vulnerability of the animals. A knowledge of these parameters allows to screen the animals belonging

to the high risk group from the their general population before inducing experimental brain ischemia. We suggest also the clinical significance of these NMR-spectroscopy data for prophylactic screening of the persons belonging, for instance, to special high risk professional groups or individual treatment of patients after cerebral blood flow disturbances. Our data can also be utilized in the development of new brain protecting drugs, correcting balance between the system of hydrogen acceptors and macroergic adenylate pool and creatine phosphate. Our results suggest that energy metabolism in animals highly sensitive to brain ischemia and during development of brain ischemia became more stiffly organized. According to the "chaos" theory of Prigojin the more rigid systems are more vulnerable. That is why the individuals highly sensitive to brain ischemia need more intensive and specific treatment of the disease process. Moreover, if this phenomenon — different sensitivity to brain ischemia — is not taken into consideration, errors may arise in the evaluation of the experimental results.

OSOBNICZE WŁAŚCIWOŚCI METABOLIZMU ENERGETYCZNEGO I ICH ZMIANY W WARUNKACH NIEDOKRWIENIA MÓZGU

Badania *in vivo* za pomocą ^{31}P magnetycznego rezonansu jądrowego

Streszczenie

Przeprowadzono analizę metabolizmu energetycznego mózgu *in vivo* za pomocą spektroskopii ^{31}P magnetycznego rezonansu jądrowego u szczurów, u których wywołano niedokrwienie mózgu przez obustronne podwiązanie tętnic szyjnych wspólnych. Rejestrację prowadzono przed podwiązaniem tętnic, w pierwszej godzinie po podwiązaniu, a u zwierząt przeżywających incydent niedokrwienny dodatkowo po upływie 24 godzin.

Obserwacje kliniczne pozwoliły na wyodrębnienie 2 grup zwierząt doświadczalnych, z których pierwsza (9 szczurów) przeżywała incydent niedokrwienny bez deficytu neurologicznego lub z zespołem ubytkowym nie przekraczającym 3 punktów w 10-punktowej skali McGrowa. Szczury drugiej grupy (35 zwierząt) ginęły z ciężkim zespołem neurologicznym w 24 godziny po podwiązaniu tętnic szyjnych. Spektroskopia NMR, wykonana w okresie poprzedzającym podwiązanie tętnic szyjnych, wykazała istotne różnice metabolizmu energetycznego mózgu u obu grup zwierząt. Ich powtarzalność pozwoliła na wyodrębnienie zwierząt „wrażliwych" i „opornych" na niedokrwienie na podstawie właściwości metabolizmu wysokoenergetycznych fosforanów w okresie poprzedzającym okluzję tętnic szyjnych. Autorzy sugerują, że podobne różnice metaboliczne między poszczególnymi formacjami oun mogą mieć decydujące znaczenie w ich zróżnicowanej wrażliwości na niedokrwienie.

REFERENCES

1. Campbell I. D., Dobson C. M., Williams R. S. P.: Resolution and enhancement of protein PMR spectra using the difference between a broadened and a normal spectrum. J Magn Res, 1973, 11, 172-181.

2. Germano I. M., Pitts L. H., Berry I., De Armond S. J.: High energy phosphate metabolism in experimental permanent focal cerebral ischemia: an *in vivo* ^{31}P magnetic resonance spectroscopy study. J Cereb Blood Flow Metab, 1988, 8, 24-31.
3. Horikawa J., Naruse S., Horikawa K., Tanaka C., Hishikawa H., Watari H.: Studies of energy metabolism in experimental cerebral ischemia using topical magnetic resonance. Changes in ^{31}P NMR spectra compared with electroencephalograms and regional cerebral blood flow. J Cereb Blood Flow Metab, 1985, 5, 235-240.
4. Kopp S. I., Krieglstein I., Freidank A., Rachman A., Seibert A., Cohen M. M.: ^{31}P nuclear magnetic resonance analysis of brain: II. Effects of oxygen deprivation on isolated perfused and nonperfused rat brain. J Neurochem, 1984, 43, 1716-1731.
5. Likhody S. St., Semionova N. A., Dubinsky W. Z., Likhody St. S., Sibeldina L. A.: Study of the phosphorus containing metabolite levels in the rat brain by means of ^{31}P NMR. Neurochimija, USSR, 1987, 6, 439-441.
6. Lukjanova L. D., Korobkov A. V.: Some physiological and metabolic individual sensitivity of the animals to hypoxia in normal condition and during adaptation. In: Physiological and clinical problems of adaptation to hypoxia, hypodynamia and hyperthermia. Moscow, 1981, pp. 73-76.
7. Naritomi H., Sasaki M., Kanashiro M., Kitani M., Sawada T.: Flow thresholds for cerebral energy disturbance and Na^{++} pump failure as studied by *in vivo* ^{31}P and ^{23}Na nuclear magnetic resonance spectroscopy. J Cereb Blood Flow Metab, 1988, 8, 16-23.
8. Thulborn K. R., Bonlay G. H., Duchen L. W., Radda G.: A ^{31}P nuclear magnetic resonance *in vivo* study of cerebral ischemia in the gerbil. J Cereb Blood Flow Metab, 1982, 2, 299-306.
9. Tzika A.: ^{31}P NMR of rat brain energy metabolism in neonatal hypothyroidism and rehabilitation. Magn Res in Med, 5th Annual Meeting, 1986, 1100, 693-694.
10. Welch K. M. A., Chopp M., Smith M. B., Helpern J. A., Walton D., Frinak S.: The utility of *in vivo* NMR — spectroscopy for the study of ischemic stroke. Neurology, 1987, 37 (Suppl. 1), 249.

Authors' address: Institute of Neurology, Academy of Medical Sciences of USSR, Moskow, USSR.

NEUROPAT. POL. 1990, 28, 3-4
PL ISSN 0028-3894

RYSZARD PLUTA

EXPERIMENTAL TREATMENT WITH PROSTACYCLIN OF GLOBAL CEREBRAL ISCHEMIA IN RABBIT — NEW DATA

Department of Neuropathology, Medical Research Centre,
Polish Academy of Sciences, Warsaw, Poland

After the discovery of prostacyclin (PGI_2) (Gryglewski et al. 1976) it was soon recognized that this substance might exert some curative effects on acute or chronic cerebrovascular diseases of ischemic origin. It is now well established that PGI_2 is the main prostaglandin synthesized in the vascular endothelial layer (Moncada et al. 1977). It has also been demonstrated in experimental animals that PGI_2 is continuously secreted from the endothelial surface of the vascular bed into the systemic circulation, and the concept of PGI_2 acting as a circulating hormone controlling platelet aggregability and vascular resistance has been put forward (Moncada et al. 1978). The assumption that such a therapy would be beneficial was based in part on the vasodilator, fibrinolytic and platelet antiaggregatory properties of PGI_2 (Gryglewski et al. 1976; Dembińska-Kieć et al. 1982). On the other hand, it has been noted that PGI_2 protects platelets against damage (Radomski, Moncada 1983). Moreover a diminished level of PGI_2 was noted in transient ischemic attacks (Jarman et al. 1979), also in the "no-reflow phenomenon" (Hallenbeck, Furlow 1979), cerebral vascular spasm (Uchida, Murao 1981), in atherosclerosis (Gryglewski et al. 1978), and after brain ischemia (Gaudet, Levine 1979). Finally, it has been demonstrated that acute cerebral ischemia stimulates the formation of platelet aggregates (Dougherty et al. 1979) and increases microcirculatory resistance during reperfusion (Hart et al. 1978; Pluta et al. 1989). The demonstration that platelet aggregates tend to concentrate in cortex zones coextensive with zones of hypoperfusion suggests that platelets may contribute to perfusion impairment. This sequence is termed the blood-damaged tissue interaction. These findings indicated that treatment of ischemic vascular diseases (e.g. complete ce-

Paper presented at Symposium on Neurobiology of Cerebral Ischemia and Hypoxia, Poznań, June 29-July 1, 1989.

rebral ischemia) with PGI_2 may compensate the endogenous loss of vasodilator and platelet-controlling activity.

The aim of the present work were the curative effects of prostacyclin on the ischemic brain.

MATERIALS AND METHODS

Rabbits (n = 30; 2.5-3.5 kg) of both sexes were anesthetized with 30 mg/kg b.w. of pentobarbital (Vetbutal — Biowet) together with 2.5 ml noraminophenazonum methanosulfonicum natrium (Pyralginum — Polfa) and Xylocain (Astra Chemicals — local pain-killer), tracheostomized, relaxed with gallaminum triaethiodidum (Tricuran — Germed, 3 mg/kg) and artificially ventilated (Pluta 1987). Global 15 or 20 min cerebral ischemia was induced by occlusion of the brachiocephalic trunk, the left subclavian and both internal thoracic arteries with reduction of the systemic arterial blood pressure to 60 ±10 mm Hg (Pluta 1987). General physiological parameters and EEG in the cortex were recorded during the experiments (6 h) (Pluta 1987). These data were referred to morphological changes in the brain (Pluta 1987). Prostacyclin (Sigma — 2 μg/kg/min) was applied intravenously to all treated animals continuously 3 min before, during and for 15 min after ischemia (Pluta 1985). The vehicle control was run parallel.

RESULTS

Untreated ischemia produced:

— disappearance of EEG activity in 10-20 s with first signs of recovery 21-55 min after ischemia, and continuous activity from 40-93 min of the recirculation period, with or without normalization of EEG recordings during 6 h postischemic observation (Fig. 1);

— hypotension;

— progressive bradycardia;

— changes typical in EKG for myocardial infarct;

— alterations in heart which consisted of massive hemorrhages in whole myocardium;

— ultrastructural changes in adrenal medulla and cortex cells cytoplasm;

— ultrastructural damages in adrenal medulla and cortex cells nuclei (clumping and marginal shifh of chromatin, vesicular structures, granulofibrillar bodies, intranuclear filamentous inclusions);

— constriction of most cerebral blood vessels (particularly capillary network);

— brain edema (cytotoxic and vasogenic types);

— neuronal changes;
— ultrastructural changes in neuronal and neuroglial cells cytoplasm;
— ultrastructural damages in neuronal and neuroglial cells nuclei (clumping and marginal shift of chromatin, vesicular structures, intranuclear membraneous or filamentous inclusions);

Ischemia with prostacyclin *i.v.*:

— advanced both EEG recovery and normalization of the recordings during reperfusion (Fig. 1);
— reduced hypotension;
— reduced bradycardia;
— prevented changes in EKG;
— reduced intensity of hemorrhages in cardiac muscle;
— produced severe destruction of adrenal cortex cells cytoplasmic organization;
— did not influence the ultrastructural damages in adrenal medulla and cortex cells nuclei;
— reduced number of constricted cerebral blood vessels;
— reduced brain edema;
— reduced the spectrum of neuronal changes and decreased the number of pathologically changed neurons;
— protected the ultrastructural changes in neuronal and neuroglial cells cytoplasm (Figs. 2, 3);
— did not affect the ultrastructural damages in neuronal and neuroglial cells nuclei (Figs. 2, 3, 4) — increased in the neuronal nuclei the number of vesicular structures and inclusions;

DISCUSSION

The major aim in the treatment of acute ischemic stroke is to minimize irreversible brain damage, but specific treatments for brain ischemia have so far proved disappointing. Currently, the possibility that PGI_2 may attenuate ischemic brain damage is being investigated extensively, and experimental and clinical studies showed that in some cases this agent may improve the neurologic outcome after ischemia (Huczyński et al. 1985; Pluta 1985). The immediate beneficial effect of the PGI_2 treatment in this study correlates very well with the results of clinical observation in humans (Huczyński et al. 1983). On the other hand, the disappearance of the statistical significance of this beneficial treatment 2 weeks later in stroke patients (Huczyński et al. 1985) or the generally lack of effect of treatment (Kerckhoff et al. 1983) are not clear. In this situation the crucial question is how to explain these differences? The conclusion that the administration of PGI_2 was responsible for these early improvements in outcome is beyond discussion. With the present

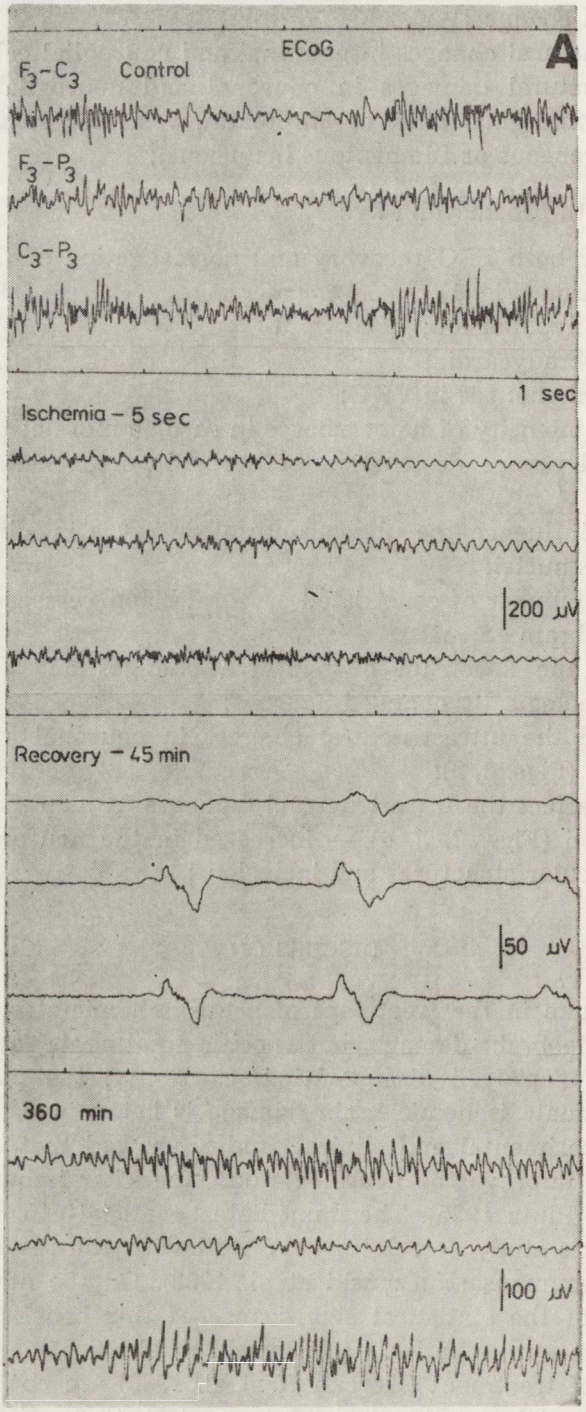

Fig. 1. Representative ECoG recordings from rabbits with 20 min complete cerebral ischemia: untreated (A) and treated (B) with PGI_2. Time constant 0.03 s

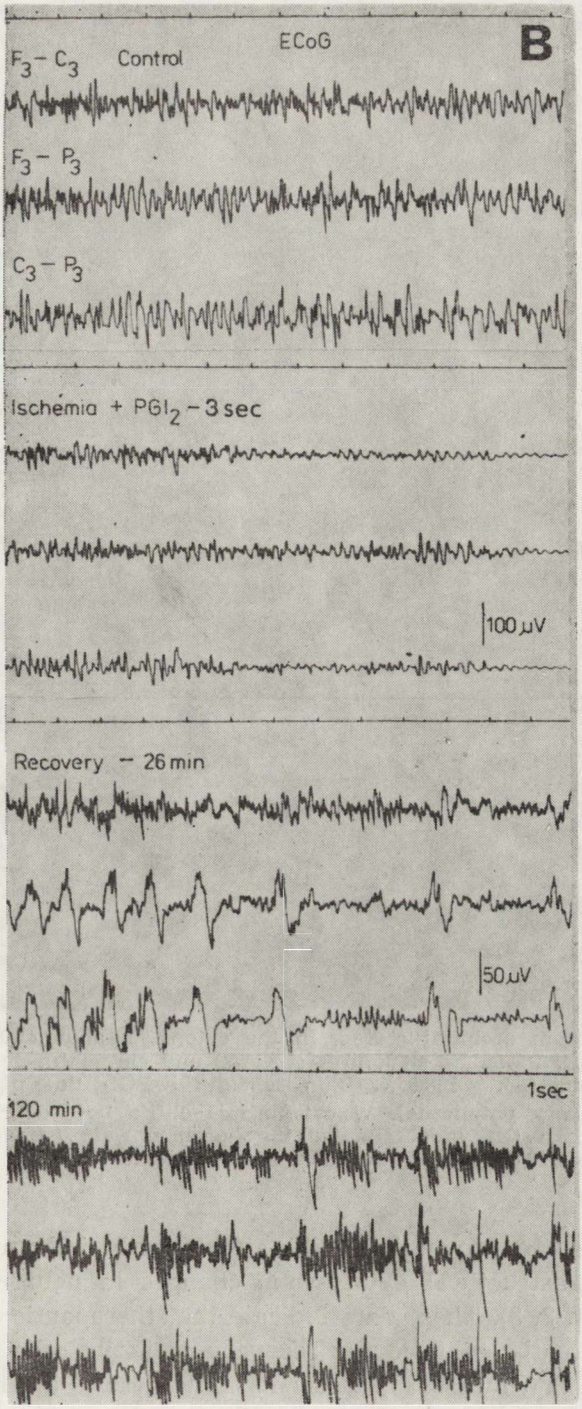

Ryc. 1. Reprezentatywne elektrokortikogramy królików po 20-minutowym całkowitym niedokrwieniu mózgowia: A — bez podawania leku, B — po podawaniu PGI_2. Stała czasu 0,03 s

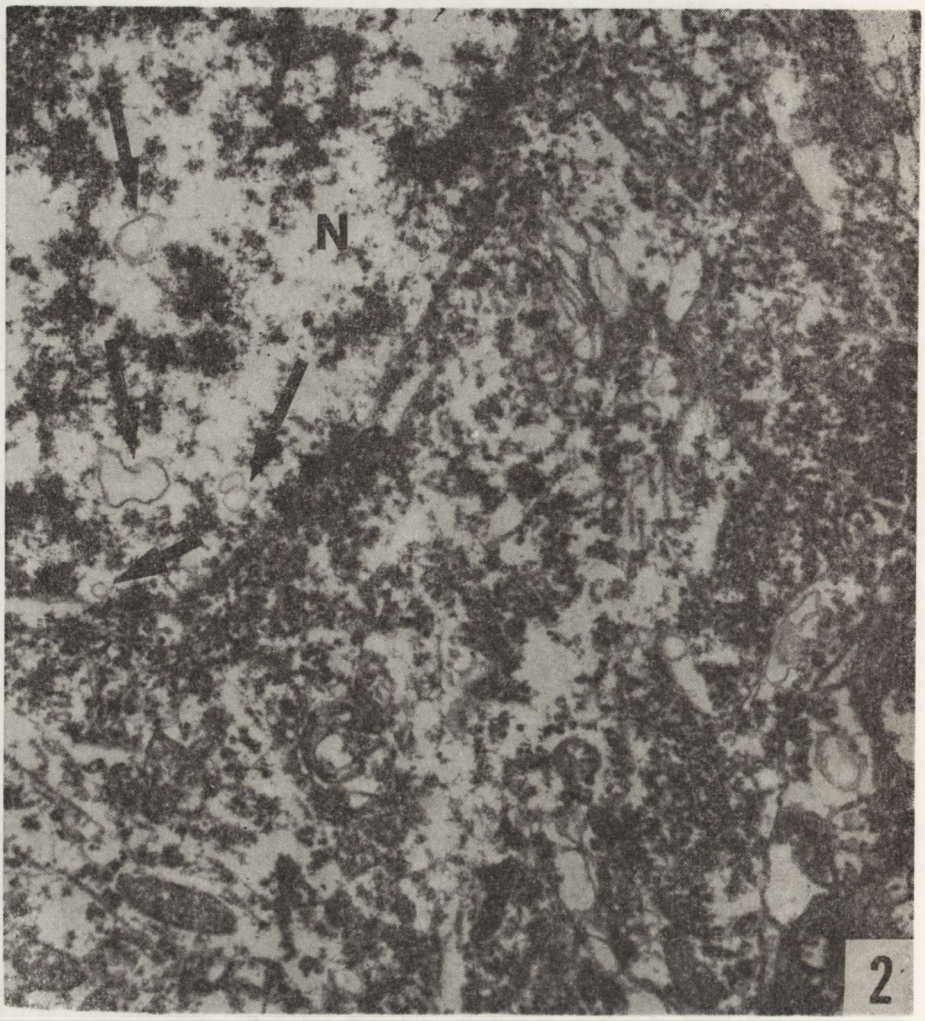

Fig. 2. Neuron from occipital cortex. In the cytoplasm abundant well preserved cellular organelles. Vesicular structures (arrows) and chromatin clumping are present within nucleus (N). × 10 800. 20 min ischemia + PGI_2; time of observation 3 h
Ryc. 2. Neuron kory potylicznej. W cytoplazmie obfita ilość dobrze zachowanych organelli. W jądrze (N) widoczne struktury pęcherzowate (strzałki) i skupienia chromatyny. Pow. 10 800 ×. 20-minutowe niedokrwienie + PGI_2. Czas obserwacji 3 godz.

knowledge, we can prove that PGI_2 affects early ischemic changes by preventing ultrastructural cytoplasmic changes in neurons and neuroglial cells (Figs. 2, 3). These data indicate that therapeutic administration of PGI_2 can greatly enhance the recovery of nerve cells function after ischemia (Fig. 1) (Pluta 1985). It seems that there is a direct causal relation between the early effects of PGI_2 on the ultrastructure of the neuronal and neuroglial cytoplasm and the final effect of this treatment, the facilitation of postischemic bioelectric recovery and metabolism.

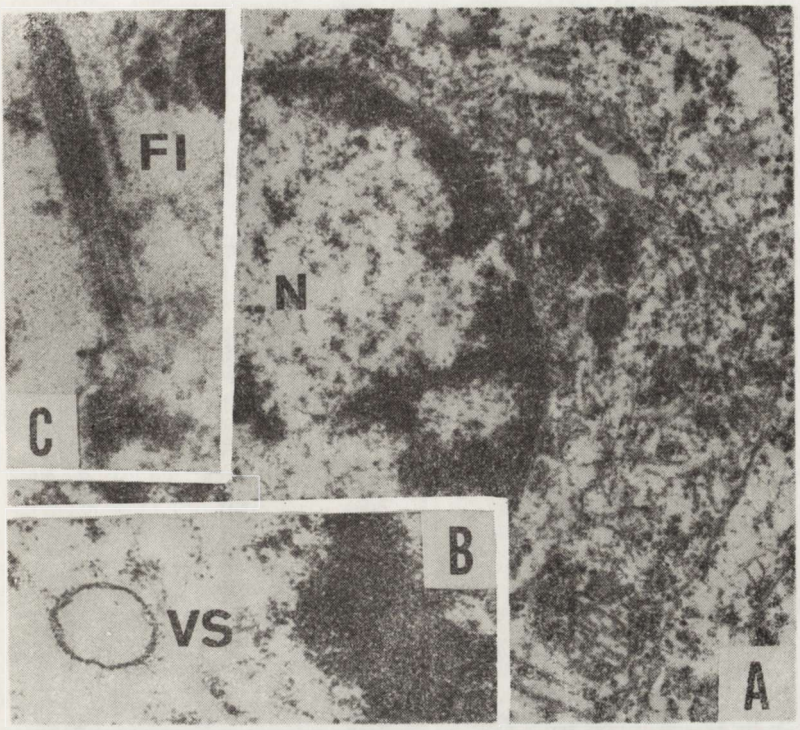

Fig. 3. Astrocyte (occipital cortex). The cytoplasmic organelles are well preserved. Electron-lucent karyoplasm (N) with clumping and marginal shift of chromatin. × 10 800. A — Intranuclear filamentous inclusion (FI). × 90 000. B — Intranuclear vesicular structure (VS). × 45 000. 20 min ischemia + PGI_2; time of observation 6 h

Ryc. 3. Astrocyt (kora potyliczna). Dobrze zachowane struktury cytoplazmatyczne. Elektronowo jasna karioplazma (N) ze skupieniami i brzeżnym przemieszczeniem chromatyny. Pow. 10 800 ×. A — śródjądrowy wtręt filamentarny (FI). Pow. 90 000 ×. B — śródjądrowa struktura pęcherzowata (VS). Pow. 45 000 ×. 20-minutowe niedokrwienie + PGI_2. Czas obserwacji 6 godz.

PGI_2 affects directly postischemic impairment of microvascular cerebral perfusion (Hallenbeck, Furlow 1978), however, it is not the only mechanism which might be responsible for the early therapeutic effect of PGI_2 in cases with ischemic stroke. PGI_2 also has a disaggregatory (Gryglewski et al. 1976) action on platelet thrombi and it inhibits the platelet release reaction. Fibrinolytic activity of PGI_2 (Dembińska-Kieć et al. 1982) and its protective effect on the blood-brain barrier (Pluta et al. 1990) also might be of importance. The influence of PGI_2 on platelet-vascular interactions could explain this early clinical phenomenon. Platelets delay healing of vascular endothelium at the site of vascular damage during recirculation. PGI_2, by dispersing platelet clumps stuck at the damaged site, and by protecting endothelial structures (Vane 1983), could promote healing of the endothelium. Since this positive effect of PGI_2 was observed also in the platelet-free systems and seemed to be independent of vessel vasodilation, it seems to indicate that a direct

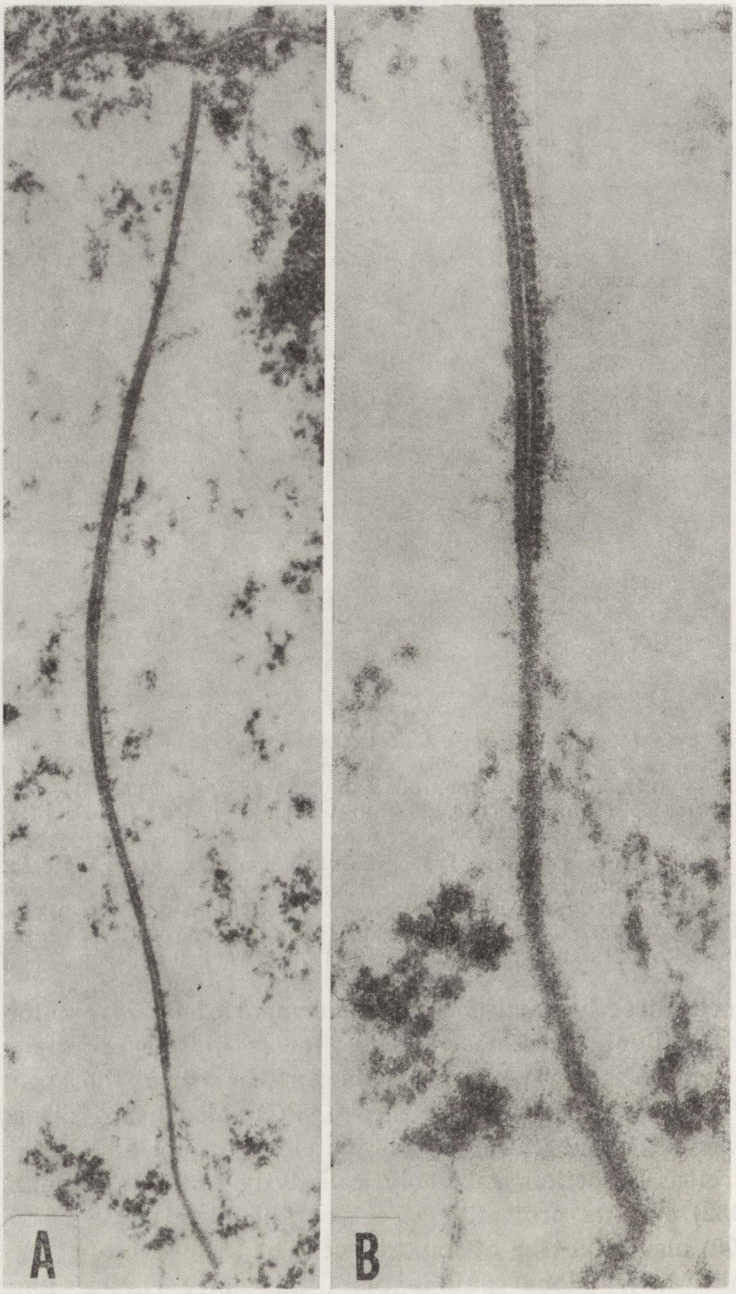

Fig. 4. Neuronal nucleus. Intranuclear filamentous inclusion. A — × 27 000. B — × 90 000. Occipital cortex. 20 min ischemia + PGI_2; time of observation 6 h

Ryc. 4. Jądro komórki nerwowej. Śródjądrowa filamentarna inkluzja. A — pow. 27 000 ×. B — pow. 90 000 ×. Kora potyliczna. 20-minutowe niedokrwienie + PGI_2. Czas obserwacji 6 godz.

"cytoprotective" or "membrane-stabilizing" action of PGI_2 might be partly responsible for the cell protection (Ogletree, Lefer 1978; Ogletree et al. 1979; Araki, Lefer 1980). In this way, the vicious circle evoking ischemic changes in the cytoplasm would be broken temporalily, but this is not sufficient to stop nuclear damages (clumping and marginal shift of chromatin, and formation of vesicular structures and intranuclear inclusions) (Figs. 2, 3, 4). These damages are accelerated with time from the end of ischemia and depict the progressive destruction of the neuronal, neuroglial and adrenal cells nuclei (reduced volume of the karyoplasm), suggest that they may cause severe functional and metabolic disturbances in the cell. It may be hypothesized that structural damages in nuclei of this nature can cause secondary metabolic disturbances (without relation with hypoperfusion or brain edema — condensed chromatin fibrils (Figs. 2, 3) are inactive — this resulting in an impairment of synthesis and transport of RNA to the cytoplasm) in the whole cell which further lead to an arrest of the function of the nucleus and next the cytoplasm, and result in death of the neurons, neuroglial and adrenal cells. In this situation nuclear damages (Figs. 2, 3, 4) (nuclear necrosis) may be responsible for the lack of effect or disappearance of early beneficial effect of treatment with PGI_2 (Huczyński et al. 1985).

In summary, this study on the therapeutic effects of PGI_2 in ischemic brain disease, is not sufficient, although conclusive. Firstly these data concern the possible mechanisms of ischemic irreversible injury. Neuronal and neuroglial survival after ischemia untreated and treated with PGI_2 seems to be restricted by a nuclear abnormal function. It is thus attractive to hypothesize that disturbed nuclear normal activity or lack of its function mediate postischemic late irreversible cell damage. It seems that PGI_2 might not be a drug of choice for permanent treatment of acute ischemic stroke. It would be unrealistic to expect that a single type of treatment would be fully and durably beneficial in cases with ischemic insult, as various different ethiopathological factors are involved in the development of stroke, and therapy with PGI_2 may not be a causative treatment for all of them. If the protective action of PGI_2 is limited to the neuronal and neuroglial cytoplasm (Figs. 2, 3), adequate postinfarction therapy has consequently, to await further pharmaceutical and pharmacological research.

DOŚWIADCZALNE LECZENIE PROSTACYKLINĄ CAŁKOWITEGO NIEDOKRWIENIA MÓZGU U KRÓLIKA — NOWE DANE

Streszczenie

Na podstawie własnych prac doświadczalnych skonfrontowanych z danymi piśmiennictwa, dotyczącymi klinicznego i doświadczalnego zastosowania prosta-

cykliny, autor omawia wpływ prostacykliny na niedokrwienne zaburzenia czynności i uszkodzenia strukturalne mózgu. Autor zwraca uwagę na korzystne działanie leku w stosunku do wczesnych strukturalno-czynnościowych, niedokrwiennych zaburzeń mózgu i jego brak wobec następstw odległych. Podkreśla, iż zjawisko to wiąże się z brakiem oddziaływania prostacykliny na uszkodzenia jąder komórek nerwowych i glejowych, które w dalszej ewolucji prowadzą zapewne do nieodwracalnych zmian populacji komórkowej wraz z ich czynnościowymi następstwami.

REFERENCES

1. Araki H., Lefer A. M.: Role of prostacyclin in the preservation of ischemic myocardial tissue in the perfused cat heart. Circ Res, 1980, 47, 757-763.
2. Dembińska-Kieć A., Kostka-Trąbka E., Gryglewski R. J.: Effect of prostacyclin on fibrinolytic activity in patients with arteriosclerosis obliterans. Thromb Haemostas, 1982, 47, 190-196.
3. Dougherty J. H. Jr., Levy D. E., Weksler B. B.: Experimental cerebral ischemia produces platelet aggregates. Neurology, 1979, 29, 1460-1465.
4. Gaudet R. J., Levine L.: Transient cerebral ischemia and brain prostaglandins. Biochem Biophys Res Comm, 1979, 86, 893-901.
5. Gryglewski R. J., Bunting S., Moncada S., Flower R. J., Vane J. R.: Arterial walls are protected against deposition of platelet thrombi by a substance (prostaglandin X) which they make from prostaglandin endoperoxides. Prostaglandins, 1976, 12, 685-713.
6. Gryglewski R. J., Dembińska-Kieć A., Żmuda A., Gryglewska T.: Prostacyclin and thromboxane A_2 biosynthesis capacities of heart, arteries and platelets at various stages of experimental atherosclerosis in rabbits. Atherosclerosis, 1978, 31, 385-394.
7. Hallenbeck J. M., Furlow T. W.: Prostaglandin I_2 and indomethacin prevent impairment of post-ischemic brain reperfusion in the dog. Stroke, 1979, 10, 629-637.
8. Hart M. N., Sokoll M. D., Davies L. R., Henriquez E.: Vascular spasm in cat cerebral cortex following ischemia. Stroke, 1978, 9, 52-57.
9. Huczyński J., Kostka-Trąbka E., Sotowska W., Bieroń K., Grodzieńska L., Dembińska-Kieć A., Pykosz-Mazur E., Peczak E., Gryglewski R. J.: Double-blind controlled trial of the therapeutic effects of prostacyclin in patients with completed ischemic stroke. Stroke, 1985, 16, 810-814.
10. Jarman D. A., DuBoulay G. H., Kendall B., Boulin D. J.: Responses of baboon cerebral and extracerebral arteries to prostacyclin and prostaglandin endoperoxcide *in vitro* and *in vivo*. J Neurol Neurosurg Psychiat, 1979, 42, 677-686.
11. Kerckhoff van den W., Hossmann K. A., Hossmann V.: No effect of prostacyclin on blood flow, regulation of blood flow and blood coagulation following global cerebral ischemia, Stroke, 1983, 14, 724-730.
12. Moncada S., Higgs E. A., Vane J. R.: Human arterial and venous tissues generate prostacyclin (prostaglandin X) a potent inhibitor of platelet aggregation. Lancet, 1977, 1, 18-21.
13. Moncada S., Korbut R., Bunting S., Vane J. R.: Prostacyclin is a circulating hormone. Nature, 1978, 273, 267-268.
14. Ogletree M. L., Lefer A. M.: Prostaglandin-induced preservation of the ischemic myocardium. Circ Res, 1978, 42, 218-224.
15. Ogletree M. L., Lefer A. M., Smith J. B., Nicolaou K. C.: Studies on the protective effect of prostacyclin in acute myocardial ischemia. Eur J Pharmacol, 1979, 56, 95-103.

16. Pluta R.: Influence of prostacyclin on early morphological changes in the rabbit brain after complete 20 min ischemia. J Neurol Sci, 1985, 70, 305-316.
17. Pluta R.: Resuscitation of the rabbit brain after acute complete ischemia lasting up to one hour: Pathophysiological and pathomorphological observations. Resuscitation, 1987, 15, 267-287.
18. Pluta R., Tomida S., Ikeda J., Nowak T. S. Jr., Klatzo I.: Cerebral vascular volume after repeated ischemic insults in gerbil: Comparison with changes in CBF and brain edema. J Cereb Blood Flow Metab, 1989, 9, 163-170.
19. Pluta R., Salińska E., Łazarewicz J. W.: Prostacyclin reduces early ischemic changes in central nervous system. Acta Neurobiol Exp. 1990, 50 (in press).
20. Radomski M., Moncada S.: An improved method for washing of human platelets with prostacyclin. Thromb Res, 1983, 30, 383-389.
21. Uchida Y., Murao S.: Role of prostaglandin I_2 and thromboxane A_2 in recurring reduction of carotid and cerebral blood flow in dogs. Stroke, 1981, 12, 786-792.
22. Vane J. R.: Prostaglandins and the cardiovascular system. Br Heart J, 1983, 49, 405-409.

Author's address: Department of Neuropathology, Medical Research Centre, Polish Academy of Sciences, 3, Dworkowa Str., 00-784 Warsaw, Poland.

NEUROPAT. POL. 1990, 28, 3-4
PL ISSN 0028-3894

MILENA LAURE-KAMIONOWSKA, MARIA DĄMBSKA,
STANISŁAW KRAJEWSKI

LATE CHANGES IN CEREBRAL HEMISPHERES AFTER PERINATAL ANOXIC DAMAGE

Laboratory of Developmental Neuropathology, Medical Research Centre,
Polish Academy of Sciences, Warsaw, Poland

Clinical investigations of infants who survived asphyxia or other types of perinatal hypoxia, performed with the use of ultrasonography, computerized tomography or magnetic resonance imaging of their brains, directed our attention to the bilateral lesions of hemispheric white matter (Saia et al. 1989). This topography of changes was reported in children who developed cerebral palsy, mostly of the spastic diplegia type (Dekaban 1959).

The brains of children with this syndrome are seldom available for neuropathological investigations. In our previous paper we tried to correlate the perinatal white matter lesions with the changes found in cases with longer survival (Dąmbska et al. 1989). In the present paper we would like to respect the features of structure and topography of cerebral lesions in the brains of children with diplegic type of cerebral palsy.

MATERIAL AND METHODS

Five children were studied with clinical symptoms of psycho-motor retardation, tone-posture abnormalities, and with the features of brain atrophy in the neuropathological macroscopic examination.

Brain sections were examined on the slides passing through five levels of the cerebral hemispheres, cerebellum and brain stem. Cresyl violet, hematoxylin-eosin, luxol fast blue, Kanzler-Arendt methods of staining were applied. The number of astrocytes was quantitatively analysed. It was done on sections from the atrophic frontal lobes. The number of astrocytes in the white matter was evaluated with the aid of immunohistochemical reaction for glial fibrillary acidic protein (GFAP). GFAP-

Paper presented at Symposium on Neurobiology of Cerebral Ischemia and Hypoxia. Poznań, June 29-July 1, 1989.

-positive cells were counted according to the method of Takashima and Becker (1983), in the subcortical, intermediate and deep white matter. The number of GFAP-positive glial cells was compared to age-matched controls elaborated by Takashima and Becker (1983).

RESULTS

The clinical and the neuropathological observations are summarized in Table 1.

Table 1. Clinical and neuropathological data

Number case age	Clinical data	Neuropathological examination				
		Cerebral cortex lesions	Cerebral white matter lesions			
			atrophy	reactive gliosis GFAP	fibrillary gliosis K—A	demyelination
1 33/86 6 months	Normal pregnancy, full-term delivery. Weak respiratory movements and defective sucking since birth. Delay of developmental milestones. Laryngeal spasm. Bronchopneumonia	—	+	+	+	—
2 14/88 7 months	Normal pregnancy, spontaneous full-term delivery. Apgar score 7, weight 3600 g. Frequent cyanotic attacks during the first day of life. Microcephaly, head circumference 40 cm. Retarded psychomotor development. Bilateral spastic type of weakness and epilepsy.	++	+	+++	+	—
3 470/81 10 months	Perinatal brain damage. Frequent seizures. Failure to thrive.	+	+	+	++	—
4 49/86 18 months	Perinatal brain damage. Infantile spasm. Epileptic attacks, Spasticity. Bronchopneumonia	+	+	++	++	—
5 37/84 6 years	Normal pregnancy, induced labor — vacuum extractor. Apgar score 2, Psychomotor retardation. Since fourth month of life epileptic attacks — infantile spasms. Spastic quadriparesis.	+	+	++	+++	+

+ present; + normal number of GFAP-positive cells; ++ increased number; +++ intensity of fibrillary gliosis; — lack of demyelination; + slight, ++ moderate, +++ intensive.

There were 3 females and 2 males. Their ages ranged from 6 months to six years. Pregnancy was uneventful in all and delivery was normal in four of them. During the neonatal period two had frequent seizures, one had respiratory difficulties, and vomiting and defective sucking were noted in others. The neurologic features of each case revealed a delay of psychomotor development. Features of spasticity in the younger cases and an evident spastic tetraplegia in the oldest one were observed. Recurrent seizures were recorded in 4 cases.

The neuropathological gross examination demonstrated brain atrophy in all cases, particularly frontal lobes had narrowed convolutions and sparse white matter. In the fifth case diffuse atrophy of all white matter of cerebral hemispheres was evident. The lateral ventricles were enlarged. The brain weight was low in one case, in two normal, in others no data were available.

Microscopical examination confirmed the topography of the grossly observed lesions.

The gray structures revealed moderate lesions while the white matter damage was more pronounced. There were no abnormalities in the appearance of the cerebral cytoarchitecture. Recent neuronal changes attributable to terminal respiratory complications were frequent. The first case showed minimal cortical lesions, in two others moderate neuronal loss was seen. Case 5 showed severe neuronal damage without glial reaction. There were few GFAP-positive glial cells in the cerebral cortex, except the molecular layer under the pia. The second case showed scattered neuronal loss in the depth of sulci with evident GFAP-positive glial cell reaction in all the cortical layers. The hippocampus was normal in all cases except case 5 in which some loss of cells in the Sommer sector was found. The cerebellar cortex did not present evident lesions. Only in case 5 cerebellar cortex revealed great loss of Purkinje cells with proliferation of Bergmann's glia. Other gray structure lesions were unremarkable in all cases.

The white matter was affected in all cases but to a different degree.

Case 1 demonstrated paucity of the white matter in the frontal lobe, especially the superior frontal gyrus. The white matter revealed edema and rarefacted tissue with hypertrophied astrocytes. The Kanzler-Arendt staining was slightly positive around the vessels in the center of cortical convolutions. GFAP-positive cells were localized also around the vessels (Fig. 1). In cases 2, 3, and 4 the sparseness of frontal white matter was more pronounced. In the periventricular white matter small perivascular cavities surrounded by more advanced gliosis were seen. Diffuse gliosis was also present in the subcortical white matter. The fibrillary gliosis was demonstrated by Kanzler-Arendt staining in the subcortical white matter (Fig. 2). Star- and bouqet-shaped GFAP-positive cells were scattered in the white matter and around the vessels (Fig. 3). Myelination

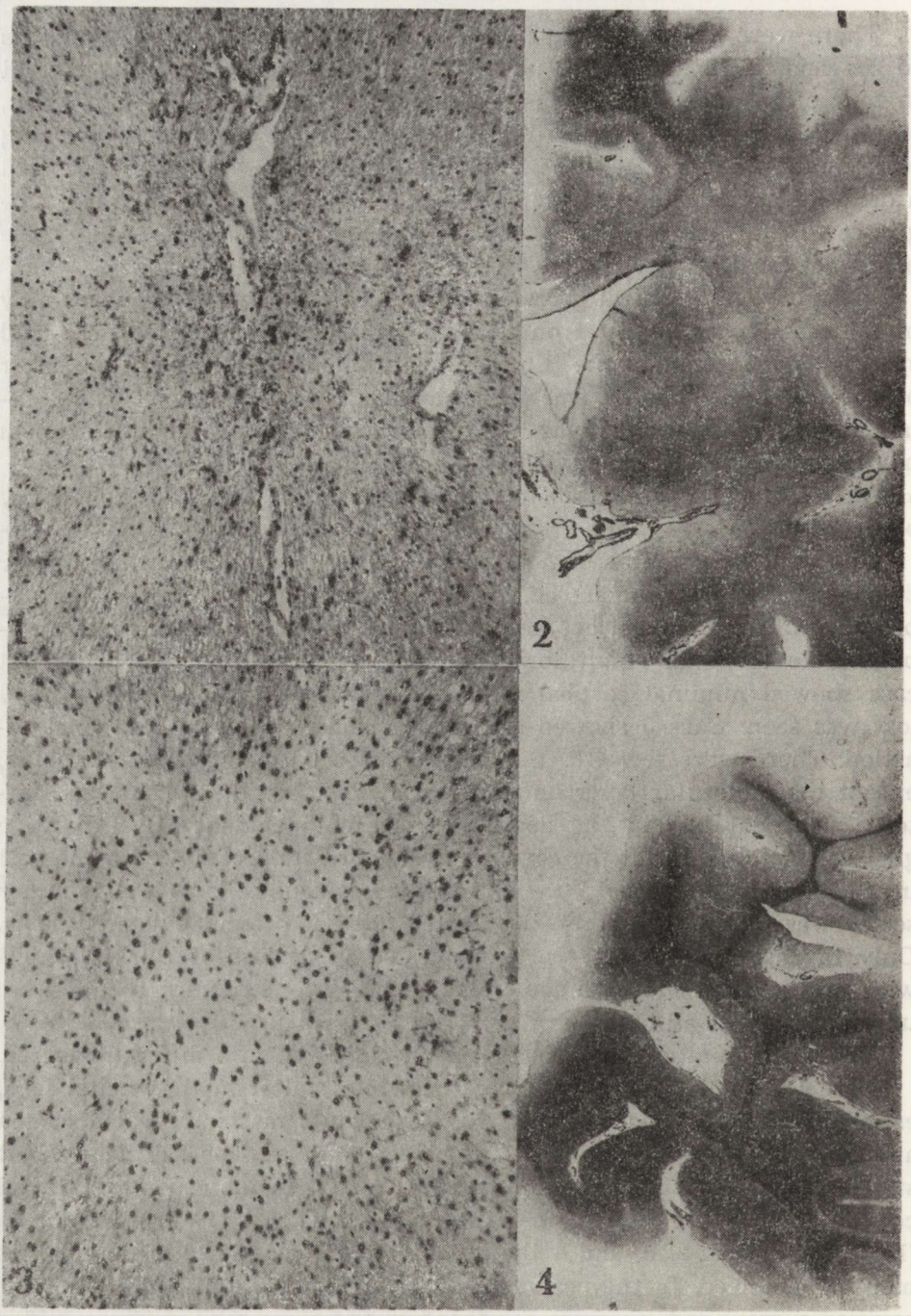

Fig. 1. Case 1. GFAP-positive cells around the vessels. × 60

Ryc. 1. Przypadek 1. Komórki GFAP-dodatnie wokół naczyń. Pow. 60 ×

Fig. 2. Case 2. Fibrillary gliosis in the superior frontal gyrus. Kanzler-Arendt. Magn. glass

Ryc. 2. Przypadek 2. Glejoza włóknista w zakręcie czołowym górnym. Kanzler-Arendt. Pow. lupowe

showed no impairment. In case 5 with the longest survival, the white matter was most severly damaged. Atrophy of the white matter was diffuse, mainly in the periventricular area and the center of convolutions. Periventricular cavities with macrophages were surrounded by thick glial wall. Dense fibrillary network spread around the cavities and in the axis of convolutions (Fig. 4). Star-shaped GFAP-positive cells were localized mainly in the subcortical white matter, under the depth of sulci. In the old necrotic foci there were GFAP positive astrocytes with cytoplasm that was less prominent than in the surrounding glia. The paucity of myelin was mostly periventricular and in the center of several cortical convolutions. Quantitative evaluation of GFAP-positive cells in frontal lobe white matter as compared to controls is shown on Fig. 5.

In the control cases adapted from Takashima and Becker (1983) GFAP-positive cells showed a transient increase in the cerebral white matter during the postnatal period. With the age these glial cells shift from the depth to the subcortical white matter. In our material the number of both boquet- and star-shaped GFAP-positive glia was high in 3 cases. A distinct increase in the number of glial cells was seen in case 2 in all the white matter zones, most pronounced in the subcortical zone. An increased number of GFAP-positive glia was also present in two other cases. Case 4 demonstrated increased number of cells in all white matter zones. In case 5 glial reaction was prominent only in the subcortical white matter.

DISCUSSION

This group of cases with perinatal asphyxia in anamnesis and cerebral palsy showed the predominance of the white matter changes. The hemispheric white matter lesions were more severe than in the gray structures. The outstanding neuropathological feature of all cases was the enlargement of ventricular system, dilatation of lateral ventricles, atrophy of cerebral hemispheres particularly frontal lobes and sparseness of the white matter most conspicuous in the semiovale centrum and involving the axis of cerebral convolutions. In the case with the longest survival small cavities surrounded by dense fibrillary gliosis were seen in the periventricular and subcortical white matter. They may be regarded as the late sequellae of the periventricular white matter infarcts

Fig. 3. Case 2. Increased GFAP-positive glia localized in the subcortical white matter. × 60

Ryc. 3. Przypadek 2. Zwiększona liczba GFAP-dodatnich komórek w podkorowej istocie białej. Pow. 60 ×

Fig. 4. Case 5. Diffuse atrophy of the white matter with intensive fibrillary gliosis. Kanzler-Arendt. Magn. glass

Ryc. 4. Przypadek 5. Zanik istoty białej z intensywną glejozą włóknistą. Kanzler-Arendt. Pow. lupowe

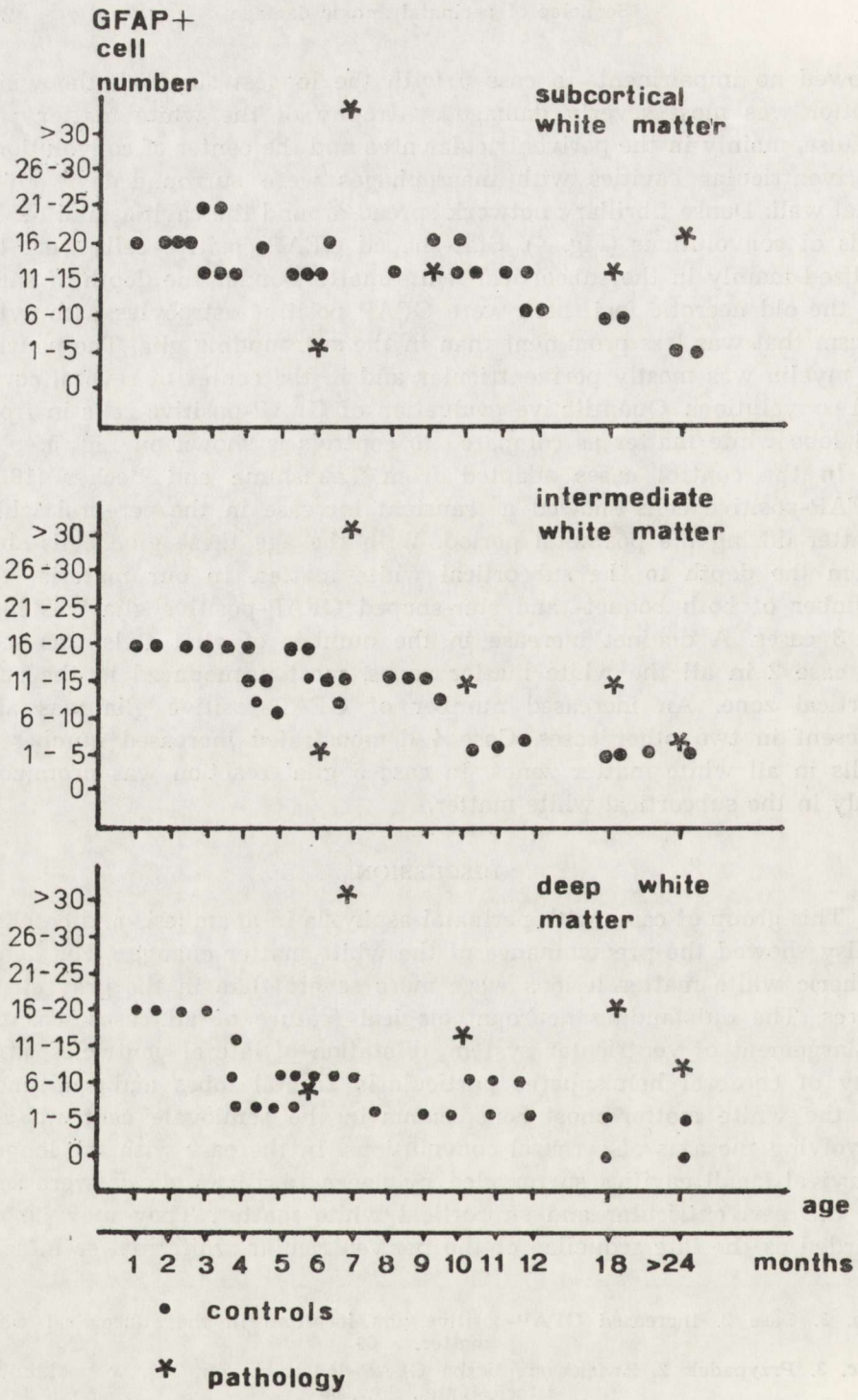

Fig. 5. Comparison of the number of GFAP-positive cells in the cerebral white matter between the cases after perinatal anoxic damage and controls. Control cases adapted from Takashima and Becker (1983)

Ryc. 5. Porównanie liczby komórek GFAP-dodatnich w istocie białej półkul w przypadkach po przebytym niedotlenieniu okołoporodowym i kontrolnych. Przypadki kontrolne wg Takashima i Beckera (1983)

or of severe edematous changes. Such lesions are similar to those reported by Feigin and Budzilowich (1978) as the result of subcortical edema. The pathologic gradient of perinatal white matter changes from classical periventricular ischemic infarcts, periventricular colliquative necrosis, through diffuse white matter damage as a background of late white matter lesions was demonstrated previously by Dąmbska et al. (1989).

The neuropathological particularity of the observed changes in the white matter was Kanzler-Arendt's positive fibrillary changes exceeding the myelin lesions and GFAP-positive reaction. The intensity of fibrillary gliosis in Kanzler-Arendt staining increased with survival. The production of glial fibrils demonstrable in Holzer preparations, persists into adulthood following neonatal lesions (Gilles 1983).

Increased production of glial filaments showed in GFAP method characterizes both the normal maturation of astrocytes and their response to various pathological conditions in the central nervous system.

The increase of GFAP-positive glia shifted with age from the deep to the superficial layers of the cerebral white matter (Takashima, Becker 1983). This shift may be related to the regions of susceptibility for noxious agent. The reactive increase of GFAP-positive cells may be induced by toxic or hypoxic insults during a time of high metabolic activity. Among our cases this reactive GFAP-positive glia proliferation which may be secondary to recent hypoxia is demonstrated in the second case. Takashima and Becker (1984) demonstrated reactive GFAP-positive response secondary to hypoxia in cases with bronchopulmonary dysplasia. Localization of GFAP-positive glial cells in the depth of sulci may indicate special vulnerability of the area under the depth of cortical sulci with impaired vascularization. It appears as triangular areas between the perforating arteries from both sides of the deep sulcus in early infancy (Takashima et al. 1978). Necroses of focal subcortical white matter and cortical neurons with compensatory proliferation of GFAP-positive glia may be produced at end zones by cerebral hypoperfusion associated with hypoxic insults in our second case. In the other cases the number of GFAP-positive cells was normal or slightly increased. Miller et al. (1986) observed that reactive "hyperplasia" of astrocytes is reversible. Miyake et al. (1988) did not report an increased number of astrocytes in an atrophic adult human brain. Our material suggests that the structure of the white matter lesions alters with the time of survival. Reactive gliosis demonstrated by GFAP-positive cells proliferation may be considered as a recent response of the nervous tissue to the noxious agent. The network of glial fibrils demonstrated by Kanzler-Arendt method is like the final residual appearance of longlasting gliosis.

ODLEGŁE ZMIANY W PÓŁKULACH MÓZGU PO USZKODZENIU OKOŁOPORODOWYM

Streszczenie

Celem pracy było prześledzenie topografii i struktury odległych zmian w istocie białej półkul mózgu będących następstwem okołoporodowego niedotlenienia. Praca dotyczy 5 przypadków dzieci w wieku od 6 miesięcy do 6 lat z niedorozwojem psychoruchowym, dwustronnym porażeniem spastycznym kończyn. W sekcyjnym badaniu mózgu były widoczne cechy zaniku istoty białej półkul. W obrazie neuropatologicznym uszkodzenie istoty białej dominowało nad zmianami w innych strukturach. Widoczny był zanik istoty białej, zwłaszcza płata czołowego, z poszerzeniem układu komorowego, a w najstarszym przypadku z obecnością jam. W celu zobiektywizowania reakcji glejowej zmieniającej się z wiekiem policzono komórki glejowe GFAP-dodatnie. Reaktywna glejoza uwidoczniająca się pomnożeniem liczby komórek GFAP-dodatnich widoczna była u dzieci młodszych i może być uważana za bezpośrednią odpowiedź na działający czynnik szkodliwy. Glejoza włóknista narastała z czasem przeżycia dzieci, od okołonaczyniowej do sieci obejmującej całą istotę białą zarówno okołokomorową, jak i w osi zawojów. Należy ją uznać za zejściowy stan długotrwającego procesu przerostu gleju.

REFERENCES

1. Dąmbska M., Laure-Kamionowska M., Schmidt-Sidor B.: Early and late neuropathological changes in perinatal white matter damage. J Child Neurol, 1989, 4, 291.
2. Dekaban A.: Neurology of infancy. Williams and Wilkins Comp., Baltimore, pp. 217-221.
3. Feigin I., Budzilowich G. N.: Laminar scars in cerebral white matter: a perinatal injury due to oedema. J Neuropathol Exp Neurol, 1978, 37, 314-325.
4. Gilles F. H.: Neuronal damage: inconstancy during gestation. In: The developing human brain. Eds.: F. H. Gilles, A. Leviton, E. Dooling. J. Wright, PSG Inc., Boston, Bristol, London, 1983, p. 243.
5. Miller R. H., Abney E. R., Davis S., Lindsay R., Patel R., Stone J., Raff M. C.: Is reactive gliosis a property of a distinct subpopulation of astrocytes? J Neurosci, 1986, 6, 22-29.
6. Miyake T., Kitamura T., Takamatsu T., Fujita S.: A quantitative analysis of human astrocytosis. Acta Neuropathol (Berl), 1988, 75, 535-537.
7. Saia O. S., Vozzi A., Fiore A., Griffith P., Angonese I., Zorzi C., Cantarutti F.: Periventricular leukomalacia: ultrasound diagnosis and follow-up. Abstract. Annual Meeting of European Society for Pediatric Research, Krakow, 1989.
8. Takashima S., Armstrong D., Becker L.: Subcortical leukomalacia Relationship to development of the cerebral sulcus and its vascular supply. Arch Neurol, 1978, 35, 470-472.
9. Takashima S., Becker L.: Developmental changes of glial fibrillary acidic protein in cerebral white matter. Arch Neurol, 1983, 40, 14-18.
10. Takashima S., Becker L.: Developmental neuropathology in bronchopulmonary dysplasia: alteration of glial fibrillary acidic protein and myelination. Brain and Development, 1984, 5, 451-457.

Authors' address: Laboratory of Developmental Neuropathology, Medical Research Centre, Polish Academy of Sciences, 3 Pasteura Str., 02-093, Warsaw, Poland.

NEUROPAT. POL. 1990, 28, 3-4
PL ISSN 0028-3894

PETER von BOSSANYI, KNUT DIETZMANN

INFANTILE BRAIN DAMAGE DUE TO HYPOXIA WITH SPECIAL REFERENCE TO FORMATION OF DENDRITIC SPINES

Institute of Morbid Anatomy, School of Medicine, Division of Neuropathology, Magdeburg

Many attempts have been made to correlate impaired brain functions such as mental retardation with various structural abnormalities (Vestergaard 1949; Penrose 1963; Jellinger 1972; Christensen, Vestergaard 1975; Shaw 1987). At present the most important causes of brain damage in the newborn are subependymal plate hemorrhages and hypoxic damages, which themselves are often ischemic, referred to subsequently as HID (Hypoxic-Ischemic Disease). A wide pattern of different structural disturbances due to HID has been described in the literature. We wish to give a rough review of this in the following:

Types of neuropathological lesions due to HID

1. Major lesions:
   sclerotic gyri,
   focal subcortical cystic lesions,
   multilocular cystic alterations,
   paraventricular softening,
   hydranencephaly,
   état marbré (*status marmoratus*).
2. Minor lesions:
   patchy loss of neurons and mild degree of gliosis,
   no anatomical lesions.

The impaired function can be correlated to major lesions of brain, but there exist patients who show profound mental retardation without any detectable anatomic abnormalities at the level of light microscopy.

Paper presented at Symposium on Neurobiology of Cerebral Ischemia and Hypoxia. Poznań, June 29-July 1, 1989.

The paper presented here intends to focus attention on the minor lesions.

Only a few quantitative analyses of dendritic spines could be found in the literature concerning human brain. Several of these studies pointed out changes in the morphology and number of dendritic spines as a correlation of aging and psychiatric diseases. Therefore the present quantitative Golgi study was undertaken to establish whether changes in the number and distribution of spines exist in deceased patients with severe mental retardation following HID.

MATERIAL AND METHODS

Specimens from area 10 of the frontal cortex were taken from nine children and adolescents of both sexes with infantile hypoxic brain damage, aged 6 to 25 years, and processed according to the Golgi-Kopsch procedure. For comparison samples from seven non-neuropsychiatric patients of age ranging between 6 to 26 years were examined in the same manner. Twenty pyramidal neurons of the lamina V from each hemisphere were examined. All visible dendritic spines on the apical dendrite were counted on consecutive segments, each 50 micrometers long. The spine density, identical with the number of spines per one micrometer of the dendrite resulted from the quotient of the total number of spines divided by the length of the apical dendrite.

RESULTS

Figure 1 shows details of the middle segments of the apical dendrites. A lower number of spines and predomination of stubby spines are findings stressed in children with infantile brain damage. Marked protrusions could be a hint for degenerative processes. The middle parts of the apical dendrite from affected adolescents (Fig. 2b) show similar changes. In comparison with control persons short and thin spines prevail in these cases.

Otherwise one can see a remarkable reduction or lack of spines in cases of infantile brain damage. The diagram (Fig. 3) reveals spine density, number of spines and the length of apical dendrite in brains with infantile damages. Brackets denote cases in which no significant differences could be found by means of the H-test. There were significant differences between all cases respectively the factor spines per apical dendrite (AD). The spine density did not indicate such considerable results, several cases, however, differ from each other. A good correlation could be found between spines per AD and length of this dendrite. The spine densities also correlate to spine numbers. Hence it can be concluded that the different spine densities result from variable spines on apical dendrite.

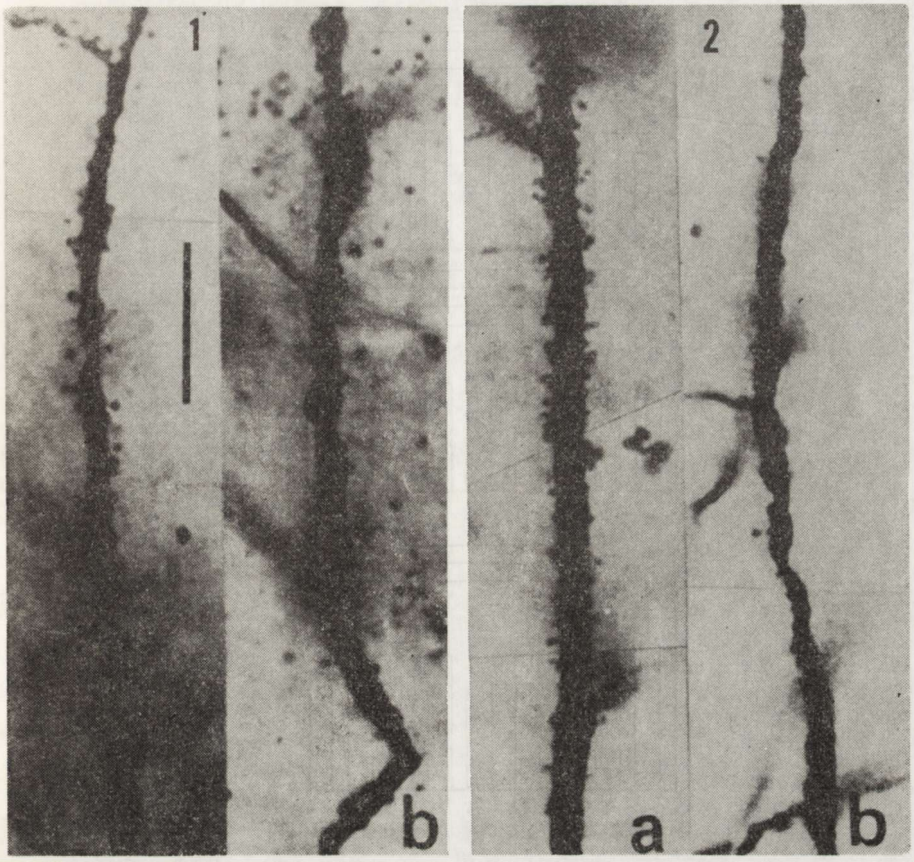

Fig. 1. Details from middle segments of apical dendrites of layer V pyramidal neurons (area 10). Golgi-Kopsch impregnation. Bar = 20 μm. *a* — child aged 9 years, *b* — child with infantile damage aged 11 years

Ryc. 1. Środkowy odcinek dendrytów wierzchołkowych neuronów piramidowych V warstwy (pole 10). Impregnacja wg Golgi-Kopscha. Kreska = 20 μm. *a* — dziecko lat 9, *b* — dziecko lat 11, z dziecięcym uszkodzeniem mózgu

Fig. 2. Details from middle parts of apical dendrite of layer V pyramidal neurons (area 10). Golgi-Kopsch impregnation. Bar = 20 μm. *a* — normal adolescent aged 18 years, *b* — adolescent with infantile brain damage aged 17 years

Ryc. 2. Środkowy odcinek dendrytów wierzchołkowych neuronów piramidowych V warstwy (pole 10). Impregnacja wg Golgi-Kopscha. Kreska = 20 μm. *a* — normalny osobnik 18-letni, *b* — osobnik w wieku 17 lat z dziecięcym uszkodzeniem mózgu

In the next step we averaged the survival time of children and adolescents with HID in order to prove the possibly existing changes between both groups (Fig. 4). Neither spine density nor spine number on the AD, the length of the apical dendrite as well gave considerable differences. Consequently, neither the density nor the distribution of spines allow to state a dependence on age or life span after hypoxic damages. As examined with the U-test, described by Mann and Whitney,

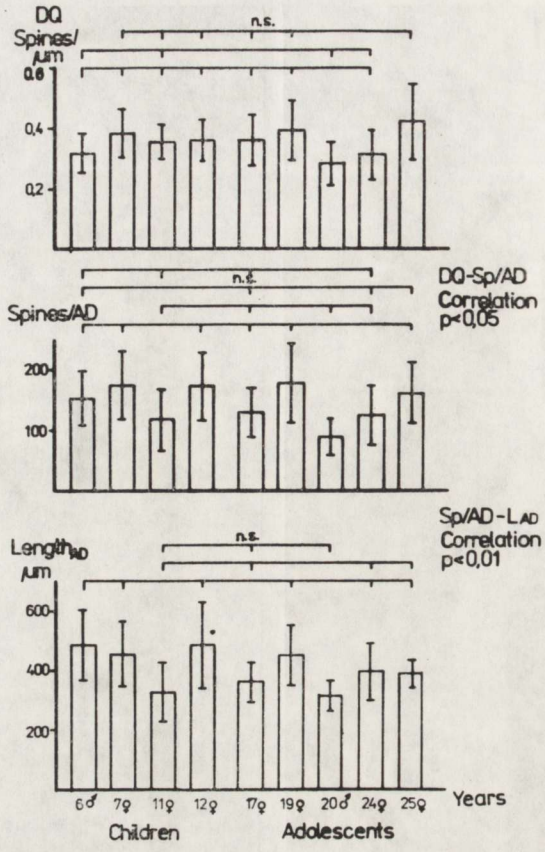

Fig. 3. Mean values ($\bar{x} \pm SD$) of spine density, number of spines and length of apical dendrite from children (< 14 years) and adolescents (> 14 years) with infantile brain damage; n.s. — not significant (H-test)

Ryc. 3. Wartości średnie ($\bar{x} \pm SD$) gęstości kolców, liczby kolców i długości dendrytów wierzchołkowych u dzieci (< 14 lat) i u młodzieży (> 14 lat) z dziecięcym uszkodzeniem mózgu; n.s. — nieznamienne (test H)

the spine density was less significant in children with prenatal hypoxic disturbances when compared with the controls. For this fact the number of spines on the AD is responsible, because the length of the evaluated dendrite is unchanged (Fig. 5). The number of spines on the AD is diminished only a little in affected adolescents. But the AD are somewhat longer, and thus there follows a significant lower spine density (about 17%).

A very interesting result in the normal control group was a decreased spine density, about 40%, and a reduction of spine numbers, about 50%, on the apical dendrite in adolescents as compared with children. Obviously, this decrease in the course of development, named spine overshoot, is similar to that previously reported in the cerebral cortex of rats and other animals.

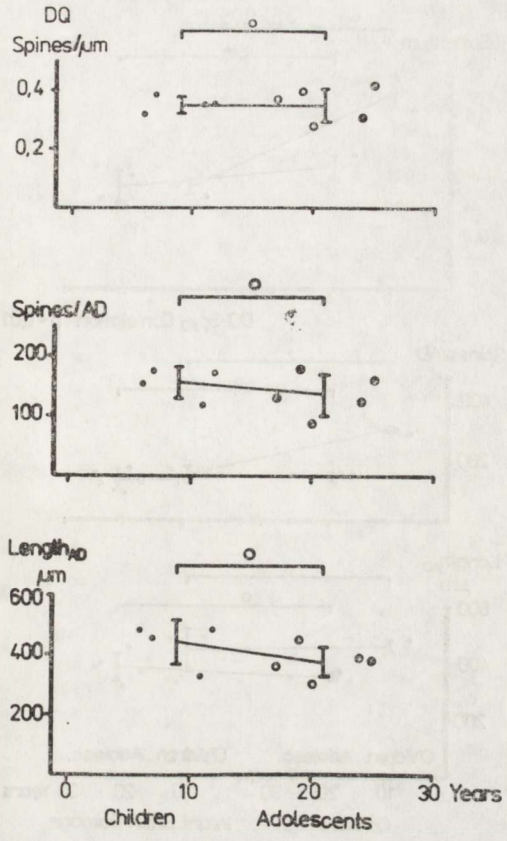

Fig. 4. Spine density, number of spines and length of apical dendrite (AD) from children (n = 4) affected as compared with adolescents (n = 5) with mental retardation due to HID. O — not significant (Mann-Whitney's U-test)

Ryc. 4. Gęstość kolców, liczba i długość dendrytów wierzchołkowych (AP) u dzieci (n = 4) z uszkodzeniem mózgu w porównaniu z młodzieżą (n = 5) z upośledzeniem umysłowym w następstwie hipoksyjno-ischemicznym uszkodzeniem mózgu w okresie wczesnodziecięcym. O — wartości nieznamienne (test U Manna-Whitneya)

The diminished number of spines characterizing infantile brain damage appears also if they were plotted on a graph as a function of the distance from the cell body (Fig. 6). We could observe the reduced number of spines, particularly in childhood, in the middle and distal segments.

DISCUSSION

The result presented here, should reveal that infantile brain damage combined with severe mental and physical retardation are associated with a decreased number of spines and abnormal spines on the apical dendrite of pyramidal neurons within layer V, investigated in area 10.

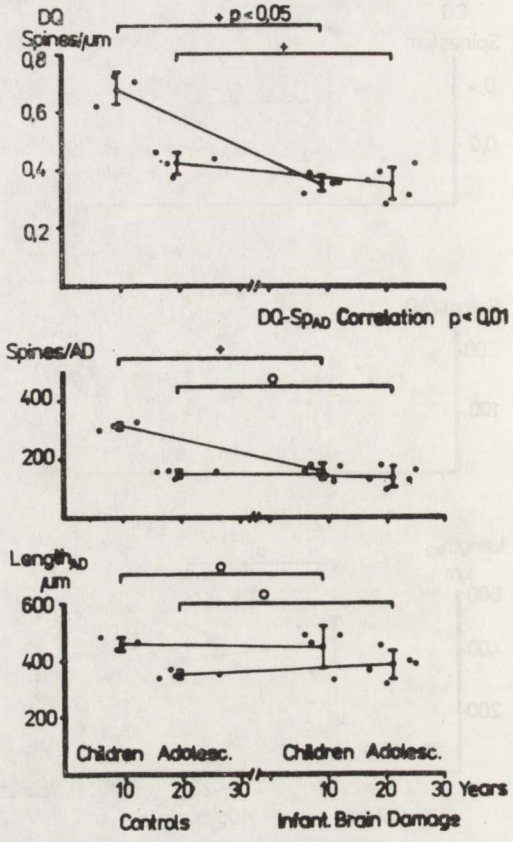

Fig. 5. Spine density, number of spines and length of apical dendrite (AD) from children and adolescents with infantile brain damage in comparison with those of the control groups. + — $p \leqslant 0.05$, O — not significant (U-test)

Ryc. 5. Gęstość kolców, liczba kolców oraz długość dendrytów wierzchołkowych (AD) u dzieci i młodzieży z uszkodzeniem mózgu we wczesnym okresie życia w porównaniu z kontrolą. + — $p \leqslant 0{,}05$, O — nieznamienne (test U)

This finding is further supported by the fact that similar observations have been made in a number of diseases in which low intellectual performance is the most common clinical symptom, such as Down's syndrome, alcoholism and Alzheimer disease. Thus, the changes observed in this study could be a morphological equivalent to mental retardation. Experimental interruption of thalamic connections to the cortex in animals resulted in reduction of dendritic spines in the middle of the apical dendrite. Provided that these facts are true also for area 10 of the human cortex, the reduced number of spines could point to a lack or loss of thalamocortical afferents as a result of brain damage.

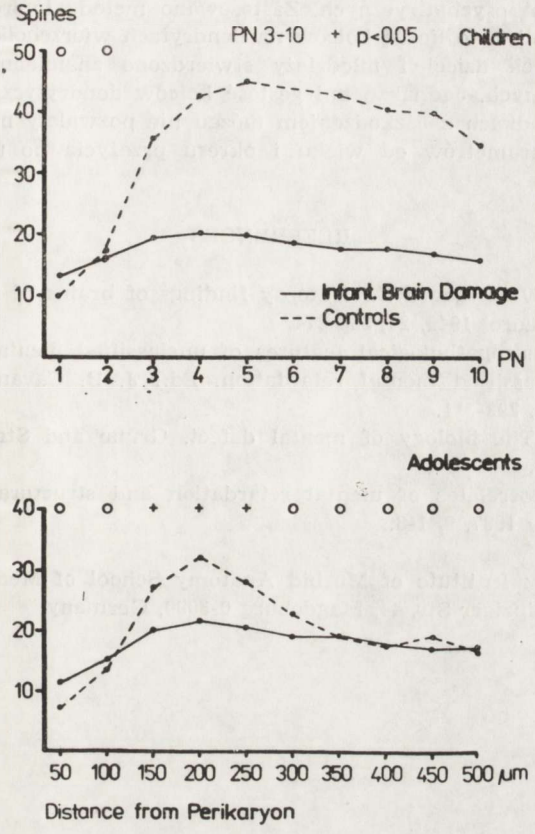

Fig. 6 Number of dendritic spines per 50 µm (PN) as a function of the distance from the cell body on apical dendrites (layer V) in affected and nonaffected children as well as adolescents. + — $p \leqslant 0.05$, O — not significant (U-test)

Ryc. 6. Liczba kolców dendrytycznych przypadająca na odcinek 50 µm PN jako funkcja odległości od ciała komórkowego u chorych i zdrowych dzieci i młodzieży. + — $p \leqslant 0,05$, O — nieznamienne (test U)

WCZESNODZIECIĘCE USZKODZENIA MÓZGU W NASTĘPSTWIE NIEDOKRWIENIA ZE SZCZEGÓLNYM UWZGLĘDNIENIEM TWORZENIA KOLCÓW DENDRYTYCZNYCH

Streszczenie

Badano anatomicznie drugorzędne uszkodzenia mózgu, towarzyszące głębokiemu upośledzeniu umysłowemu i fizycznemu po przebytym HID (zespół hipoksyjno-ischemiczny). Materiał stanowiły mózgi dziewięciorga dzieci i młodzieży z uszkodzeniem mózgu we wczesnym okresie życia oraz mózgi 7 osobników w tym samym

wieku bez zaburzeń psychiatrycznych. Zastosowano metodę impregnacyjną według Golgi-Kopscha i obliczano liczbę kolców na dendrytach wierzchołkowych.

U upośledzonych dzieci i młodzieży stwierdzono znamiennie niższą gęstość kolców dendrytycznych. Jednakże ani gęstość kolców dendrytycznych, ani ich dystrybucja w przypadkach z uszkodzeniem mózgu nie pozwalały na ustalenie zależności badanych parametrów od wieku i okresu przeżycia po uszkodzeniu hipoksyjnym.

REFERENCES

1. Christensen E., Vestergaard E.: Autopsy findings of brains of mental defectives. Acta Psyhiatr Neurol 1949, 24, 363-374.
2. Jellinger K.: Neuropathological features of unclassified mental retardation, In: The brain unclassified mental retardation. Ed.: J. B. Cavanagh, Livingstone, London 1972, pp. 293-311.
3. Penrose L. S.: The biology of mental defect. Grune and Stratton, New York 1963, pp. 172-174.
4. Shaw C. M.: Correlates of mental retardation and structural changes of the brain. Brain Dev 1987, 9, 1-8.

Autors' address: Institute of Morbid Anatomy School of Medicine, Division of Neuropathology, Leipziger Str. 44, Magdeburg 0-3090, Germany.

NEUROPAT. POL. 1990, 28, 3-4
PL ISSN 0028-3894

MIECZYSŁAW WENDER, ZOFIA ADAMCZEWSKA-GONCERZEWICZ,
DANUTA TALKOWSKA, JADWIGA PANKRAC

MYELIN PROTEINS IN THE LATE PERIOD AFTER MODERATE HYPOXIA

Department of Neurology, School of Medicine, Poznań, Poland

The important question is whether the physicochemical and morphological changes occurring in the myelin sheath as sequelae of noxious agents depend on factors affecting any particular component of the protein or lipid moiety of the complex multilayer structure of the myelin.

As a late effect of moderate hypoxia only minor changes in lipid chemistry of myelin have been found (Wender et al. 1989a). That is why, as the next step in the evaluation of late changes induced by moderate hypoxia in the myelin we have studied the pattern of myelin proteins.

MATERIAL AND METHODS

Experiments were performed on white Wistar rats, each weighing 200-250 g. The animals were placed for 30 min in a gaseous mixture of 7% oxygen, 92.9% nitrogen and 0.1% carbon dioxide. The experimental animals in groups of 10 each were sacrificed 14 days or 2 months after hypoxia, by decapitation in light halothane anesthesia. The heads were immediately frozen in liquid nitrogen.

Biochemical methods. The myelin was obtained by fractionation using the method of Norton and Poduslo (1973). The myelin proteins were fractionated according to Agrawal (1974) and quantitated by means of densitometry. More details of chemical methods may be found in our previous publication (Wender et al. 1989b).

Paper presented at Symposium on Neurobiology of Cerebral Ischemia and Hypoxia. Poznań, June 29-July 1, 1989.

RESULTS

Most pronounced alterations concern the high molecular weight Wolfgram protein which shows a decrease in the late period after the action of moderate hypoxia, i.e. after 14 days and 2 months. The main myelin protein Folch-Lees proteolipid and Agrawal protein decreased in the later period after the experiment (2 months after hypoxia). Both fractions of basic protein (LBP and SBP) ahowed a relative increase. The results are ilustrated in Figure 1.

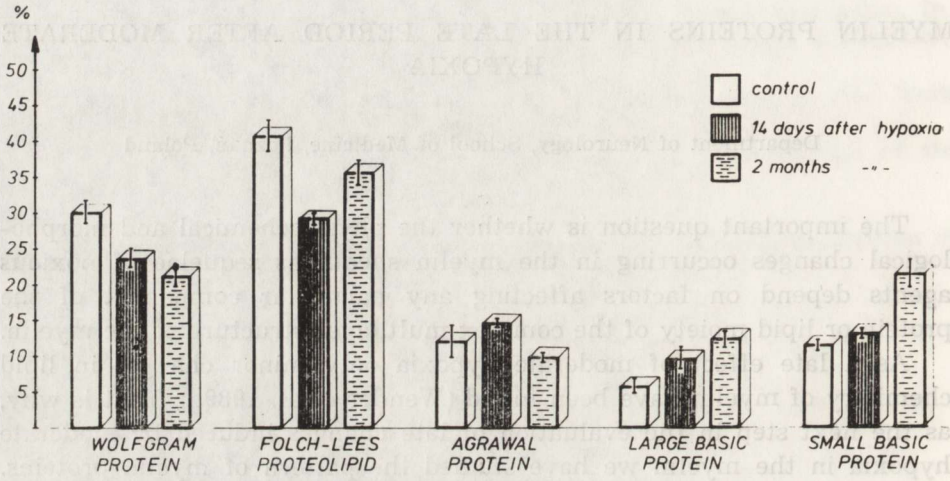

Fig. 1. Myelin proteins of the rat brain in the late period after moderate hypoxia
Ryc. 1. Białka mieliny w mózgu szczura w późnym okresie po niedotlenieniu

DISCUSSION

The pattern of late changes in myelin proteins found as a consequence of severe hypoxia was characterized by the mostly marked deviations in Wolfgram protein and in Folch-Lees proteolipid (Wender et al. 1989b). A similar pattern was found as sequela of moderate hypoxia, because among the various protein fractions Wolfgram protein happened to be most markedly affected, exhibiting a considerably lowered percentage in the late period after experimental hypoxia. The changes of both fractions of basic proteins are of minor importance being only the result of concomitant relative shifts. Norton et al. (1978) advocated the view that the degradation of basic protein by neutral proteinases, excreted by macrophages might be primarily responsible for demyelination. The fact that hypoxia does not lead to decomposition of basic proteins should be, therefore, considered as a significant factor explaining that after cerebral hypoxia demyelination only rarely occurs.

Our findings compared with those obtained in other experimental conditions (Mathieu et al. 1974; Iyoyama et al. 1980; Wender et al. 1983a, b) lead to the conclusion, that various noxious agents affect different proteins, and changes in the myelin proteins pattern are characteristic for particular morbid processes, evoked by various pathogenic factors. Therefore, it does not seem probable that a special molecular part of the myelin bilayers is the general weak point in its architecture.

The degradation of high molecular weight proteins in the myelin starting in the early period after hypoxia, is even exaggerated in the course of the next weeks . It must mean that the pathological processes in the myelin membranes start immediately after hypoxia, but continue for months.

BIAŁKA MIELINY W PÓŹNYM OKRESIE NIEDOTLENIENIA

Streszczenie

Badano wpływ łagodnego niedotlenienia, wywołanego umieszczeniem szczurów rasy Wistar przez 30 min w komorze zawierającej mieszaninę gazów z 7% zawartością tlenu, na obraz białek mieliny. Po 14 dniach i po 2 miesiącach po niedotlenieniu stwierdzono wyraźny spadek zawartości białka Wolfgrama w mielinie, a jedynie w 2 miesiące po niedotlenieniu występuje również spadek zawartości proteolipidu Folch-Lees oraz białka Agrawala. Nie ma natomiast cech rozpadu białek zasadowych. Wyniki badań, w porównaniu ze stwierdzanymi w innych warunkach doświadczalnych, prowadzą do wniosku, że zmiany w obrazie białek mieliny są charakterystyczne dla poszczególnych procesów chorobowych wywołanych przez różne czynniki patogenne. Demielinizacja przebiega łącznie z dużym spadkiem białka zasadowego, podczas gdy uszkodzenia mieliny innych typów są połączone ze zmianami w białkach o wyższej masie cząsteczkowej.

REFERENCES

1. Agrawal H.: Analysis of membrane proteins by sodium dodecyl-sulfate-polyacrylamide gel electrophoresis. In: Fundamentals of lipid chemistry. Eds.: R. Burton, F. Guerra. Science Publ Div.
2. Iyoyama Y., Sternberger N., de Webster H., Quarles R., Cohen S., Richardson J.: Immunocytochemical observation in the distribution of myelin-associated glycoprotein and myelin basic protein in multiple sclerosis lesions. Ann Neurol, 1980, 7, 167-177.
3. Mathieu J., Zimmerman A., de Webster H., Ulsomer A., Brady P., Quarles R.: Hexochloropheno-intoxication, characterisation of myelin and myelin related fractions in rats during early postnatal development. Exp Neurol, 1974, 45, 558-574.
4. Norton W., Cammer W., Bloom B., Gordon S.: Neutral proteinase secreted by macrophages degrade basic protein: a possible mechanism of inflammatory demyelination. In: Myelination and demyelination. Ed.: J. Palo. Plenum Publ Corp, New York, 1978, pp. 365-381.

5. Norton N., Poduslo S.: Myelination in rat brain: method of myelin isolation. J Neurochem, 1973, 21, 749-758.
6. Wender M., Adamczewska-Goncerzewicz Z., Stanisławska J., Pankrac J., Talkowska D., Grochowalska A.: Myelin lipids of the rat brain in experimental mild hypoxia. Exp Pathol, 1989a (in press).
7. Wender M., Adamczewska-Goncerzewicz Z., Talkowska D., Pankrac J., Grochowalska A.: Influence of experimental acute hypoxia on myelin proteins. Neuropatol Pol, 1989b, 27 (in press).
8. Wender M., Zgorzalewicz B., Piechowski A., Spieszalski W., Bucholc M.: The pattern of myelin proteins in triethyltin (TET) intoxication. Exp Pathol, 1983a, 23, 193-195.
9. Wender M., Zgorzalewicz B., Śniatała-Kamasa M., Piechowski A.: Myelin proteins in Wallerian degeneration of the optic tract. Exp Pathol, 1983b, 23, 215-217.

Authors' address: Department of Neurology, School of Medicine, 49, Przybyszewskiego Str., 60-355 Poznań.

NEUROPAT. POL. 1990, 28, 3-4
PL ISSN 0028-3894

ZOFIA ADAMCZEWSKA-GONCERZEWICZ, MIECZYSŁAW WENDER, EUGENIUSZ SROCZYŃSKI, DANUTA TALKOWSKA, JOLANTA DORSZEWSKA, JADWIGA PANKRAC

FREE FATTY ACIDS OF CEREBRAL WHITE MATTER IN THE LATE PERIOD AFTER SEVERE HYPOXIA

Department of Neurology, School of Medicine, Poznań, Poland

Most of the conducted studies in hypoxia pertained to the brain as a whole and the observed alterations were related to disturbances in cell membrane metabolism with no attempts of pinpointing the structure affected. However, little is known on the effects of hypoxia on cerebral white matter with a lipid-rich myelin sheath. Considering the role played by some fatty acids in stimulation of cellular processes, determination of changes in their content and of their transformations may be of basic significance for understanding the involved pathomechanism. Therefore in continuation of our scientific efforts concerning this subject, we studied the content and composition of free fatty acids in the cerebral white matter in the late period after acute hypoxia.

MATERIAL AND METHODS

The experiments were performed on white rats of Wistar strain, each weighing 200-250 g. Severe hypoxia was induced by placing the animals for 3 min in a air-tight glass chamber with gas mixture containing 2% O_2 in 97.9% N_2 and 0.1% CO_2. The control level of body temperature was maintained by heating the experimental rats with a lamp. The animals were sacrificed 14 days and 2 months after hypoxia by decapitation in a light halothane anesthesia. The heads were immediately placed in liquid nitrogen. The white matter was isolated in a cold room at a temperature of 0°C.

Biochemical methods

Free fatty acids were extracted from the cerebral white matter of rats according to the method described by Doll and Meinertz (1960),

Paper presented at Symposium on Neurobiology of Cerebral Ischemia and Hypoxia. Poznań, June 29-July 1, 1989.

Table 1. Free fatty acids of cerebral white matter in the late period after acute hypoxia (2% oxygen) (in mg/100 g of dry weight)

Tabela 1. Wolne kwasy tłuszczowe istoty białej mózgu w późnym okresie po ostrym niedotlenieniu (2% tlenu) (w mg/100 g suchej wagi)

Free fatty acids Wolne kwasy tłuszczowe	Control Norma	14 days after hypoxia 14 dni po niedotlenieniu	2 months after hypoxia 2 miesiące po niedotlenieniu
Total content of FA Całkowita zawartość kwasów tłuszczowych	73.08±7.80	224.42**±26.21	138.93**±11.79
12 : 0	0.23±0.10	1.12**± 0.54	0.28 ± 0.11
14 : 0	0.97±0.21	6.06**± 2.19	1.11 ± 0.30
15 : 0	0.38±0.32	2.24**± 0.73	0.56 ± 0.23
16 : 0	16.86±2.39	57.22**± 1.92	22.09**± 2.07
16 : 1	0.99±0.40	7.41**± 4.05	1.95**± 0.66
17 : 0	0.56±0.13	1.57**± 0.70	0.70 ± 0.12
18 : 0	26.16±4.34	95.82**±18.43	47.64**± 2.94
18 : 1	22.18±6.27	30.52 ±19.17	35.62**± 3.42
18 : 2	0.39±0.09	0.80**± 0.18	2.08**± 0.29
18 : 3	0.31±0.29	1.67 ± 0.20	0.06**± 0.02
20 : 0	0.37±0.07	2.69**± 0.92	1.11**± 0.09
21 : 1	0.95±0.22	1.12 ± 0.70	5.56**± 0.52
20 : 2	0.13±0.08	1.12**± 0.80	0.28**± 0.11
20 : 3	0.74±0.89	0.67 ± 0.36	0.56 ± 0.08
20 : 4	0.51±0.10	3.82**± 1.33	12.50**± 2.81
20 : 5	0.45±0.11	1.80 ± 0.90	1.25**± 0.34
24 : 0	0.91±0.33	8.08**± 3.00	4.03**± 0.46
24 : 1	0.00±0.00	0.67 ± 1.10	1.39**± 0.18
Total saturated Całkowite nasycone	46.44±7.02	174.80**±20.08	77.52**± 3.52
Total unsaturated Całkowite nienasycone	26.64±4.03	49.60* ±10.50	61.35**± 3.54
Total monoenes Całkowite jednonienasycone	24.12±2.31	39.72 ±11.00	44.62**± 3.40
Total dienes Całkowite dwunienasycone	0.52±0.99	2.92* ± 1.10	2.36 ± 1.60
Total trienes Całkowite trójnienasycone	1.05±0.60	1.34 ± 0.89	0.62 ± 0.11
Total tetraenes Całkowite czteronienasycone	0.51±0.12	3.82**± 1.33	12.50**± 2.61
Total pentaenes Całkowite pięcionienasycone	0.74±0.12	1.80**± 0.85	1.26**± 0.34

Number of animals in each group: 6±SD.
Liczba zwierząt w każdej grupie: 6.

* Differences significant at the level $p < 0.05$.
Różnice istotne przy poziomie $p < 0.05$.

** Differences significant at the level $p < 0.01$.
Różnice istotne przy poziomie $p < 0.01$.

separated by means of thin layer chromatography according to Fishwich (1968) in the modification of Sroczyński and Fiedler (1978) and determined by the method of Düncombe (1964). Then free fatty acids eluted from thin-layer chromatograms were methylated and separated by means of gas liquid chromatography as described in our previous publication (Wender et al. 1988a). The results were subjected to statistical analysis by Student's t test.

RESULTS

The clinical and morphological patterns of the brain after severe hypoxia in experimental animals were identical to those reported in our previous publication (Wender et al. 1987). A well defined myelinopathy was never found.

Results obtained in chemical studies are presented in Table 1. The total content of free fatty acids increased 3-fold 14 days after the experiment in acute hypoxia. Even in the chronic period after hypoxia (2 months) it was twice as high as that found in control animals.

In analysis of the fatty acids spectrum, obtained by means of gas liquid chromatography, it would appear that in absolute values nearly all fatty acids showed an increased content. The most evident reproducible alterations can be noted in the levels of two saturated fatty acids, palmitic (16 : 0) and stearic (18 : 0). The increase was 3-fold 14 days after the experiment. In the group examined 2 months after hypoxia a slight decrease in free fatty acids was noted, but the level of these acids still remained higher than in the control group.

However, the highest rise involved polyunsaturated fatty acids: linolic, linoleic and arachidonic. The latter in the chronic phase (2 months) after hypoxia showed a 24-fold increase of level. In two late periods after hypoxia, the presence of nervonic acid (24 : 1), not detectable in normal white matter, was observed.

DISCUSSION

Lipids of cell membranes are particularly sensitive to lesions in conditions of disturbed basal metabolism in the central nervous system (hypoxia, hypoglycemia, seizures). As far as the mechanism of the changes is concerned, two hypotheses have been advanced. Bazan (1970, 1971) postulated an increase in the levels of free fatty acids released from phospholipids due to their hydrolysis as the primary cause of a chain of secondary metabolic and structural lesions in the central nervous system. Demopoulos (1977) and Majewska et al. (1978), pointed to a possibility of activated processes of free radical oxidation of lipids and of free fatty acids in the course of or after hypoxia. Release of fatty acids

and stimulated lipid peroxygenation in pathological conditions are accompanied by less drastic changes in the composition and metabolism of cell membrane lipid components.

The studies of Strosznajder (1981) and of Domańska-Janik (1985) have shown that the lipid fraction, the main structural component of the cell membrane is particularly sensitive to hypoxia, as compared with other macromolecular compounds. This is reflected mainly in decreased phospholipid and ganglioside levels in the brains of rats exposed to hypoxia. Disturbances of longest duration, however, have been noted in acid glycerophospholipid containing mostly inositol phospholipid. In the later period after hypoxia Wender et al. (1987) have demonstrated a pronounced increase in contents of lysoglycerophospholipids and cholesterol esters. This may indicate that hypoxia leads to a lesion in the molecular structure of myelin, but owing to the absence of lymphocyte and macrophage reaction no myelinolytic factors are produced and no demyelination takes place.

Disturbances in the dynamic balance between free fatty acids and the acyl groups of membrane phospholipids in brain hypoxia result in an increased pool of free fatty acids. This pool consists primarily of saturated fatty acids, palmitic (16 : 0) and stearic (18 : 0), and unsaturated acids, oleic (18 : 1), arachidonic (20 : 4) and eicosapentaenic (22 : 5). This composition has been observed also in experimental transient and bilateral ischemia in gerbils, as described by De Medio et al. (1980). This spectrum reflects, according to Strosznajder (1981) disturbed processes of glycerophospholipid deacylation-reacylation in the brain cell membrane of animals subjected to hypoxia. Stimulated acylation results from augmented amounts of lysoglycerophospholipids formed by calcium-activated phospholipase A_2. An increased sensitivity of the enzyme to the stimulatory action of calcium ions in hypoxia may constitute one of the factors responsible for the increase in the pool of unsaturated fatty acids in the brain (particularly of arachidonic acid). A decreased activity of acylCoA ligase may represent another factor responsible for this effect.

In our experiments on rats subjected to severe hypoxia, we have also noticed the sharp rise in the free fatty acids pool. This pertains in particular to polyunsaturated acids, including arachidonic acid. Similar results have been obtained by Bazan (1976) and de Medio et al. (1980). These authors examined distribution of arachidonic acid and specific activity of neutral and polar brain lipids, pointing to phosphatidylethanolamine and phosphatidylinositol as the main source of arachidonic acid during ischemia and hypoxia.

An interesting finding in this study involves the observation that the free fatty acids pool is maintained for a prolonged period, throughout the studied time point after hypoxia. The high free fatty acids level in

experimental animals corresponds to a high content of cholesterol esters noted in the earlier study by Wender et al. (1988b). The mechanism of this phenomenon remains unclear.

WOLNE KWASY TŁUSZCZOWE ISTOTY BIAŁEJ MÓZGU W PÓŹNYM OKRESIE PO CIĘŻKIM NIEDOTLENIENIU

Streszczenie

Badano wpływ ciężkiego niedotlenienia na zawartość i obraz wolnych kwasów tłuszczowych istoty białej mózgu. Badania przeprowadzono na szczurach rasy Wistar przez umieszczenie zwierząt na okres 3 min w komorze zawierającej mieszaninę gazów z zawartością 2% tlenu.

Kwasy tłuszczowe ekstrahowano według sposobu Dolla i Meinertza (1960), oznaczano ilościowo metodą Düncomba (1964), a następnie rozdzielano techniką chromatografii gazowej.

W wyniku badań stwierdzono trzykrotny (w 14 dni po niedotlenieniu oraz dwukrotny po 2 miesiącach) wzrost puli wolnych kwasów tłuszczowych. Największy wzrost wykazywały dwa kwasy nasycone palmitynowy i stearynowy oraz kwasy wielonienasycone, szczególnie kwas arachidonowy, który w okresie chronicznym (2 miesiące) wzrastał aż dwudziestoczterokrotnie.

Tak długo utrzymujący się po niedotlenieniu wzrost zawartości wolnych kwasów tłuszczowych może tłumaczyć narastanie objawów klinicznych, występujących w niektórych przypadkach po udarze mózgu.

REFERENCES

1. Bazan N. G.: Effect of ischemia and electroconvulsive shock on free fatty acid pool in the brain. Biochim Biophys Acta, 1970, 218, 1-10.
2. Bazan N. G.: Phospholipase A_1 and A_2 in brain subcellular fraction. Acta Physiol Pharmacol Latinoam, 1971, 21, 101-106.
3. Bazan N. G.: Function and metabolism of phospholipids in central and peripheral nervous system. Plenum Press, New York, 1976.
4. De Medio G., Goracci G., Horrocks L., Łazarewicz J., Mazzari S., Porcelatti G., Strosznajder J., Trovarelli G.: The effect of transient ischemia on fatty acid and lipid metabolism in the gerbil brain. Ital J Biochem, 1980, 29, 412-432.
5. Demopoulos H., Flamm E., Soligmann M., Power R., Pretronigro D., Ranschoff J.: Molecular pathology of lipids in CNS membranes. In: Oxygen and physiological function. Ed.: F. F. Jöbis. Professional Inform Library, Dallas, Texas, 1977, pp. 491-508.
6. Doll W., Meinertz H.: Microdetermination of long-chain fatty acids in plasma and tissues. J Biol Chem, 1960, 235, 2595-2599.
7. Domańska-Janik K.: Zaburzenia metabolizmu glukozy w energetycznie wyrównanym niedotlenieniu mózgu szczura. Praca habilitacyjna, 1985, 1-131.
8. Düncombe W.: The colorimetric microdetermination of non-esterified fatty acid plasma. Clin Chim Acta, 1964, 9, 122-126.
9. Fishwick B.: Changes in the lipids of turkey muscle during storage of chilling and freezing temperature. J Sci Food Agric, 1968, 19, 440-445.

10. Majewska M. D., Strosznajder J., Łazarewicz J.: Effect of ischemic anoxia and barbiturate anesthesia on free radical oxydation of mitochondrial phospholipids. Brain Res, 1978, 158, 423-434.
11. Sroczyński E., Fiedler A.: Evaluation of the degree of rancidity of poultry fat (in Polish). Przemysł Spożywczy, 1978, 11, 233-238.
12. Strosznajder J.: Regulation of glycerophospholipids metabolism in the brain in normal conditions and in hypoxia (in Polish). Neuropatol Pol. 1981, 19, 145-154.
13. Wender M., Adamczewska-Goncerzewicz Z., Stanisławska J., Pankrac J., Talkowska D., Grochowalska A.: Effect of acute hypoxia on myelin lipids. Neuropatol Pol, 1987, 25, 107-115.
14. Wender M., Adamczewska-Goncerzewicz Z., Żórawski A., Sroczyński E., Grochowalska A.: Effect of moderate hypoxia on content and pattern of free fatty acids in cerebral white matter. Neuropatol Pol, 1988a, 26, 39-46.
15. Wender M., Adamczewska-Goncerzewicz Z., Stanisławska J., Pankrac J., Talkowska D., Grochowalska A.: Myelin lipids of the rat brain in experimental hypoxia. Exp Pathol, 1988b, 33, 59-63.

Authors' address: Department of Neurology, School of Medicine, 49, Przybyszewskiego Str., 60-355 Poznań, Poland.

NEUROPAT. POL. 1990, 28, 3-4
PL ISSN 0028-3894

ANTONI GODLEWSKI, JÓZEF SZCZECH, HANNA HEJDUK-HANTKE, MIECZYSŁAW WENDER

MORPHOMETRIC STUDIES OF THE MYELIN-OLIGODENDROGLIA COMPLEX IN THE LATE PERIOD AFTER HYPOXIA

Department of Neurology, School of Medicine, Poznań, Poland

Pathological changes in the brain following hypoxia have been the subject of many reports examining the problem from its morphological side, ultrastructure and neurochemistry (Brierley 1976). Morphological studies evaluated the lesions of myelin sheaths, sometimes in the form of markedly disseminated or diffuse demyelination (Raine 1984) and changes in neuroglia (Kraśnicka et al. 1973). Hypoxia induces changes in the chemistry of myelin: an increase of cholesterol esters and lysophosphatidylcholine content (Wender et al. 1988a).

In the presented work we investigated the morphometric picture of the myelin-oligodendroglia complex in the late period after hypoxia. In the early period after hypoxia we observed edematous changes in the oligodendroglia (Wender et al. 1988c) and in myelinated nervous fibers (Wender et al. 1988b).

MATERIAL AND METHODS

The experiment was performed on Wistar rats. The animals were exposed to hypoxia in a special glass chamber in two experimental groups. Severe hypoxia was induced by flushing the chamber with a gas mixture containing 2% O_2, 97.9% N_2 and 0.1% CO_2 for 3 min. Mild hypoxia was induced by flushing the chamber with a gas mixture containing 7% O_2, 92.9% N_2 and 0.1% CO_2 for 30 min. The animals of both experimental groups were sacrificed 14 days and 60 days after hypoxia.

Karyometric measurements of oligodendroglia cell nuclei of the *corpus callosum* were performed on Feulgen-stained slices using an automatic analyzer of microscopic pictures (Morphoquant). More details of the

Paper presented at Symposium on Neurobiology of Cerebral Ischemia and Hypoxia. Poznań, June 29-July 1, 1989.

measurements were published in our previous paper (Wender et al. 1988c).

Morphometric measurements of myelin fibers were performed on EM prints magnified × 35 000 using a Reichert planimeter. The method was identical as in previous work (Wender et al. 1988b).

RESULTS

Results of karyometric estimations of oligodendroglia nuclei are presented in Table 1.

Results of morphometric measurements are visible in Table 2.

Table 1. Results of karyometric studies of oligodendroglia in *corpus callosum* of rats after hypoxia
Tabela 1. Wyniki pomiarów kariometrycznych oligodendrogleju spoidła wielkiego szczurów po niedotlenieniu

Parameter Współczynnik	Control Norma	Mild hypoxia Łagodne niedotlenienie		Acute hypoxia Ostre niedotlenienie	
		14 days dni	60 days dni	14 days dni	60 days dni
KONL	85± 8	85± 7	82± 8	76± 7**	78± 5**
KOFL	244±40	282±34**	228±35**	181±32**	223±26**
FOFA	149±11	150±12	146±12**	161±18**	142± 7**
DMVH	69±10	71±11	71±11**	61±13**	77± 9**
EXTS	78±12	73± 9**	77± 7**	64± 6**	73± 5**
KOMP	65± 3	65± 5	65± 3	65± 3	62± 3**
ZNTR	77± 6	67± 9**	78± 9	85± 6	70± 7**

All values in working units. KONL — length of nuclear cross-section circumference. KOFL — area of nuclear cross-section. FOFA — form factor of length square to area. DMVH — ratio of the smallest to the biggest diagonal. EXTS — sum of nuclear chromatin extinction, in Feulgen method proportional to DNA amount. KOMP — nuclear chromatin compactness index. ZNTR — nuclear chromatin concentration in the centre index.

Wszystkie wartości podano w jednostkach roboczych. KONL — długość obwodu przekroju jądra komórkowego. KOFL — pole powierzchni przekroju jądra komórkowego. FOFA — współczynnik kształtu, stosunek kwadratu długości obwodu do pola powierzchni. DMVH — stosunek długości najmniejszej do największej przekątnej. EXTS — suma ekstynkcji chromatyny jądrowej, w metodzie Feulgena proporcjonalna do zawartości DNA. KOMP — współczynnik zbitości chromatyny jądrowej. ZNTR — współczynnik centryczności ułożenia grudek chromatyny jądrowej.

** Difference highly statistically significant in Kolmogorov-Smirnov test ($p < 0.01$).

** Różnice wysoce istotne statystycznie w tekście Kołmogorova-Smirnova ($p < 0.01$).

CONCLUSIONS

1. In the late period after hypoxia the mean thickness of myelin and the number of myelin lamellae are greater, whereas the mean diameter and area of axons are smaller than in the control group.

Table 2. Nervous fibers of *corpus callosum* in rats exposed to the action of mild hypoxia

Tabela 2. Włókna nerwowe spoidła wielkiego szczurów poddanych działaniu łagodnego niedotlenienia

Parameter Współczynniki	Control Norma	14 days after hypoxia 14 dni po niedotlenieniu	60 days after hypoxia 60 dni po niedotlenieniu
Thickness of myelin (in working units) Grubość mieliny (w jednostkach roboczych)	0.08±0.04	0.11±0.02*	0.10±0.02*
Number of myelin lamellae Liczba blaszek mieliny	8.0 ±3.3	9.1 ±3.2*	9.2 ±3.0*
Axon diameter (in working units) Przekrój aksonu (w jednostkach roboczych)	0.83±0.28	0.71±0.16*	0.74±0.36**
Axon area (in working units) Pole aksonu (w jednostkach roboczych)	15.91±6.2	13.16±5.74*	11.23±4.62**

* Difference statystically significant in analysis of variance ($p < 0.05$).
* Różnice statystycznie istotne przy analizie wariancji ($p < 0.05$).
** Difference highly statistically significant in analysis of variance ($p < 0.01$).
** Różnice wysoce istotne statystycznie przy analizie wariancji ($p < 0.01$).

2. Mild hypoxia induces selective destruction and disappearance of myelinated fibers. The selective disappearance of nervous fibers in *corpus callosum*, secondary to neuronal and oligodendroglial degeneration, is evidently the decisive factor provoking the changes observed in myelin and axons in our morphometric studies.

3. In the late period after hypoxia the karyometric changes, typical for the degenerative processes, are observed in oligodendroglia nuclei. The intensity of these changes varied according to the degree of hypoxia and the time elapsing after hypoxia.

4. Cytophotometric analysis of the relative DNA content in the cell nuclei of oligodendroglia demonstrated a decreased extinction in the late period after acute or mild hypoxia.

5. The changes in oligodendroglia may be primarily responsible for the structural lesion in myelin observed as a result of hypoxia.

BADANIA MORFOMETRYCZNE KOMPLEKSU MIELINA-OLIGODENDROGLEJ W PÓŹNYM OKRESIE PO NIEDOTLENIENIU

Streszczenie

W pracy przedstawiono wpływ ostrego (2% O_2 przez 3 min) i łagodnego (7% O_2 przez 30 min) niedotlenienia na kompleks mielina-oligodendroglej w późnym okresie po doświadczeniu (14 i 60 dni).

Zaobserwowano zmiany we włóknach mielinowych (wzrost grubości mieliny i liczby blaszek mielinowych, zmniejszenie średnicy i pola powierzchni aksonu) oraz zmiany zwyrodnieniowe w oligodendrogleju. Uszkodzenie oligodendrogleju wydaje się pierwotne w stosunku do zmian strukturalnych w mielinie, obserwowanych w następstwie niedotlenienia.

REFERENCES

1. Brierley J. B.: Cerebral hypoxia. In: Greenfield's Neuropathology. Eds.: W. Blackwood, J. A. N. Corsellis. E. Arnold, London, 1976, pp. 43-83.
2. Kraśnicka Z., Renkawek K., Gajkowska B.: Effect of short-term anoxia on the ultrastructural picture of the glial tissue *in vitro*. Neuropatol Pol, 1973, 11, 399-404.
3. Raine C.: The neuropathology of myelin disease. In: Myelin. Ed.: P. Morell. Plenum Press, New York, London, 1984, pp. 259-310.
4. Wender M., Adamczewska-Goncerzewicz Z., Stanisławska J., Pankrac J., Talkowska D., Grochowalska A.: Myelin lipids of the rat brain in experimental hypoxia. Exp Pathol, 1988a, 33, 59-63.
5. Wender M., Hejduk-Hantke H., Goncerzewicz A., Wyglądalska-Jernas H.: Morphometric studies of the nerve fibers in corpus callosum of rats exposed to mild hypoxia. Neuropatol Pol, 1988b, 26, 185-191.
6. Wender M., Szczech J., Godlewski A., Grochowalska A.: Karyometric and cytophotometric studies of the oligodendroglia in the corpus callosum of the rat after hypoxia. Exp Pathol, 1988c, 32, 249-255.

Authors' address: Department of Neurology, School of Medicine, 49, Przybyszewskiego Str., 60-355 Poznań, Poland.

NEUROPAT. POL. 1990, 28, 3-4
PL ISSN 0028-3894

JÓZEF SZCZECH, JÓZEF GODLEWSKI

KARYOMETRIC ANALYSIS OF VASCULAR ENDOTHELIA IN THE FORNIX COLUMNS OF RAT BRAIN IN THE LATE PERIOD AFTER HYPOXIA

Department of Neurology, School of Medicine, Poznań, Poland

The sequence of changes in structural elements of the brain resulting from hypoxia is well known. Morphological changes appear first in the neurons, later in oligo- and astroglia, while microglia and cells of blood vessels are considered to be less sensitive to oxygen deficit (Jacob 1963). On the other hand, the vascular factor play a significant role in the development of brain damage after hypoxia (Lindenberg 1955; Klatzo 1967). The damage of parenchymal elements in the brain has permanent features (Mossakowski et al. 1986).

Changes in the morphological components of blood vessels are rarely examined and their reversibility is not evident. For these reasons, we present the karyometric and cytophotometric findings which we obtained in the late period after hypoxia.

MATERIAL AND METHODS

Investigations were performed on adult Wistar rats subjected to moderate hypoxia in a gaseous mixture containing 7% of oxygen for 30 min and severe hypoxia in a mixture with 2% oxygen for 3 min. The animals of both experimental groups and the control group were sacrificed in trifluoroethane anesthesia on the 14th and 60th day after hypoxia. To visualize in the blood vessels the endothelial nuclei brain slices of the control and experimental animals were subjected to the Feulgen reaction (Krygier-Stojałowska 1982). The nuclei were measured with a Morphoquant measuring microscope (Zeiss, Jena). Each index and coefficient of size, shape and the nuclear chromatin of the 100 endothelial nuclei of each experimental group were compared with the respective parameter of the 100 nuclei of the control group. The lambda statistic and

Paper presented at Symposium on Neurobiology of Cerebral Ischemia and Hypoxia. Poznań, June 29-July 1, 1989.

Kolmogorov-Smirnov test (Greń 1982) were applied as method for comparison and the accepted lowest significant level of changes was $p \leqslant 0.05$.

RESULTS

Fig. 1 presents the microscopic picture of the fornix columns 60 days after hypoxia. Arrows indicate the endothelial nuclei which are darker and more irregular than the surrounding oligodendroglial nuclei.

The results of karyometric and cytophotometric measurements are compared in Table 1.

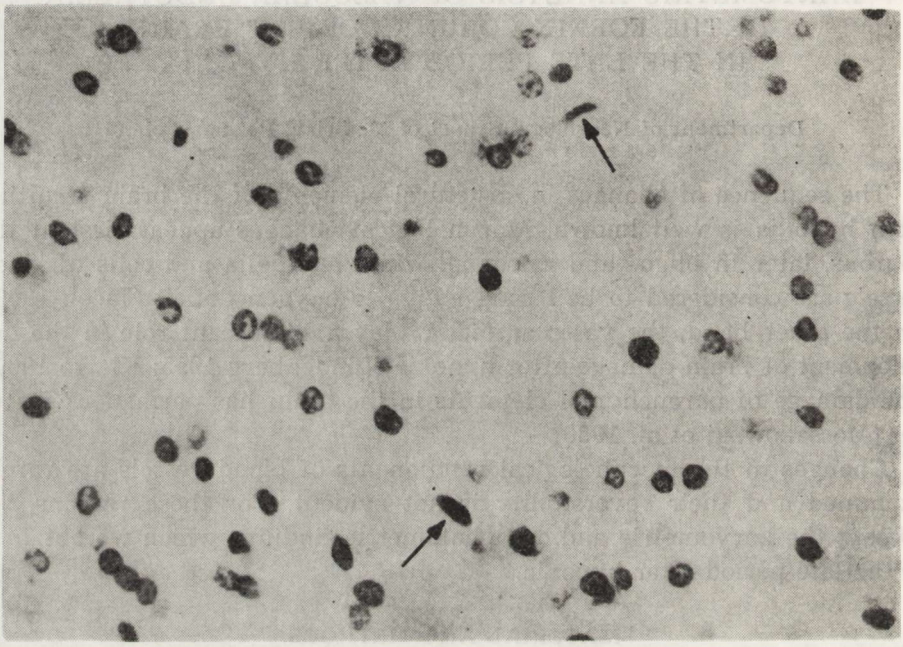

Fig. 1. Feulgen's reaction in column of fornix. Arrows indicate the nuclei of capillary endothelia. × 800

Ryc. 1. Reakcja Feulgena w kolumnie sklepienia. Strzałki wskazują jądra śródbłonków naczyń włosowatych. Pow. 800 ×

CONCLUSIONS

1. Many statistically significant changes of karyometric and cytophotometric parameters were observed in nuclei of blood vessel endothelia in the late period after hypoxia.

2. In comparison with the control group the nuclei of endothelial cells were larger and rounder. With respect to the 14th day group, the increase of the cross section was diminished on 60th day after hypoxia. However, in the late experimental group a decrease of roundness and loss of the nuclear membrane fold were observed.

Table 1. Karyometric measurements of blood vessel endothelia in the fornix columns in the late period after hypoxia

Tabela 1. Pomiary kariometryczne śródbłonków naczyń kolumn sklepienia w późnym okresie po niedotlenieniu

Parameter Współczynnik	Control Norma	Mild hypoxia Łagodne niedotlenienie		Acute hypoxia Ostre niedotlenienie	
		14 days dni	60 days dni	14 days dni	60 days dni
KONL	94±15	96±10	91±10	97±12	92±11
KOFL	192±38	211±30**	206±32*	214±32***	208±29**
FOFA	232±47	219±27*	205±29**	223±41	206±30**
DMVH	47±10	44± 8**	48±9	45±10	48± 8
FLVH	74± 7	76± 6	77± 5**	75± 7	77± 6**
EXTS	50±12	61± 8***	66± 8***	67± 7***	63± 8***
KOMP	56± 6	58± 4	58± 4	57± 4	56± 5*
ZNTR	75± 8	77± 7	80± 7***	77± 8	78± 7**

Numerical values of the parameters are expressed in numbers of the measuring sceen points: mean value ± standard deviation. KONL — length of nucleus cross-section circumference, KOFL — area of nucleus cross-section, FOFA — ratio of $KONL^2$ to KOFL, DMVH — ratio of smallest and biggest diagonals of nuclei, FLVH — ratio of cross-section area to convex area (folding index), EXTS — sum of nuclear chromatin extinction, KOMP — nuclear chromatin compactness index, ZNTR — nuclear chromatin concentration index. Statistical significance level of changes (Kolmogorov-Smirnov test). * $p \leq 0.05$, ** $p \leq 0.02$, *** $p \leq 0.01$.

Wartości liczbowe parametrów wyrażone w liczbie punktów siatki pomiarowej w układzie: średnia arytmetyczna ± odchylenie standardowe. KONL — długość obwodu przekroju poprzecznego, KOFL — pole przekroju poprzecznego, FOFA — stosunek $KONL^2$ do KOFL, DMVH — stosunek przekątnych, FLVH — stosunek przekroju poprzecznego do powierzchni konweksyjnej (wskaźnik pofałdowania), EXTS — suma ekstynkcji chromatyny jądrowej, KOMP — wskaźnik zbitości chromatyny, ZNTR — wskaźnik koncentracji chromatyny. Poziom istotności statystycznej zmian (test Kołmogorova-Smirnova): * $p < 0{,}05$, ** $p < 0{,}02$, *** $p < 0{,}01$.

3. Independently of the time after hypoxia a considerable increase of the nuclear chromatin extinction was recorded in both experimental groups.

4. In some aspects of observation, the type of the observed degenerative changes of capillary endothelia after hypoxia is similar to an accelerated process of ageing.

BADANIA KARIOMETRYCZNE ŚRÓDBŁONKÓW NACZYŃ WŁOSOWATYCH KOLUMN SKLEPIENIA MÓZGU SZCZURA W PÓŹNYM OKRESIE PO NIEDOTLENIENIU

Streszczenie

Oceniono wpływ niedoboru tlenu w mieszaninie gazowej na jądra śródbłonków włośniczek kolumn sklepienia, w 14 i 60 dniu po niedotlenieniu w modelu hipoksji ostrej i umiarkowanej. Za pomocą komputerowej metody analizy obrazu mikro-

skopowego i analizy statystycznej zaobserwowano, że niedotlenienie wywołuje zmiany zwyrodnieniowe, które w odniesieniu do niektórych wyników mogą odpowiadać przyspieszonemu procesowi starzenia.

REFERENCES

1. Greń J.: Statystyka matematyczna. Modele i zadania. PWN, Warszawa, 1982.
2. Jacob H.: CNS tissue and cellular pathology in hypoxaemia states In: Selective vulnerability of the brain in hypoxaemia. Eds.: J. P. Schade, W. H. McMenemey. Blakwell Scientific, Oxford, 1963.
3. Klatzo I.: Neuropathological aspects of brain oedema. J Neuropathol Exp Neurol, 1967, 26, 1-14.
4. Krygier-Stojałowska A.: Zasady cytofotometrii. W: Topochemiczne metody badania komórek i tkanek. PWN, Warszawa, 1982.
5. Lindenberg R.: Compression of brain arteries as a pathogenetic factor for tissue necrosis and their areas of predilection. J Neuropathol Exp Neurol, 1955, 14, 223-243.
6. Mossakowski M. J., Hilgier W., Januszewski S.: Ocena zmian morfologicznych w ośrodkowym układzie nerwowym w doświadczalnym zespole poreanimacyjnym. Doniesienie wstępne. Neuropatol Pol, 1986, 24, 471-489.

Authors' address: Department of Neurology, School of Medicine, 49, Przybyszewskiego Str., 60-355 Poznań, Poland.

NEUROPAT. POL. 1990, 28, 3-4
PL ISSN 0028-3894

ROLF WARZOK, BERNDT WATTIG, ANDREAS TIMMEL

THE ROLE OF HYPOXIA IN DISEASES OF PERIPHERAL NERVES

Institute of Pathology, University of Greifswald, GDR

Ischemic neuropathy is a term used to describe neurological disorders that accompany obstructive vascular disease. Although neurological symptoms occur both in acute and chronic ischemia, ischemic neuropathy is generally associated with chronic conditions such as *atherosclerosis*, *thrombangiitis obliterans* and *diabetes mellitus*.

With regard to blood supply, there are striking differences between the brain and peripheral nerves. Nutritional arteries are known to penetrate the epineurial tissue and subsequently give off smaller arteries that anastomose within this tissue. The epineurial arterial plexus then gives rise to smaller vascular channels (precapillaries and capillaries) which penetrate the epineurium and anastomose within the endoneurium thus forming a second rich plexus. Because of these connections peripheral nerves have a strong collateral blood supply and consequently they acquire resistance to damage by segmental ischemia.

Ischemic neuropathy related to the occlusion of large arteries is encountered as a result of atherosclerosis, embolism, compression and compartment syndromes. The consequences have been most closely studied in relation to the lower limb atherosclerotic disease, but so far even these have not been extensively examined using modern techniques. Such studies are currently done in our laboratory.

Microangiopathy is generally thought to be of major importance in the development of diabetic polyneuropathy. But, here again detailed studies are lacking. Therefore, we analysed the relationship between the degree of microangiopathy and nerve fiber loss of the sural nerve in autopsy material.

Paper presented at Symposium on Neurobiology of Cerebral Ischemia and Hypoxia. Poznań, June 29-July 1, 1989.

MATERIAL AND METHODS

Pieces 3 cm long were taken from sural nerves of 16 deceased individuals with diabetes mellitus and 12 age-related controls without diabetes. Cases with malignant neoplasms were not considered. Nerve tissue was fixed in glutaraldehyde, postfixed in osmium tetroxide and embedded in durcupan. Semithin sections were stained with thionin and acridin orange (Sievers 1971). Morphometry was performed with the aid of the automatic microscope image analysis system A 6471-AMBA/R (Robotron, Dresden). The software program Axon-2 was used (Wattig et al. 1989a,b). The following parameters were registered: number of fibers per mm^2, mean area of nerve fibers, mean area of axons and myelin sheaths, thickness of myelin sheaths, ratio of total area of axons to total area of nerve fibers. The degree o diabetic angiopathy was determined according to the parameters in Table 1. For statistical analysis Student's t-test and the Kolmogorov-Smirnov test (for histograms) were used.

Table 1. Degrees of diabetic microangiopathy
Tabela 1. Stopnie mikroangiopatii cukrzycowej

Degree Stopień	Relation Stosunek		
	thickness of capillary wall grubość ściany kapilarów	versus versus	diamater of capillary średnica światła kapilarów
1	1	:	> 2
2	1	:	1.5
3	1	:	1
4	1.5	:	1
5	> 2	:	1

RESULTS

The most striking finding was a significant decrease of the number of myelinated fibers in diabetics as compared with controls ($p > 0.0001$, Fig. 1). The histograms of myelinated fibers showed no shift, e.g. loss of nerve fibers occurs in all fiber classes. In the preserved fibers a decrease of the area of myelin sheaths was registered ($p > 0.05$). Microangiopathy was observed in all nerve specimens of diabetics (Fig. 2). The loss of nerve fibers did not correspond to the degree of microangiopathy. Nerves with low and high fiber density were randomly distributed (Fig. 3).

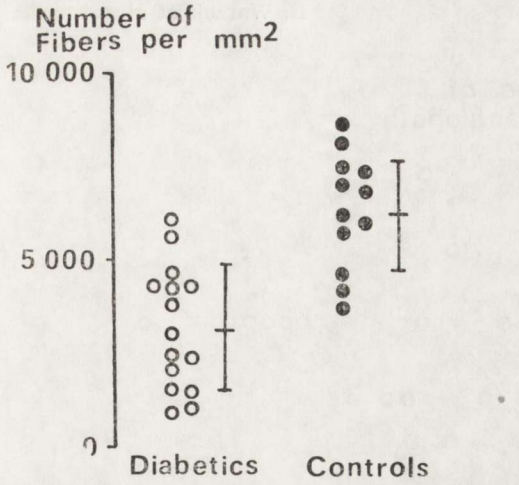

Fig. 1. Number of nerve fibers in diabetics and controls
Ryc. 1. Liczba włókien nerwowych u osobników z cukrzycą i w kontroli

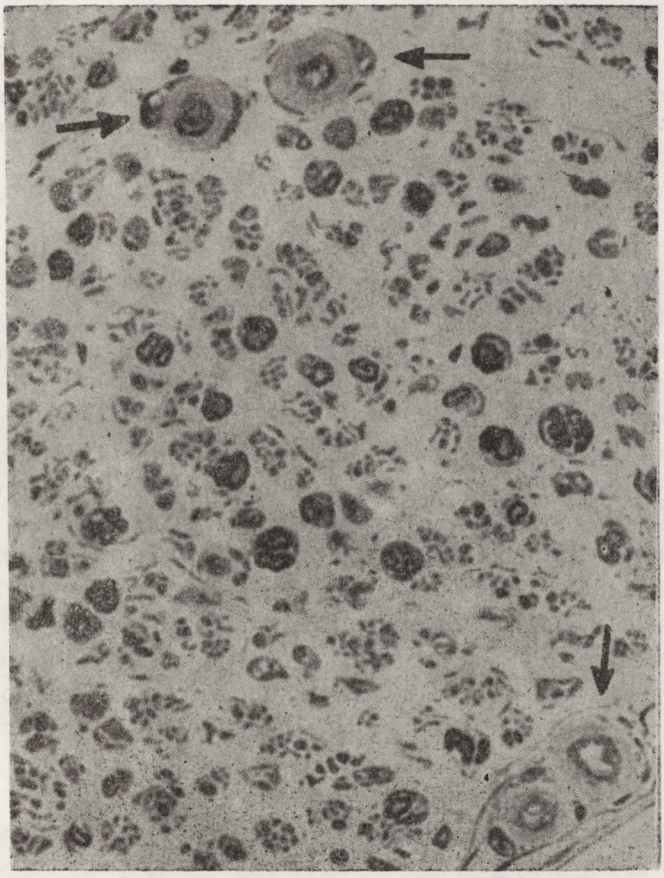

Fig. 2. Diabetic microangiopathy with marked thickening and homogenization of vascular walls (arrows), decrease of nerve fiber density and clusters of regenerating fibers. TAO. × 450

Ryc. 2. Mikroangiopatia cukrzycowa ze znacznym zgrubieniem ścian naczyń i ich homogenizacją (strzałki). Zmniejszenie gęstości włókien nerwowych i gniazda regenerujących włókien. TAO. Pow. 450 ×

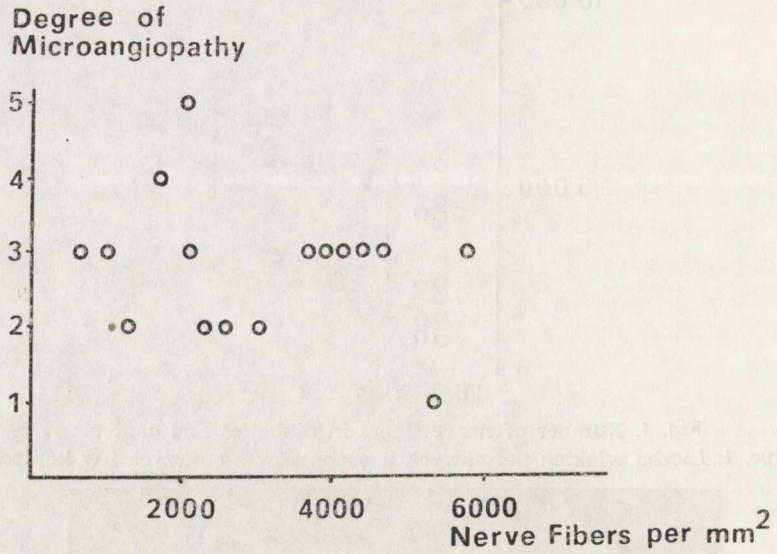

Fig. 3. Correlation between the degree of microangiopathy and fiber density
Ryc. 3. Zależność pomiędzy nasileniem mikroangiopatii i gęstością włókien

DISCUSSION

Diabetes mellitus is a disease that affects a vast number of patients and manifests itself through a large array of signs and symptoms (Thomas, Eliasson 1975; Warzok et al. 1987). More than 50 per cent of patients afflicted with diabetes for 30 years complain of different neurological disturbances which are often difficult to treat. The symptoms are persistent and, at times, unrelenting. To date various causes of diabetic peripheral neuropathy have not been elucidated fully. However, several theories have been proposed, among them microangiopathy with ischemia, sorbitol accumulation, myoinositol deficiency and membrane glycosylation (Clements 1979, Greene 1983, Warzok et al. 1986, 1987). The first theory proposes that microangiopathy results in damage to the nerve cell through hypoxia and neuronal infarction. These microangiopathic changes are thought to affect vessels supplying nutrition to peripheral nerves and lead to sensory, motor and autonomous dysfunctions. The exact mechanisms by which ischemia might cause these changes in nerve morphology are as yet unknown. Although more extensive studies are necessary before a definite answer can be given, our results suggest that other factors that hypoxia caused by microangiopathy are of major importance in the development of nerve fiber loss in diabetic polyneuropathy. We do not deny than hypoxia and microangiopathy play a role in the pathogenesis of diabetic polyneuropathy, however, it seems that it is not justified to regard the diabetic neuropathy first of all as an

expression of microangiopathy. Our own experimental studies showed that in rats, as early as two weeks after the administration of streptozotocin significant electrophysiologic and morphometric changes can be registered. At this time, vessels do not show any changes (Wattig 1985, 1989a,b).

In general the development of diabetic polyneuropathy depends on glucose regulation. However, patients with poor control can be observed, in whom neuropathy never develops although they show microangiopathic changes such as retinopathy. In other cases peripheral neuropathy is registered in newly diagnosed diabetics in whom microvessels show no or unsignificant abnormalities. Our results favour the idea that diabetic neuropathy is the result of metabolic disturbances caused by hyperglycemia and that microangiopathy which develops later in the course of the disease plays a minor role. The role of exogenous and endogenous factors such as drug administration, alcoholism, other concomitant diseases and metabolic disturbances need further elucidation.

ROLA NIEDOTLENIENIA W CHOROBACH NERWÓW OBWODOWYCH

Streszczenie

Przedyskutowano rolę niedotlenienia w chorobach nerwów obwodowych ze szczególnym uwzględnieniem mikroangiopatii cukrzycowej. Za pomocą badań morfometrycznych wykazano znamienny spadek liczby włókien w 1 mm^2 w nerwie strzałkowym pacjentów cukrzycowych w porównaniu z kontrolą. Ustalono ponadto, że nasilenie mikroangiopatii (zgrubienie ściany kapilarów i zwężenie ich światła) wzrasta wraz z czasem trwania cukrzycy. Ubytek włókien nerwowych natomiast nie był skorelowany z nasileniem mikroangiopatii. Autorzy nie negują, że mikroangiopatia może stanowić czynnik patogenny w rozwoju polineuropatii cukrzycowej (zwłaszcza w późniejszych okresach) uważają jednak, że inne zaburzenia metaboliczne, a nie niedotlenienie spowodowane mikroangiopatią, mają większy udział w uszkodzeniu nerwów obwodowych.

REFERENCES

1. Greene D. A.: Metabolic abnormalities in diabetic peripheral nerves: relation to impaired function. Metabolism, 1983, 32 (Suppl. 1), 118-123.
2. Sievers J.: Basic two-dye stains for epoxy embedded 0.3-1 μ sections. Stain Technol, 1971, 46, 195-199.
3. Thomas P. K., Eliasson S. G.: Diabetic neuropathy. In: Peripheral neuropathy. Eds.: Dyck P. J., Thomas P. K., Lambert E. W. Saunders, Philadelphia, 1975, pp. 1773-1810.
4. Warzok R., Rudel J., Wattig B.: Biochemische Aspekte der diabetischen Polyneuropathie. Wiss Z Univ Greifswald, 1986, 35, 33-35.
5. Warzok R., Wattig B., Rudel J., Schwanengel H., Timmel A.: Morphologie der diabetischen Neuropathie. Zentralbl Allg Pathol, 1987, 133, 119-126.

6. Wattig B.: Die experimentelle diabetische Polyneuropathie — Morphometrische Untersuchungen am *N. suralis* und *N. tibialis posterior* der Ratte. Thesis, Universität Greifswald, 1985.
7. Wattig B., Warzok R., Röder H., Hufnagl P., Huyoff K.: Untersuchungen an peripheren Nerven der nichtdiabetischen Ratte nach Streptozotocin-Applikation mit Hilfe der automatischen Mikroskopbildanalyse. Gegenbauers Morphol Jahrb, 1989a, 135, 103-108.
8. Wattig B., Warzok R., Zglinicki T.: Morphometrische Untersuchungen an peripheren Nerven und Spinalganglien bei Streptozotocin-diabetischen Ratten. Gegenbauers Morphol Jahrb, 1989b, 135, 207-210.

Authors' address: Prof. Dr. R. Warzok, University of Greifswald, Department of Pathology, DDR 2200 Greifswald, GDR

NEUROPAT. POL. 1990, 28, 3-4
PL ISSN 0028-3894

PRZEMYSŁAW NOWACKI, ANNA STAŃKOWSKA-CHOMICZ,
MARIA BORODIN

FIBRINOGEN DEGRADATION PRODUCTS IN SERUM AND CEREBROSPINAL FLUID IN CEREBROVASCULAR DISEASES

Department of Neurology and Department of Clinical Biochemistry Pomeranian School of Medicine, Szczecin, Poland

The increase of fibrinogen degradation products (FDP) represents a very sensitive test for activated secondary fibrinolysis, concomitant with many diseases (McNicol 1971; Hewitt, Davies 1983; Kuratowska 1984; Rybicki et al. 1987). Recently, much attention is devoted to the presence of FDP in cerebrospinal fluid (CSF) in patients with neurological disorders (Brueton 1976; Myśliwiec 1978; Nowak et al. 1984). It could be interesting to become closer acquinted with FDP in the CSF of patients with ischemic stroke. The increase of FDP in these cases can testify to activated fibrinolysis and blood-brain barrier efficiency in stroke. We have attempted to establish what is the serum and CSF FDP level in patients with ischemic stroke. We have also tried to answer whether there is a relationship between FDP levels in the serum and CSF.

MATERIAL AND METHODS

The investigations were carried out in 66 patients of both sexes divided into two groups. Group 1 included 20 patients aged from 25 to 87 years ($\bar{x} = 60.7$) suffered from a transient ischemic attack or reversible ischemic stroke. Group 2 was subdivided into 2 groups: 2a — consisted of 16 patients with progressive or complete stroke uncomplicated by serious general state; 2b — included 10 patients with the same type of stroke as in group 2a, but complicated by severe general condition. The patients' age in the group 2 ranged from 51 to 82 years ($\bar{x} = 61.6$). The control group consisted of 20 patients aged 18-59 years ($\bar{x} = 35.9$), who suffered from neurosis, vasomotor headache or essential epilepsy.

Paper presented at Symposium on Neurobiology of Cerebral Ischemia and Hypoxia. Poznań, June 29-July 1, 1989.

The concentration of FDP in the serum and CSF was determined accordin to Merskey.

RESULTS

Table 1 presents FDP level in serum and CSF.

A statistically significant increase of FDP in the CSF was observed in group 2b as compared with groups 1, 2a and the control one. Some patients of the group 2b exhibited moderately elevated FDP levels in the serum.

Table 1. FDP level in serum and CSF

Tabela 1. Poziom produktów rozpadu fibrynogenu (FDP) w surowicy i w płynie mózgowo-rdzeniowym (CSF)

Group Grupa	FDP (μg/ml) serum	 CSF
1	$\bar{x} = 5.33$ 3.0—15.0	$\bar{x} = 0.34$ 0.14—0.6
2a	$\bar{x} = 6.35$ 2.0—17.0	$\bar{x} = 0.38$ 0.10—0.6
2b	$\bar{x} = 7.24$ 2.0—25.0	$\bar{x} = 1.22$* 0.50—6.0
Control Kontrola	$\bar{x} = 4.20$ 3.0—6.0	$\bar{x} = 0.29$ 0.10—0.5

* Statistically significant.
* Statystycznie znamienny.

Table 2 shows correlation between FDP level in serum and CSF.

In the group 1 and 2a positive correlations were found between the FDP level in the serum and CSF. No such correlation was noted for patients included in group 2b.

Table 2. Correlation between FDP level in serum and CSF

Tabela 2. Korelacja pomiędzy poziomem produktów rozpadu fibrynogenu (FDP) w surowicy i w płynie mózgowo-rdzeniowym (CSF)

Group 1 Grupa 1	Group 2a Grupa 2a	Group 2b Grupa 2b
$R = 0.5741$ $p < 0.05$	$R = 0.5387$ $p < 0.05$	$R = 0.3651$ SN

SN — statistically nonsignificant.
SN — statystycznie nieznamienne.

DISCUSSION

It seems that FDP are transferred from the blood to the CSF becoming a normal constituent of CSF, also in cases with normal FDP concentration in the serum (1-10 μg/ml). Therefore FDP were found in the CSF in different neurological disorders for example multiple sclerosis, amyotrophic lateral sclerosis, and even in muscular diseases (Nowak et al. 1984). We believe that FDP presence in the CSF in our patients depends on the penetration of FDP from the serum into CSF. This has been confirmed by the positive correlations between FDP levels in the serum and CSF in our cases. It is worth noting that patients in group 2b had a statistically significant increase of FDP in CSF, while elevation of FDP in the serum was little pronounced (12-25 μg/ml). The FDP content in the CSF was never higher than the level in the serum. This contradicts FDP production in the CSF. Maybe a serious general condition complicating severe ischemic stroke increases the permeation of FDP into the CSF due to blood-brain barrier impairment. Most patients with high FDP concentration in the CSF died a few days after stroke onset, so such a distinct FDP elevation in the CSF in patients with complete severe ischemic stroke could be an indicator of unfavourable prognosis. The normal FDP levels in serum in patients groups 1 and 2a, and usually a slight increase in group 2b, suggest that activated fibrinolysis does not play an important role in the pathogenesis of ischemic stroke.

CONCLUSIONS

1. In patients with ischemic stroke FDP levels in the serum and CSF are usually low. Activated fibrinolysis does not play an important role in the pathogenesis of ischemic stroke.

2. The positive correlation between FDP levels in serum and CSF also in cases with normal FDP concentration in serum, suggests that FDP are transferred from the blood to the CSF and appear as the normal constituent of the latter.

3. Distinct FDP elevation in the CSF occurring in some patients with severe stroke complicated by serious general state is an unfavourable prognostic factor.

PRODUKTY ROZPADU FIBRYNOGENU W SUROWICY KRWI I W PŁYNIE MÓZGOWO-RDZENIOWYM W CHOROBACH NACZYNIOWYCH MÓZGU

Streszczenie

Oceniono zawartość produktów rozpadu fibrynogenu (FDP) w surowicy i w płynie mózgowo-rdzeniowym u 66 pacjentów w wieku 25-87 lat, z udarem niedokrwiennym mózgu. W zależności od ciężkości udaru i stanu ogólnego chorych ma-

teriał podzielono na 2 grupy: z przemijającym, odwracalnym udarem (20 pacjentów) oraz z postępującym lub pełnym udarem i dobrym (16 pacjentów) oraz ciężkim (10 pacjentów) stanem ogólnym. Ustalono, że poziom FDP u pacjentów z udarem niedokrwiennym jest niski zarówno w surowicy, jak i w płynie mózgowo-rdzeniowym, z czego wynika, że aktywacja procesu fibrynolizy nie ma istotnego znaczenia w patomechanizmie udaru niedokrwiennego. Wykazano ponadto dodatnią korelację pomiędzy zawartością FDP w surowicy i w płynie mózgowo-rdzeniowym, również w przypadkach z prawidłowym stężeniem FDP w surowicy, co wskazuje, że FDP są transportowane z krwi do płynu mózgowo-rdzeniowego. Znaczny wzrost poziomu FDP w płynie mózgowo-rdzeniowym, jaki stwierdzono u pacjentów udarowych będących w ciężkim stanie ogólnym, można traktować jako czynnik rokujący niepomyślny przebieg choroby.

REFERENCES

1. Brueton M. J.: Fibrinogen degradation products in cerebrospinal fluid. J Clin Pathol, 1976, 29, 341-346.
2. Hewitt P., Davies S.: The current state of DIC. Intensive Care Med, 1983, 9, 249-253.
3. Kuratowska Z.: O produktach rozpadu fibrynogenu (FDP) i hemostazie. Pol Tyg Lek, 1984, 39, 349-351.
4. McNicol G. P.: Fibrinogen degradation products (FDP) in renal disease, estimation and significance of FDP in urine. Scand J Haematol, 1971, 13, 329-335.
5. Myśliwiec B.: Produkty degradacji fibrynogenu (FDP) w ropnych zapaleniach opon mózgowo-rdzeniowych u dzieci. Pol Tyg Lek, 1978, 31, 1213-1216.
6. Nowak S., Zioło H., Błaszczyk B.: Produkty degradacji fibryny-fibrynogenu w płynie mózgowo-rdzeniowym chorych neurologicznie. Neurol Neurochir Pol, 1984, 18, 542-545.
7. Rybicki Z., Szepietowski J., Zalewski A., Kański A., Żmijewski Z.: Doświadczenia własne w rozpoznawaniu i leczeniu zespołu wykrzepiania wewnątrznaczyniowego. Anest Intens Terap, 1987, 19, 5-11.

Authors' address: Dept. of Neurology, 1, Unii Lubelskiej Str., 71-344 Szczecin, Poland.

NEUROPAT. POL. 1990, 28, 3-4
PL ISSN 0028-3894

MIECZYSŁAW WENDER, ZOFIA ADAMCZEWSKA-GONCERZEWICZ, ANDRZEJ ŻÓRAWSKI, JOLANTA DORSZEWSKA, DANUTA TALKOWSKA, JADWIGA PANKRAC

INFLUENCE OF MODERATE HYPOXIA ON THE COMPOSITION OF FATTY ACIDS IN MYELIN LIPIDS

Department of Neurology, School of Medicine, Poznań, Poland

The myelin-oligodendroglia complex is relatively sensitive to the action of hypoxia or ischemia. A high intensity of these noxious agents leads to necrotic changes in the white matter or to demyelination, while less pronounced stimuli provoke only some derangement of the membraneous structures of myelin (Traugot, Raine 1984). Concomitantly with structural changes, deviations in the chemistry of myelin and other components of the white matter are observed (Aveidano, Bazan 1975; Cenedella et al. 1975; Gardiner et al. 1981). Deviations in myelin lipids involve a marked increase in cholesterol esters and lysophosphatidylcholine content in the myelin fraction (Wender et al. 1988a). In experimental rats subjected to hypoxia there occurs also a sharp increase of the free fatty acid pool in the cerebral white matter, with a striking excess of polyunsaturated fatty acids, especially of arachidonic (20 : 4) and nervonic acids (20 : 1) (Wender et al. 1988b).

The question as to which lipids of myelin or other cellular and subcellular structures of the white matter are affected by degradation and subsequently are responsible for the rise of the free fatty acids pool is unclear so far. Therefore, in order to answer this question at least partially we studied the changes in the pattern of fatty acids of the main myelin phospholipids. We also examined this spectrum in cholesterol esters and in lysophosphatidylcholine, whose contents significantly increase after hypoxia, which seems to be related with the pathomechanism of white matter lesions.

MATERIAL AND METHODS

The experiments were performed on white Wistar rats, each weighing 200-250 g, exposed to mild hypoxia (7% of oxygen in a respiratory mixture for 30 min) in a specially constructed glass chamber. Appropriate

composition of gases in the chamber was secured by feeding the gases through a flowmeter and rotameter. A normal level of body temperature (37°C) was maintained by heating the experimental rats with a lamp. The animals were sacrificed 4 hrs, 24 hrs, 14 days and 2 months after hypoxia, by decapitation in light halotane anesthesia. The heads were immediately placed in liguid nitrogen. The white matter was isolated in the cold room at 0°C.

Biomedical methods. The myelin fraction was isolated by means of differental centrifugation according to Norton and Poduslo (1973). Total lipids were extracted from the myelin fraction by the method described by Folch-Pi et al. (1957) and further separated by means of combined column and thin layer chromatography. The details of the methods used may be found in our previous publication (Wender et al. 1978).

The myelin phosphatidylcholine, lysophosphotidylcholine, phosphatidylethanolamine, plasmalogen and cholesterol esters were subjected to methanolysis, and the fatty acyl methyl esters obtained in this way were separated by means of gas-liquid chromatography on the Pye 104 gas chromatograph equipped with a ionizing detector. The columns were packed with 15% diethylene-glycol-succinate (DEGS) adsorbed on Gas-chrom Q 100/120 mesh. Column temperature 280°C with Argon as carrier gas. Gas flow 30 ml/min.

The fatty acids were identified by comparison of the respective peaks of the experimental chromatograms with those corresponding to a mixture of standard fatty acyl methyl esters (Applied Sciences Laboratories). The chromatograms were quantitated by computing the areas of the respective peaks from the retention times and the heights of these peaks. The results were expressed in relative percentages.

RESULTS

The clinical symptoms and the morphological pattern of the central nervous system after the action of moderate hypoxia on the experimental rats were identical to those presented in our previous publication (Wender et al. 1988). A well defined myelinopathy was never observed.

Results obtained in chemical studies are presented in detail in Tables 1-5.

Analysis of the fatty acid spectrum of phosphatidylcholine obtained by means of gas-liquid chromatography demonstrated in the experimental animals in all studied periods a very marked drop of total unsaturated fatty acids, of total monoenes unsaturated ones, and among the particular fatty acids of oleic acid (18 : 1).

The lysophosphatidylcholine of the myelin fraction was markedly abnormal in two experimental periods: 4 hours and 2 months after the action of hypoxia, in which the percentage of almost all subgroups of

Table 1. Fatty acids of phosphatidylcholine of the myelin fraction after moderate hypoxia
Tabela 1. Kwasy tłuszczowe fosfatydylocholiny frakcji mielinowej po umiarkowanym niedotlenieniu

Fatty acids Kwasy tłuszczowe	Control Norma	4 hours 4 godz.	24 hours 24 godz.	14 days 14 dni	2 months 2 miesiące
1	2	3	4	5	6
12 : 0	0.2±0.04	0.6±0.1*	0.7±0.1*	1.2±0.5	0.1±0.02
14 : 0	1.7±0.1	1.8±0.6	0.6±0.1**	1.7±0.7	0.6±0.1**
15 : 0	0.4±0.06	0.6±0.2	0.3±0.03	0.5±0.1	0**
16 : 0	19.5±1.3	24.9±1.6*	19.7±1.9	17.1±0.9	14.4±1.0
16 : 1	1.3±0.4	2.5±0.7	2.0±0.5	2.2±0.7	1.2±0.3
17 : 0	0.4±0.05	0.8±0.1**	1.6±0.6	2.0±1.3	5.3±0.7
18 : 0	14.2±1.5	20.1±0.4**	19.6±0.3**	13.3±1.6	14.9±1.3
18 : 1	29.2±2.3	19.4±1.6	8.5±1.0**	13.4±2.6**	3.5±0.5**
18 : 2	5.4±0.9	2.9±0.1*	5.9±1.3	5.2±1.2	10.1±0.7**
18 : 3	0.3±0.07	0.4±0.1	0.4±0.02	0.5±0.2	8.8±1.0**
20 : 0	1.8±0.09	1.2±0.2*	5.6±1.5*	2.2±1.2	0.3±0.03**
20 : 1	2.3±0.3	2.8±1.7	5.0±0.3**	0.4±0.1**	9.3±0.9**
20 : 2	1.1±0.2	0.7±0.2	1.0±0.3	0.9±0.3	0.6±0.05**
20 : 3	1.7±0.2	1.2±0.3	1.0±0.2*	1.4±0.9	5.8±0.5
20 : 4	5.0±0.6	1.1±0.2**	1.9±0.2**	20.2±3.9**	1.8±0.3**
20 : 5	1.5±0.6	4.8±0.7**	4.8±0.6**	1.8±0.6	2.0±0.1
24 : 0	6.3±1.2	3.2±0.4*	1.4±0.1**	8.0±1.5	1.3±0.3
24 : 1	1.2±0.2	0.8±0.4	2.3±0.3**	0**	0.1±0.1**
22 : 5	0	2.3±0.3**	2.5±0.2	1.8±0.5**	3.9±0.4**
22 : 6	3.8±0.4	0.6±0.4**	4.6±0.4	1.4±0.4**	2.0±0.5*
Unidentified Niezidentyfikowane	2.8±0.8	7.3±1.4	10.8±1.6*	4.8±1.9	13.5±1.1
Total saturated Całkowite nasycone	44.1±1.4	53.3±1.9	49.4±0.9*	45.9±1.5	37.0±0.8**
Total unsaturated Całkowite nienasycone	53.7±1.2	39.4±1.9	39.9±0.7	49.0±1.6	48.6±3.1
Total 1-unsaturated Całk. 1-nienasycone	34.5±3.3	25.3±1.5	17.9±1.4	19.2±4.0	14.0±1.1
Total 2-unsaturated Całk. 2-nienasycone	8.9±0.9	3.6±0.2	7.0±1.0	6.1±1.2	10.8±1.1
Total 3-unsaturated Całk. 3-nienasycone	1.6±0.1	1.7±0.4	1.1±0.2	1.9±0.8	14.7±1.4
Total 4-unsaturated Całk. 4-nienasycone	4.1±0.4	1.1±0.2	2.0±0.2	20.0±3.8	1.8±0.3
Total 5-unsaturated Całk. 5-nienasycone	0.7±0.2	7.1±0.7	7.3±0.6	3.6±0.4	5.9±0.5
Total 6-unsaturated Całk. 6-nienasycone	3.9±0.4	0.6±0.4	4.6±0.4	1.4±0.2	1.4±0.3
Unidentified Niezidentyfikowane	2.2±0.5	7.3±1.4	10.7±0.8	5.1±0.7	14.4±2.6

Mean ± SEM.
Średnia ± średni błąd średniej.
* Difference significant at the level $p \leqslant 0.05$.
Różnica istotna przy poziomie $p \leqslant 0{,}05$.
** Difference significant at the level $p \leqslant 0.01$.
Różnica istotna przy poziomie $p \leqslant 0{,}01$.
Number of animals in each group: 6.
Liczba zwierząt w każdej grupie: 6.

Table 2. Fatty acids of lysophosphatidylcholine of the myelin fraction after moderate hypoxia
Tabela 2. Kwasy tłuszczowe lizofosfatydylocholiny frakcji mielinowej po umiarkowanym niedotlenieniu

Fatty acids Kwasy tłuszczowe	Control Norma	4 hours 4 godz.	24 hours 24 godz.	14 days 14 dni	2 months 2 miesiące
1	2	3	4	5	6
12 : 0	0.2±0.05	1.3±0.3**	1.3±0.3**	1.2±0.2**	0.6±0.2*
14 : 0	3.1±0.1	0.8±0.1**	2.0±0.5*	1.5±0.4**	0.8±0.2**
15 : 0	0.6±0.04	0.3±0.2	0.4±0.08*	0.6±0.04	0**
16 : 0	17.8±1.3	19.1±0.9	19.0±0.7	17.5±1.6	10.2±1.7**
16 : 1	1.9±0.4	3.8±0.5*	2.4±0.1	2.5±0.6	2.4±0.6**
17 : 0	0.5±0.05	1.0±0.1**	0.7±0.1	0.8±0.1	5.8±1.2**
18 : 0	11.0±1.5	12.5±0.7	16.0±1.3*	11.9±1.5	11.3±0.4
18 : 1	26.6±2.6	26.6±1.8	21.4±1.9	26.4±1.8	11.4±2.2**
18 : 2	10.1±0.9	5.4±0.8**	5.3±0.1**	9.6±1.0	13.0±1.5
18 : 3	0.3±0.07	0.8±0.3	0.4±0.05	0.6±0.1	10.6±2.0**
20 : 0	2.9±0.2	1.2±0.1**	1.5±0.1**	3.2±0.6	1.5±1.1
20 : 1	1.4±0.3	7.5±1.5**	8.0±1.1**	0.7±0.5	11.4±0.7**
20 : 2	0.8±0.3	1.2±0.2	1.1±0.2	1.1±0.3	0.9±0.2
20 : 3	1.1±0.1	2.2±0.4*	1.0±0.1	2.4±0.5*	5.5±0.7**
20 : 4	4.2±0.3	1.4±0.6**	0.4±0.2**	7.3±1.6	0.7±0.07**
20 : 5	1.2±0.5	2.2±0.4	2.5±0.4	1.3±0.4	1.0±0.1
24 : 0	8.8±1.4	2.6±0.4**	2.4±0.3**	6.6±1.9	0.8±0.4**
24 : 1	0.4±0.1	0.5±0.3	1.5±0.6	0	0.6±0.6
22 : 5	0	1.9±0.7*	3.8±1.6	0.6±0.4	4.2±0.9
22 : 6	5.0±0.7	4.3±0.7	5.4±1.5	0.7±0.5**	0.2±0.1
Unidentified Niezidentyfikowane	1.6±0.5	3.4±1.5	3.5±1.3	3.5±2.0	7.1±1.5
Total saturated Całkowite nasycone	44.9±1.1	38.7±1.0**	43.2±1.6	43.2±2.2	31.1±0.9**
Total unsaturated Całk. nienasycone	53.3±0.7	57.6±1.6*	53.3±2.5	53.4±1.9	62.0±1.3**
Total 1-unsaturated Cał. 1-nienasycone	30.4±1.5	38.3±1.2**	33.3±1.8	29.4±2.1	25.9±2.3
Total 2-unsaturated Całk. 2-nienasycone	11.1±0.5	6.6±0.9**	6.4±0.2**	9.2±0.6	13.7±1.6
Total 3-unsaturated Całk. 3 nienasycone	1.4±0.1	3.0±0.6*	1.4±0.1	3.2±0.6*	16.4±2.2**
Total 4-unsaturated Całk. 4-nienasycone	4.2±0.3	1.4±0.6**	0.4±0.2**	8.5±1.5*	0.7±0.1**
Total 5-unsaturated Całk. 5-nienasycone	1.2±0.5	4.0±0.8*	6.4±2.0*	2.4±0.5	5.1±0.9**
Total 6-unsaturated Całk. 6-nienasycone	5.0±0.7	4.3±0.7	5.4±1.5	0.7±0.4	0.2±0.1**
Unidentified Niezidentyfikowane	1.8±0.6	3.7±1.0	3.5±1.0	3.4±1.2	6.9±0.8**

Mean ± SEM.
Średnia ± średni błąd średniej.
* Difference significant at the level $p < 0.05$.
Różnica istotna przy poziomie $p < 0{,}05$.
** Difference significant at the level $p < 0.01$.
Różnica istotna przy poziomie $p < 0{,}01$.
Number of animals in each group: 6.
Liczba zwierząt w każdej grupie: 6.

Table 3. Fatty acids of phosphatidylethanolamine of the myelin fraction after moderate hypoxia
Tabela 3. Kwasy tłuszczowe fosfatydyloetanoloaminy frakcji mielinowej po umiarkowanym niedotlenieniu

Fatty acids Kwasy tłuszczowe	Control Norma	4 hours 4 godz.	24 hours 24 godz.	14 days 14 dni	2 months 2 miesiące
1	2	3	4	5	6
12 : 0	0.2±0.04	0.7±0.1**	1.1±0.3**	1.2±0.2**	0.4±0.1
14 : 0	2.4±0.3	1.2±0.5	1.3±0.4*	1.7±0.2	0.8±0.2**
15 : 0	0.4±0.05	0.5±0.2	0.4±0.1	0.3±0.04	0**
16 : 0	15.2±1.2	16.7±1.1	15.6±1.9	13.3±1.2	9.9±1.4*
16 : 1	1.5±0.2	3.2±0.4**	2.6±0.5	1.8±0.3	2.0±0.3
17 : 0	0.5±0.2	1.2±0.2*	1.4±0.3	0.4±0.05	4.8±0.9**
18 : 0	20.0±1.8	23.9±0.7	20.6±2.2	24.6±2.5	13.8±1.1*
18 : 1	27.1±1.9	25.5±1.5	16.8±1.8**	15.2±1.2**	10.1±2.3**
18 : 2	6.8±0.6	5.6±0.6	4.4±0.9*	6.5±0.7	15.7±1.9**
18 : 3	0.2±0.03	0.7±0.1**	0.6±0.2*	0.2±0.04	9.8±1.7**
20 : 0	1.8±0.1	1.7±0.3	4.2±1.5	0.7±0.1**	0.5±0.02**
20 : 1	2.9±0.4	4.2±1.7	3.6±0.4	0.3±0.1*	10.3±1.1**
20 : 2	0.4±0.03	1.0±0.1*	3.0±0.7**	0.6±0.1*	0.9±0.1**
20 : 3	1.0±0.2	2.0±0.5	0.9±0.1	0.5±0.1*	4.3±0.5*
20 : 4	4.8±0.5	0.9±0.2**	2.1±0.4**	9.6±1.7*	1.1±0.2**
20 : 5	0.2±0.06	2.6±0.1**	2.7±0.8**	0.9±0.2**	3.0±0.3**
24 : 0	6.3±1.1	2.2±0.4**	3.7±0.6	8.6±1.9	2.2±0.3**
24 : 1	0.4±0.1	0**	1.0±0.6	0**	0.2±0.1
22 : 5	0	2.3±0.6*	4.6±1.0**	4.3±0.6	1.7±0.4**
22 : 6	2.0±0.3	0**	5.5±1.6*	3.4±0.6*	2.7±0.6
Unidentified Niezidentyfikowane	5.9±1.7	3.7±1.4	3.1±1.8	5.9±2.5	5.8±0.2
Total saturated Całkowite nasycone	46.8±1.1	48.3±2.0	48.2±1.8	50.8±3.1	32.3±1.8**
Total unsaturated Całk. nienasycone	47.3±1.3	47.9±1.3	47.8±2.1	43.5±3.6	62.7±2.5**
Total 1-unsaturated Całk. 1-nienasycone	31.8±1.6	32.9±0.9	24.2±2.6**	17.3±1.4**	22.9±3.2*
Total 2-unsaturated Całk. 2-nienasycone	7.2±0.2	6.5±0.8	7.3±1.4	7.1±0.6	16.7±2.1
Total 3-unsaturated Całk. 3-nienasycone	1.2±0.2	2.7±0.5*	1.5±0.2	0.6±0.05**	14.5±2.1**
Total 4-unsaturated Całk. 4-nienasycone	4.8±0.6	0.9±0.2**	2.1±0.4**	9.9±1.7*	1.1±0.2**
Total 5-unsaturated Całk. 5-nienasycone	0.3±0.1	4.9±0.8**	7.2±1.2**	5.2±0.7**	4.8±0.6**
Total 6-unsaturated Całk. 6-nienasycone	2.0±0.3	0,0**	5.5±1.6*	3.4±0.6	2.7±0.7
Unidentified Niezidentyfikowane	5.9±1.5	3.8±1.3	4.0±1.4	5.7±1.1	5.0±1.1

Mean ± SEM.
Średnia ± średni błąd średniej.
* Difference significant at the level $p \leqslant 0.05$.
Różnica istotna przy poziomie $p \leqslant 0,05$.
** Difference significant at the level $p \leqslant 0.01$.
Różnica istotna przy poziomie $p \leqslant 0,01$.
Number of animals in each group: 6.
Liczba zwierząt w każdej grupie: 6.

Table 4. Fatty acids of plasmalogens of the myelin fraction after moderate hypoxia

Tabela 4. Kwasy tłuszczowe plazmalogenów frakcji mielinowej po umiarkowanym niedotlenieniu

Fatty acids Kwasy tłuszczowe	Control Norma	4 hours 4 godz.	24 hours 24 godz.	14 days 14 dni	2 months 2 miesiące
1	2	3	4	5	6
12 : 0	0.2±0.04	0.7±0.2*	1.6±0.7*	1.5±0.4**	0.4±0.1
14 : 0	2.1±0.2	1.6±0.3	1.6±0.3	2.0±0.3	0.6±0.1**
15 : 0	0.4±0.03	0.6±0.2	0.5±0.1	0.4±0.1	0**
16 : 0	10.6±0.8	20.9±1.6**	17.6±0.6**	14.5±0.9**	9.2±1.3
16 : 1	1.3±0.2	3.7±0.8*	4.0±1.2	1.6±0.1	1.0±0.2
17 : 0	0.4±0.1	1.0±0.2*	1.1±0.1**	0.6±0.1	7.8±0.4**
18 : 0	6.4±0.6	12.5±0.7**	12.2±0.3**	5.7±0.3	11.4±0.08**
18 : 1	37.3±1.3	29.6±1.2**	18.8±2.0**	24.9±2.8**	9.6±1.3**
18 : 2	6.6±0.8	5.3±0.5	5.0±0.3	8.6±1.1	12.5±1.0**
18 : 3	0.3±0.06	0.8±0.3	0.5±0.06*	0.3±0.1	9.6±0.8**
20 : 0	1.6±0.1	3.3±0.5**	1.3±0.1	0.8±0.1**	0.8±0.1**
20 : 1	12.5±1.0	2.8±0.7**	4.5±1.0**	0.6±0.1**	10.1±0.4*
20 : 2	0.5±0.1	1.1±0.2*	0.6±0.2	2.0±0.3**	0.8±0.1*
20 : 3	1.5±0.05	1.6±0.4	1.5±0.4	1.3±0.2	3.2±0.3**
20 : 4	4.8±0.4	2.0±0.4**	3.3±0.4*	8.6±0.8**	2.0±0.2**
20 : 5	0.3±0.1	2.8±0.4**	3.9±0.8**	1.5±0.1**	2.3±0.3**
24 : 0	7.6±1.1	2.3±0.5**	1.9±0.4**	13.0±1.0**	1.7±0.2**
24 : 1	0.2±0.05	0**	1.9±0.1**	0.2±0.2	0.5±0.3
22 : 5	0	3.3±0.6**	3.5±0.4	1.9±0.9	1.6±0.5*
22 : 6	1.2±0.5	0	5.7±0.7**	3.7±1.3	3.4±0.7*
Unidentified Niezidentyfikowane	4.2±1.3	4.1±2.7	9.0±2.8	6.3±2.4	11.5±4.5
Total saturated Całkowite nasycone	29.3±1.2	42.9±2.3**	37.9±1.1**	38.9±1.6**	31.9±1.4
Total unsaturated Całk. nienasycone	66.2±0.8	53.1±1.4**	53.1±2.2**	55.1±1.8**	56.6±1.4**
Total 1-unsaturated Całk. 1-nienasycone	51.1±1.5	36.1±1.5**	29.2±3.6**	27.3±2.9**	21.2±1.3**
Total 2-unsaturated Całk. 2-nienasycone	7.1±0.8	6.4±0.6	5.6±0.4	10.6±1.1*	13.3±1.1**
Total 3-unsaturated Całk. 3-nienasycone	1.7±0.1	2.5±0.5	1.9±0.4	1.6±0.2	12.8±0.9**
Total 4-unsaturated Całk. 4-nienasycone	4.8±0.4	2.0±0.4**	3.3±0.4*	8.5±0.8**	2.0±0.2**
Total 5-unsaturated Całk. 5-nienasycone	0.3±0.1	6.1±0.6**	7.4±1.2*	3.4±0.9**	3.9±0.5**
Total 6-unsaturated Całk. 6-nienasycone	1.2±0.6	0	5.7±0.7**	3.7±0.8*	3.4±0.7*
Unidentified Niezidentyfikowane	4.5±0.6	4.0±1.1	9.0±2.2	6.0±0.9	11.5±2.2*

Mean ± SEM.

Średnia ± średni błąd średniej.

* Difference significant at the level $p < 0.05$.
Różnica istotna przy poziomie $p < 0,05$.

** Difference significant at the level $p < 0.01$.
Różnica istotna przy poziomie $p < 0,01$.

Number of animals in each group: 6.

Liczba zwierząt w każdej grupie: 6

Table 5. Fatty acids of cholesterol esters of tjhe myelin fraction after moderate hypoxia
Tabela 5. Kwasy tłuszczowe estrów cholesterolu frakcji mielinowej po umiarkowanym niedotlenieniu

Fatty acids Kwasy tłuszczowe	Control Norma	4 hours 4 godz.	24 hours 24 godz.	14 days 14 dni	2 months 2 miesiące
1	2	3	4	5	6
12 : 0	0.5±0.4	1.0±0.1	1.1±0.1*	1.2±0.3*	0.8±0.2
14 : 0	3.8±0.4	2.8±0.7	2.7±0.8	2.0±0.4*	1.8±0.3**
15 : 0	1.1±0.1	0.6±0.05**	0.9±0.2	0.3±0.1**	0**
16 : 0	18.0±1.1	21.5±1.6	22.8±1.8*	18.8±1.5	15.6±1.6
16 : 1	6.7±0.5	5.1±0.6	4.7±1.3	5.6±1.0	4.8±0.4
17 : 0	2.3±0.7	1.8±0.2	2.1±0.3	0.8±0.1	2.6±0.4
18 : 0	9.4±0.5	16.0±1.1**	14.1±1.1**	6.6±0.5**	11.2±0.4**
18 : 1	25.5±1.1	21.3±1.2*	17.2±1.1*	21.9±2.1	16.1±1.8**
18 : 2	10.3±1.3	4.6±0.3**	4.0±0.5**	8.9±0.7	9.1±1.4
18 : 3	2.3±1.0	1.8±0.3	1.7±0.7	0.1±0.03*	6.8±1.1*
20 : 0	3.6±0.4	2.0±0.5*	0.4±0.2**	1.1±0.1**	0.5±0.05**
20 : 1	0.9±0.05	2.8±0.5**	3.7±1.2*	0.4±0.04**	9.6±0.1**
20 : 2	0.5±0.1	1.5±0.3**	4.2±1.2**	0.7±0.1	0.8±0.2
20 : 3	0.8±0.1	1.6±0.4	1.6±0.5	0.7±0.1	5.5±0.3**
20 : 4	3.8±0.6	1.2±0.4**	0.6±0.3**	7.1±1.6	1.2±0.1**
20 : 5	0.7±0.1	2.4±0.4**	1.9±0.6	1.7±0.5	2.3±0.3**
24 : 0	2.5±0.5	1.8±0.2	1.9±0.5	6.5±0.7**	2.7±0.3
24 : 1	0.7±0.1	0.5±0.5	1.6±0.5	2.1±0.8	0.3±0.3
22 : 5	0	3.6±0.7	3.2±1.0**	3.4±1.0	2.1±0.7*
22 : 6	3.3±0.4	1.1±0.9	5.0±1.4	0.9±0.6**	4.8±0.5
Unidentified Niezidentyfikowane	3.3±1.1	5.0±1.6	4.6±2.5	9.2±3 3	1.4±0.6
Total saturated Całkowite nasycone	41.1±1.5	47.6±1.0	46.1±2.2	37.4±1.6	34.8±2.2*
Total unsaturated Całk. nienasycone	55.3±1.5	47.5±0.8**	49.3±1.8*	54.5±1.7	63.7±1.8**
Total 1-unsaturated Całk. 1-nienasycone	33.6±0.3	29.6±1.1**	27.1±1.5**	30.0±1.8	30.9±1.5
Total 2-unsaturated Całk. 2-nienasycone	10.8±1.1	6.1±0.4**	8.1±1.2	9.7±0.8	10.0±1.3
Total 3-unsaturated Całk. 3-nienasycone	3.2±1.1	3.4±0.4	3.3±1.1	0.8±0.2	12.3±1.3**
Total 4-unsaturated Całk. 4-nienasycone	3.7±1.1	1.2±0.4	0.6±0.3*	8.0±1.5*	1.2±0.1
Total 5-unsaturated Całk. 5-nienasycone	0.7±0.2	6.1±1.0**	5.2±1.3**	5.1±1.0**	4.4±1.0**
Total 6-unsaturated Całk. 6-nienasycone	3.3±0.4	1.1±0.9*	5.0±1.4	0.9±0.2**	4.9±0.5*
Unidentified Niezidentyfikowane	3.6±0.9	4.9±0.9	4.6±1.8	8.1±1.5*	1.5±0.5

Mean ± SEM.
Średnia ± średni błąd średniej.
* Difference significant at the level $p \leqslant 0.05$.
Różnica istotna przy poziomie $p \leqslant 0{,}05$.
** Difference significant at the level $p \leqslant 0.01$.
Różnica istotna przy poziomie $p \leqslant 0{,}01$.
Number of animals in each group: 6.
Liczba zwierząt w każdej grupie: 6.

fatty acids (total saturated, total unsaturated, total mono- to hexaenes fatty acids) as well as of the particular fatty acids deviated significantly from that seen in the control animals.

Results of fatty acid analysis of phosphatidylethanolamine expressed in relative percentages demonstrated the greatest decrease in unsaturated monoenes and 18 : 1 (oleic) fatty acids.

The content of total unsaturated and monoenes unsaturated fatty acids as well as oleic acid (18 : 1) in plasmalogen was decreased in experimental animals in all studied periods. The fatty acid pattern of plasmalogens was almost generally abnormal 2 months after hypoxia.

The pattern of the fatty acids of cholesterol esters in the myelin fraction of the experimental animals differed also markedly from normal. Most marked are the deviations in the relative content of total pentaenoic fatty acids (20 : 5 and 22 : 5) showing a pronounced increase.

DISCUSSION

The pathomechanism of membraneous lesions in the white matter including myelin sheaths in hypoxia and ischemia is not yet fully explained. A very striking biochemical event in these conditions is the increase of the free fatty acid pool, with the dominating rise of polyunsaturated fatty acids, especially of arachidonic acid (20 : 4) (Bazan et al. 1984; De Medio et al. 1980). An exception is the predemyelinating stage of cyanide-induced encephalopathy, with only transient changes in the free fatty acid pattern (Wender et al. 1986b). The summary of the whole problem was presented in our previous publications (Wender et al. 1975, 1988a).

The increase of the free fatty acid pool is considered as the result of their release from membrane phospholipids, evoked partially by the activation of catabolic processes and by inhibition of phospholipid synthesis (Strosznajder et al. 1972; Bazan 1976; Rodriguez de Turco et al. 1983). According to De Medio et al. (1980), free arachidonate is released from phospholipids yielding diglycerides and lysophospholipids and are further transformed into free fatty acids. The alternate possible pathway woul involve phospholipid degradation through phospholipase A_2 activity.

In our recent studies of the fatty acid spectrum of the main myelin phospholipids (phosphatidylcholine, phosphatidylethanolamine and plasmalogen) after moderate hypoxia, we have noticed considerable changes. The main finding was the decrease of the content of unsaturated fatty acids, mainly of oleic acid (18 : 1). It would be reasonable to believe that the observed phenomenon is connected with the release of fatty acids into the free pool. Otherwise, it would be necessary to presume that an enhanced degradation of some fatty acids in the myelin lipids occurred.

As presented in our previous paper (Wender et al. 1988b), the highest rise after hypoxia is exhibited by polyunsaturated fatty acids (tetra- and pentaenoic fatty acids), which show a manifold higher level in the cerebral white matter of experimental animals. Very interesting is also the appearance of nervonic acid (24 : 1) in the free pool, not present at all in normal white matter. The increase of oleic acid (18 : 1) content was only mild.

The comparison of changes in fatty acids content of myelin lipids with those in the pool of free fatty acids does not demonstrate any similarities. Therefore, the results of this study testify to the assumption, that myelin is not the main source of the sharply increasing pool of free fatty acids after hypoxia. However, it is not clear which other membranes of the structural component in the white matter undergo degradation in this conditions.

The increase in the free fatty acids pool in the white matter after moderate hypoxia is a long lasting phenomenon observed even 2 months after the action of this noxious agent. The same was observed in the spectrum of fatty acids in myelin phospholipids, which was also abnormal so late after hypoxia. In plasmalogen an aggravation of deviations was noted even two months after hypoxia. These findings contribute to the understanding of the maturation phenomenon of the hypoxic brain lesions, presented so far mainly as a morphological event.

WPŁYW UMIARKOWANEGO NIEDOTLENIENIA NA SKŁAD KWASÓW TŁUSZCZOWYCH LIPIDÓW MIELINY

Streszczenie

Badano wpływ umiarkowanego niedotlenienia wywołanego przez umieszczenie szczurów rasy Wistar na okres 30 minut w komorze zawierającej mieszaninę gazów z zawartością 7% tlenu na obraz kwasów tłuszczowych fosfolipidów oraz estrów cholesterolu w mielinie. Spektrum kwasów tłuszczowych oznaczono za pomocą chromatografii gazowej.

Stwierdzono w fosfolipidach mieliny znaczny spadek zawartości nienasyconych kwasów tłuszczowych, szczególnie kwasu olejowego. Porównanie tych zmian ze wzrostem poziomu poszczególnych kwasów tłuszczowych w puli wolnych kwasów tłuszczowych w istocie białej nie wykazuje podobieństwa. Potwierdza to przypuszczenie, że lipidy błon komórkowych, innych poza mieliną, składników strukturalnych istoty białej stanowią główne źródło wzrastającej po niedotlenieniu puli wolnych kwasów tłuszczowych. Utrzymywanie się zmian w obrazie kwasów tłuszczowych fosfolipidów mieliny w późnym okresie po niedotlenieniu, a nawet ich nasilenie w odniesieniu do niektórych frakcji fosfatydów (plasmalogen) może stanowić biochemiczny odpowiednik zjawiska dojrzewania zmian po niedotlenieniu, znanego głównie od strony morfologicznej.

REFERENCES

1. Aveidano M., Bazan N.: Rapid production of diacylglycerols enriched in arachidonate during early brain ischemia. J Neurochem, 1975, 25, 919-920.
2. Bazan N.: Free arachidonic acid and other lipids in the nervous system during early ischemia and after electroshock. In: Function and metabolism of phospholipids in the central and peripheral nervous system. Eds.: G. Porcellati, L. Amaduzzi, C. Galli. Plenum Press, New York, 1976, pp. 317-335.
3. Bazan N., Politi L., Rodriguez de Turco E.: Endogenous pools of arachidonic acid-enriched membrane lipids in cryogenic brain edema. In: Recent progress in the study and therapy of brain edema. Eds.: K. Go, A. Baethmann. Plenum Publ Corp, New York, 1984, pp. 203-212.
4. Cendella R., Galli C., Paoletti R.: Brain free fatty acids level in rats sacrificed by decapitation versus focused microwave irradiation. Lipids, 1975, 10, 210-213.
5. De Medio G., Gorecci G., Horrocks L., Łazarewicz J., Mazzari S., Porcelatti G., Strosznajder J., Trovarelli G.: The effect of transient ischemia on fatty acid and lipid metabolism in the gerbil brain. Ital J Biochem, 1980, 29, 412-432.
6. Folch-Pi J., Lees M., Sloane-Stanley G.: A simple method for the isolation and purification of total lipids from animal tissues. J Biol Chem, 1957, 226, 497-511.
7. Gardiner M., Nilsson B., Rehncrona S., Siesjö B.: Free fatty acids in the rat brain in moderate and severe hypoxia. J Neurochem, 1981, 36, 1500-1505.
8. Norton N., Poduslo S.: Myelination in rat brains: method of myelin isolation. J Neurochem, 1973, 21, 749-758.
9. Rodriguez de Turco E., Morelli de Liberii S., Bazzan N.: Stimulation of free fatty acid and diacylglycerol accumulation in cerebrum and cerebellum during bicumalline-induced status epilepticus. Effect of pretreatment with α-methyl-p-tyrosine and p-chlorophenylalanine. J Neurochem, 1983, 40, 252-259.
10. Strosznajder J., Gromek A., Łazarewicz J.: Wpływ niedokrwienia na zawartość wolnych kwasów tłuszczowych w mózgu świnek morskich. Neuropatol Pol, 1972, 10, 447-455.
11. Traugott U., Raine C.: The neurology of myelin disease. In: Myelin. Ed.: P. Morell. Plenum Press, New York, London, 1984, pp. 311-335.
12. Wender M., Adamczewska-Goncerzewicz Z.: Fatty acid pattern of cerebral lipids in cyanide encephalopathy. Exp Pathol, 1975, 41, 233-238.
13. Wender M., Adamczewska-Goncerzewicz Z., Pankrac J., Wajgt A.: Myelin lipids in cyanide encephalopathy. Neuropatol Pol, 1978, 16, 153-162.
14. Wender M., Adamczewska-Goncerzewicz Z., Stanisławska J., Knitter B., Talkowska D., Pankrac J.: Influence of cyanide intoxication on the composition of myelin lipids in rats fed during development of a diet containing various amounts of lipids. Neuropatol Pol, 1986a, 24, 43-56.
15. Wender M., Adamczewska-Goncerzewicz Z., Sroczyński E., Żórawski A.: The effect of cyanide intoxication on free fatty acid pattern in the brain of rats developing on a diet with various amounts of lipids. Neuropatol Pol, 1986b, 24, 341-350.
16. Wender M., Adamczewska-Goncerzewicz Z., Stanisławska J., Pankrac J., Talkowska D., Grochowalska A.: Myelin lipids of the rat brain in experimental hypoxia. Exp Pathol, 1988a, 33, 59-63.
17. Wender M., Adamczewska-Goncerzewicz Z., Żórawski A., Sroczyński E., Grochowalska A.: Effect of moderate hypoxia on content and pattern of free fatty acids in cerebral white matter. Neuropatol Pol, 1988b, 26, 39-47.

Authors' address: Department of Neurology, School of Medicine, 49 Przybyszewskiego Str., 60-355 Poznań, Poland.

NEUROPAT. POL. 1990, 28, 3-4
PL ISSN 0028-3894

JÓZEF SZCZECH

COMPARATIVE EVALUATION OF BLOOD VESSEL ENDOTHELIA IN WHITE MATTER STRUCTURES OF RAT BRAIN FOLLOWING HYPOXIA

Laboratory of Neuropathology, Department of Neurology, School of Medicine, Poznań, Poland

The sequence of changes in the structural elements of the nervous system, taking place as a consequence of hypoxia, has been relatively well studied using numerous experimental models. Morphological alterations take place at first in the most sensitive nerve cells, and then, in oligodendroglia and astrocytes while microglia and blood vessel cells are least sensitive to oxygen deficit. Apart from different sensitivity of individual cellular elements of the CNS, selective susceptibility of individual anatomical structures or their parts is worth stressing. This phenomenon used to be explained by the vascular theory (Spielmeyer 1925; Scholtz 1963), physicochemical properties of the structures involved (Vogt, Vogt 1937), differences in chemical composition (Friede 1966) and in enzymatic activity (Wender, Kozik 1972). The vascular factor plays a significant role in post-hypoxia lesions and it participates in inducing brain edema after hypoxia (Lindenberg 1955; Klatzo 1957). Observing selective lesions of some white matter structures in the brain in natural as well as experimental pathological processes, we undertook an attempt to evaluate alterations in cell nuclei of blood vessel endothelia in various systems of nervous fibers in the CNS which may take place as a result of hypoxia.

MATERIAL AND METHODS

Studies were conducted on 60 adult rats of Wistar strain, weighing each 200 to 259 g. The animals were exposed to hypoxia in a special chamber, in two experimental groups. Moderate hypoxia was induced using a respiratory mixture consisting of 7% O_2, 92.9% N_2 and 0.1% CO_2 for 30 min while severe hypoxia was induced using a respiratory mixture

consisting of 2% O_2, 97.9% N_2 and 0.1% CO_2 for 3 min. The control group consisted of 7 rats kept in typical laboratory conditions.

Animals of both experimental groups were sacrificed in Narcotan (Spofa) anesthesia 4 and 24 h after hypoxia, on the 14th and 60th day after hypoxia. Brains of experimental and control rats were fixed in Baker's solution, paraffin embedded, sectioned at 7 μm and stained with hematoxylin-eosin, according to Nissl and Weil. Some sections were subjected to the Feulgen reaction (Krygier-Stojałowska 1982) and provided material for karyometric and cytophotometric measurements of the blood vessels endothelia in corpus callosum, fimbria hippocampi and in fornix columns. Measurements on the cell nuclei were conducted using a Morphoquant scanning measuring microscope (Zeiss, Jena) coupled to a KSR 4100 computer (Robotron), in monochromatic light of 560 nm wave length obtained from a HBO 100 lamp.

The following parameters and cross-section indices were estimated in endothelial cell nuclei:

1. Size coefficients:
   KONL * — length of cross-section circumference,
   KOFL — area of cross-section.
2. Shape coefficients:
   FOFA — ratio of circumference square to cross-section area,
   DMVH — ratio of the shortest to the longest diagonal of the convection area (i.e. the smallest octagon described on the analyzed structure),
   FLVH — ratio of the structure area in the cross-section to the convenction area.
3. Indices of nuclear chromatin:
   EXTS — sum of extinctions over the entire cross-section area,
   KOMP — density of nuclear chromatin, expressed by the ratio of mean extinction to mean maximum extinction,
   ZNTR — index of nuclear chromatin concentration in the central part of the cell nucleus, expressed by the ratio of mean extinction in the central part of the cell nucleus to mean maximum extinction.

In each experimental group, numerical values of measurements performed on 100 endothelial cell nuclei, expressed in numbers of measuring raster points (size coefficients) or in arbitrary units (indices of nuclear chromatin) were grouped into sets and compared to sets of endothelial cell nuclei in the control group vessels using trifactorial analysis of variance and Snedecor statistics F (Octaba 1966; Greń 1982). Computations were performed using a MERA 400 computer. Alterations at $p < 0.05$ level were considered as significant.

* Coefficient and index terms originate from the Mosaik computer program applied in the measuring procedure (Voss et al. 1979).

RESULTS

Histopathological examination of the brains of animals subjected to hypoxia demonstrated stasis and small perivascular hemorrhages, mainly in the gray matter. In the white matter of corpus callosum, particularly 24 h after hypoxia, widening of perivascular spaces and numerous empty, circular spaces in-between nerve fibers were noted, pointing to edema. Vascular and perivascular alterations were clearly less pronounced on the 14th and 60th days after hypoxia.

Numerical values of karyometric and cytophotometric measurements on endothelial nuclei in the examined structures of the white matter are grouped in Tables 1 to 5. Changes in the mean ratio of some studied karyometric or cytophotometric traits in experimental groups to the mean values of the traits in the control group (Q value), as affected by the extent of hypoxia and time after hypoxia, in individual regions of the white matter are shown in Figs 1 to 5.

Four hours after hypoxia, cross-section of endothelial cell nuclei underwent significant enlargement and became more spherical in the fornix columns (Figs 1-3) with more pronounced changes taking place after severe hypoxia. Cell nuclei in vascular endothelium of fimbria hippocampi became more spherical (decreased value of FOFA — Fig. 3) this being accompanied by levelling of nuclear membrane folds (increased FLVH value). The changes prevailed after moderate hypoxia. In corpus callosum no significant alterations were observed in size or shape of the endothelial cell nucleus cross-section. Alterations in nuclear chromatin indices also behaved in a different manner in vascular endothelia of various white matter structures. In fornix columns, severe hypoxia was followed by a particularly pronounced increase in chromatin extinction (Fig. 4), associated with its concentration in the central portion of the cell nuclei (Fig. 5). A less pronounced increase was observed following moderate hypoxia (Fig. 4). In the capillaries of corpus collosum, on the other hand, nuclear chromatin extinction decreased significantly in both groups of hypoxia.

In the 24th hour after hypoxia, either moderate or severe, cell nuclei cross-section in capillary endothelia of fornix columns remained enlarged, particularly in the group of severe hypoxia (Figs 1 and 2). In moderate hypoxia, the changes were associated with rounding of the cell nucleus outline and with decreased folding of the nuclear membrane (decreased FOFA value — Fig. 3, increased FLVH value). In each hypoxia group the cell nucleus chromatin extinction (Fig. 4) increased even if concentration of the chromatin slightly decreased as compared with the 4th hour after hypoxia (Fig. 5).

On the other hand, no significant size changes were observed in endothelial cell nuclei in fimbria hippocampi or corpus callosum. Only mo-

Table 1. Trifactorial analysis of variance of changes in vascular endothelia nuclei contour length (KONL) after hypoxia
Tabela 1. Trójczynnikowa analiza wariancji zmian długości obwodu (KONL) jąder śródbłonków naczyń krwionośnych po niedotlenieniu

Region Okolica	Control Grupa kontrolna	% O_2	Time Czas							
			4 h		24 h		14 d		60 d	
	$\bar{x}\pm SD$		$\bar{x}\pm SD$	Q	$\bar{x}\pm SD$	Q	$\bar{x}\pm SD$	Q	$\bar{x}\pm SD$	Q
Corpus callosum Spoidło wielkie	95±12	7%	95±11	0.9908	101±15	1.0533	91±16	0.9545	88±15	0.9246
		2%	94±12	0.9860	97±12	1.0133	95±12	0.9925	94±12	0.9835
Fimbria hippocampi Strzępek hipokampa	95±12	7%	96±11	1.0094	99±13	1.0388	100±12	1.0546	96±12	1.0107
		2%	93±12	0.9849	93±13	0.9841	95±15	1.0032	89±10	0.9408
Columnae fornicis Kolumny sklepienia	94±15	7%	93±13	0.9900	95±12	1.0170	96±10	1.0231	91±10	0.9767
		2%	97±12	1.0402	99±13	1.0626	97±12	1.0369	92±11	0.9833

$NIR_{0.05} = 0.0380$; $p_{0.05}$ $0.9620 > Q > 1.0380$.

Explanations:
Objaśnienia:

Values statistically significant are underlined.
Wartości istotne statystycznie podkreślono.

$\bar{x}\pm SD$ Arithmetical mean and standard deviation for numerical value of measurements.
Średnia arytmetyczna i odchylenie standardowe wartości liczbowych pomiarów.

$NIR_{0.05}$ Minimal significant difference at the statistical significance level 0.05.
Najmniejsza istotna różnica na poziomie istotności statystycznej 0.05.

Q Mean ratio of investigated parameter values in experimental and control groups.
Q in control is 1.000.
Średni stosunek badanej cechy grupy doświadczalnej do grupy kontrolnej.
Q w grupie kontrolnej równa się 1.000.

$P_{0.05}$ The value of Q quotient for the changes at statistical significance level $p_{0.05}$.
Wartość ilorazu Q dla zmian na poziomie istotności statystycznej $p_{0.05}$.

Table 2. Trifactorial analysis of variance of changes in vascular endothelia nuclei cross-section area (KOFL) after hypoxia

Tabela 2. Trójczynnikowa analiza wariancji zmian pola przekroju poprzecznego (KOFL) jąder śródbłonków naczyń krwionośnych po niedotlenieniu

Region Okolica	Control Grupa kontrolna	% O_2	Time Czas							
			4 h		24 h		14 d		60 d	
	$\bar{x}\pm SD$		$\bar{x}\pm SD$	Q	$\bar{x}\pm SD$	Q	$\bar{x}\pm SD$	Q	$\bar{x}\pm SD$	Q
Corpus callosum Spoidło wielkie	211±38	7%	204±33	0.9681	211±35	1.0000	183±41	0.8701	187±43	0.8857
		2%	203±34	0.9610	214±33	1.0168	204±34	0.9670	205±37	0.9712
Fimbria hippocampi Strzępek hipokampa	202±31	7%	213±33	1.0552	219±34	1.0738	215±32	1.0632	214±33	1.0575
		2%	203±36	1.0030	204±39	1.0079	201±49	0.9935	194±32	0.9605
Columnae fornicis Kolumny sklepienia	192±38	7%	211±41	1.0953	210±38	1.0901	211±30	1.0975	206±32	1.0716
		2%	216±34	1.1247	226±36	1.1743	214±32	1.1143	208±29	1.0813

$NIR_{0.05} = 0.0502$; $p_{0.05}$ $0.9498 > Q > 1.0502$.
Explanation: see table 1.
Objaśnienia: jak do tabeli 1.

Table 3. Trifactorial analysis of variance of changes in vascular endothelia nuclei form factor (FOFA) after hypoxia

Tabela 3. Trójczynnikowa analiza wariancji zmian współczynnika kształtu (FOFA) jąder śródbłonków naczyń krwionośnych po niedotlenieniu

Region Okolica	Control Grupa kontrolna	% O_2	Time Czas							
			4 h		24 h		14 d		60 d	
	$\bar{x}\pm SD$		$\bar{x}\pm SD$	Q	$\bar{x}\pm SD$	Q	$\bar{x}\pm SD$	Q	$\bar{x}\pm SD$	Q
Corpus callosum Spoidło wielkie	220±37	7%	223±40	1.0121	244±49	1.1056	230±43	1.0444	213±44	0.9687
		2%	223±42	1.0117	222±38	1.0060	223±34	1.0125	218±32	0.9902
Fimbria hippocampi Strzępek hipokampa	225±36	7%	218±38	0.9684	229±40	1.0159	235±40	1.0463	218±39	0.9669
		2%	218±33	0.9683	217±38	0.9668	234±49	1.0381	208±35	0.9251
Columnae fornicis Kolumny sklepienia	232±47	7%	211±33	0.9113	219±31	0.9457	219±27	0.9457	205±29	0.8856
		2%	222±39	0.9608	222±39	0.9578	223±41	0.9618	206±30	0.8878

$NIR_{0.05} = 0.0474$; $p_{0.05}$ $0.9526 > Q > 1.0474$.

Explanation: see table 1.

Objaśnienia: jak do tabeli 1.

Table 4. Trifactorial analysis of variance of changes in vascular endothelia extinction sum (EXTS) (relative amount of DNA) after hypoxia
Tabela 4. Trójczynnikowa analiza wariancji zmian sumy ekstynkcji (EXTS) jąder śródbłonków naczyń krwionośnych po niedotlenieniu (względna ilość DNA)

Region Okolica	Control Grupa kontrolna	% O_2	Time Czas							
			4 h		24 h		14 d		60 d	
	$\bar{x}\pm SD$		$\bar{x}\pm SD$	Q	$\bar{x}\pm SD$	Q	$\bar{x}\pm SD$	Q	$\bar{x}\pm SD$	Q
Corpus callosum	62±11	7%	51± 8	0.8223	54± 8	0.8707	43±10	0.7013	57±13	0.9297
Spoidło wielkie		2%	57±10	0.9233	52± 8	0.8481	63±10	1.0286	60± 9	0.9759
Fimbria hippocampi	57±10	7%	58± 8	1.0097	62± 7	1.0851	56± 9	0.9883	67± 7	1.1760
Strzępek hipokampa		2%	60± 8	1.0484	46±10	0.8071	55±18	0.9685	53± 8	0.9268
Columnae fornicis	50±12	7%	52± 9	1.0504	59± 8	1.1753	61± 8	1.2184	66± 8	1.3274
Kolumny sklepienia		2%	52± 9	1.1799	61±10	1.2225	67± 7	1.3380	63± 8	1.2523

$NIR_{0.05} = 0.0479$; $p_{0.05}$ $0.9521 > Q > 1.0479$.
Explanation: see table 1.
Objaśnienia: jak do tabeli 1.

Table 5. Trifactorial analysis of variance of changes in vascular endothelia nuclei chromatin concentration (ZNTR) after hypoxia
Tabela 5. Trójczynnikowa analiza wariancji zmian koncentracji chromatyny (ZNTR) jąder śródbłonków naczyń krwionośnych po niedotlenieniu

Region Okolica	Control Grupa kontrolna	% O_2	Time Czas							
			4 h		24 h		14 d		60 d	
	$\bar{x}\pm SD$		$\bar{x}\pm SD$	Q	$\bar{x}\pm SD$	Q	$\bar{x}\pm SD$	Q	$\bar{x}\pm SD$	Q
Corpus callosum Spoidło wielkie	77±6	7%	78±7	1.0107	73±8	0.9498	76±7	0.9944	79±9	1.0319
		2%	75±7	0.9811	77±7	1.0036	77±7	1.0000	77±8	0.9979
Fimbria hippocampi Strzępek hipokampa	78±7	7%	79±7	1.0132	77±7	0.9798	75±7	0.9582	77±8	0.9816
		2%	78±7	0.9989	79±7	1.0101	78±7	0.9894	79±6	1.0033
Columnae fornicis Kolumny sklepienia	75±8	7%	80±6	1.0594	77±8	1.0312	77±7	1.0220	80±7	1.0679
		2%	78±6	1.0346	78±6	1.0359	77±8	1.0230	78±7	1.0433

$NIR_{0.05} = 0.0272$; $p_{0.05}$ $0.9728 > Q > 1.0272$.
Explanation: see table 1.
Objaśnienia: jak do tabeli 1.

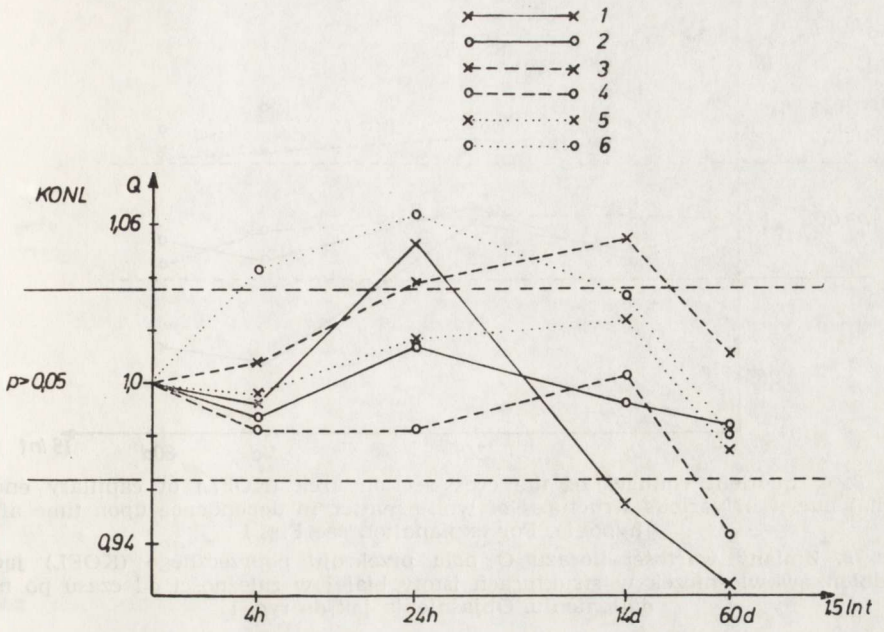

Fig. 1. Q quotient changes of the length of capillary endothelial nuclei cross-section (KONL) in various structures of white matter in dependence upon time after hypoxia. Explanation: Q — mean ratio of investigated parameter values in experimental and control groups, calculated by the use of trifactorial analysis of variance and F Snedecor statistics, $p > 0.05$ — value of Q quotient for changes statistically non significant, 4h, 24h — hours after hypoxia, 14d, 60d — days after hypoxia, 1.5 lnt — 1.5 time expressed as natural logarithm of hours, 1 — corpus callosum, moderate hypoxia, 2 — corpus callosum, severe hypoxia, 3 — fimbria hippocampi — moderate hypoxia, 4 — fimbria hippocampi, severe hypoxia, 5 — fornix columns, moderate hypoxia, 6 — fornix columns, severe hypoxia

Ryc. 1. Zmiany wartości ilorazu Q długości obwodu przekroju poprzecznego (KONL) jąder śródbłonków włośniczek w badanych strukturach istoty białej w zależności od czasu po niedotlenieniu. Objaśnienia: Q — średni stosunek badanej cechy grupy doświadczalnej do grupy kontrolnej, obliczony metodą trójczynnikowej analizy wariancji i statystyki F Snedecora, $p > 0,05$ — zakres wartości ilorazu Q nieistotny statystycznie, 4h, 24h — godziny po niedotlenieniu, 14d, 60d — dni po niedotlenieniu, 1,5 lnt — 1,5 logarytmu naturalnego czasu w godzinach, 1 — spoidło wielkie, niedotlenienie umiarkowane, 2 — spoidło wielkie, niedotlenienie ciężkie, 3 — strzępek hipokampa, niedotlenienie umiarkowane, 4 — strzępek hipokampa, niedotlenienie ciężkie, 5 — kolumny sklepienia, niedotlenienie umiarkowane, 6 — kolumny sklepienia, niedotlenienie ciężkie

derate hypoxia induced elongation of endothelial cell nuclei in corpus callosum (increased FOFA — Fig. 3, increased KONL — Fig. 1). The changes in corpus callosum were associated with a decreased extinction of nuclear chromatin, independently of how pronounced was the hypoxia (Fig. 4), associated with a decreased concentration of nuclear chromatin following moderate hypoxia (Fig. 5). In fimbria hippocampi moderate hypoxia induced an increase, while severe hypoxia caused a decrease in nuclear chromatin extinction.

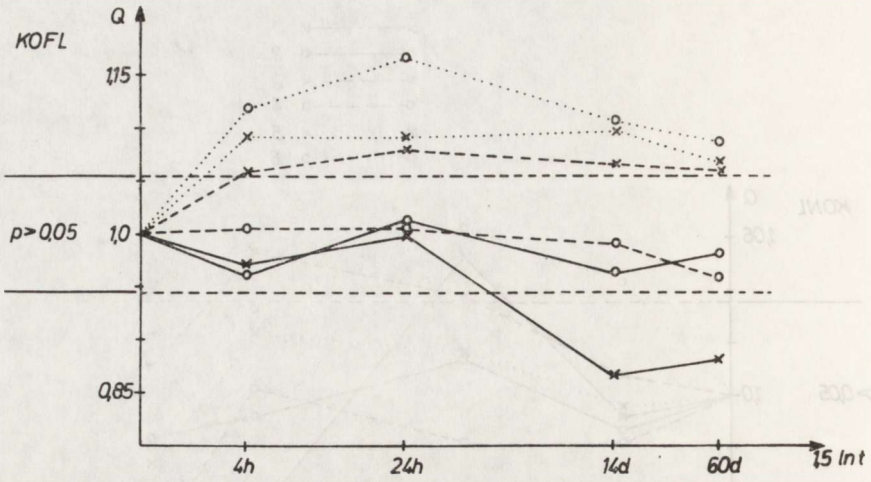

Fig. 2. Q quotient changes of the cross-section area (KOFL) of capillary endothelial nuclei in various structures of white matter in dependence upon time after hypoxia. For explanation see Fig. 1

Ryc. 2. Zmiany wartości ilorazu Q pola przekroju poprzecznego (KOFL) jąder śródbłonków włośniczek w strukturach istoty białej w zależności od czasu po niedotlenieniu. Objaśnienia jak do ryc. 1

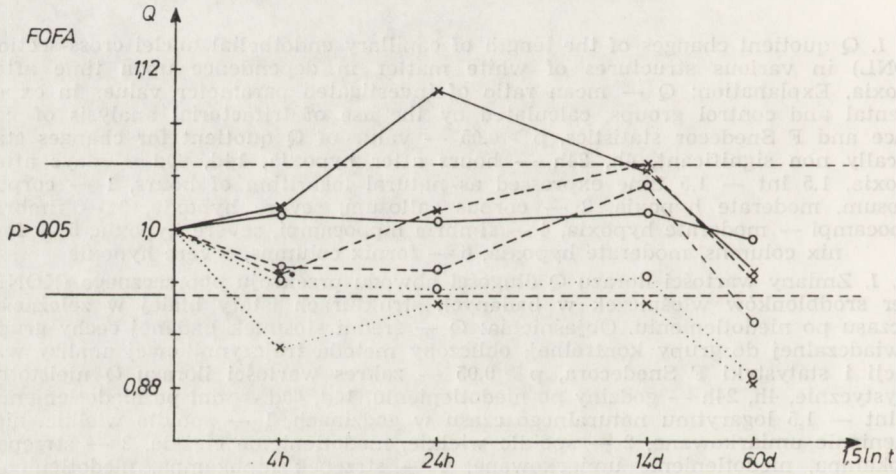

Fig. 3. Q quotient changes of the form factor (FOFA) of capillary endothelial nuclei in various structures of white matter in dependence upon time after hypoxia. For explanations see Fig. 1.

Ryc. 3. Zmiany wartości ilorazu Q wskaźnika kształtu (FOFA) jąder śródbłonków włośniczek struktur istoty białej w zależności od czasu po niedotlenieniu. Objaśnienia jak do ryc. 1

In the 14th day after hypoxia, the area of cell nuclei cross-section in capillary endothelium of fornix columns was still significantly higher in both groups of hypoxia as compared with the control group (Fig. 2). On the other hand, the cell nucleus cross-section circumference, even if greater than in the control group, did not differ from it significantly (Fig. 1). Following moderate hypoxia, endothelial cell nuclei were rounder

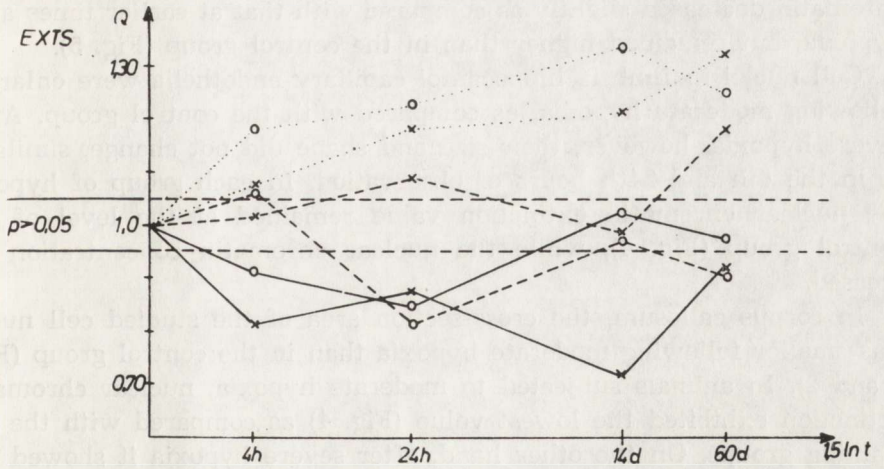

Fig. 4. Q quotient changes of the sum of nuclear chromatin (EXTS) of capillary endothelial nuclei in various structures of white matter upon time after hypoxia. For explanation see Fig. 1

Ryc. 4. Zmiany wartości ilorazu Q sumy ekstynkcji chromatyny jądrowej (EXTS) jąder śródbłonków włośniczek w strukturach istoty białej w zależności od czasu po niedotlenieniu. Objaśnienia jak do ryc. 1

as compared with the control group (Fig. 3). In each group of hypoxia augmented extinction of nuclear chromatin was observed as compared with earlier post-hypoxia stages (Fig. 4). The concentration of nuclear

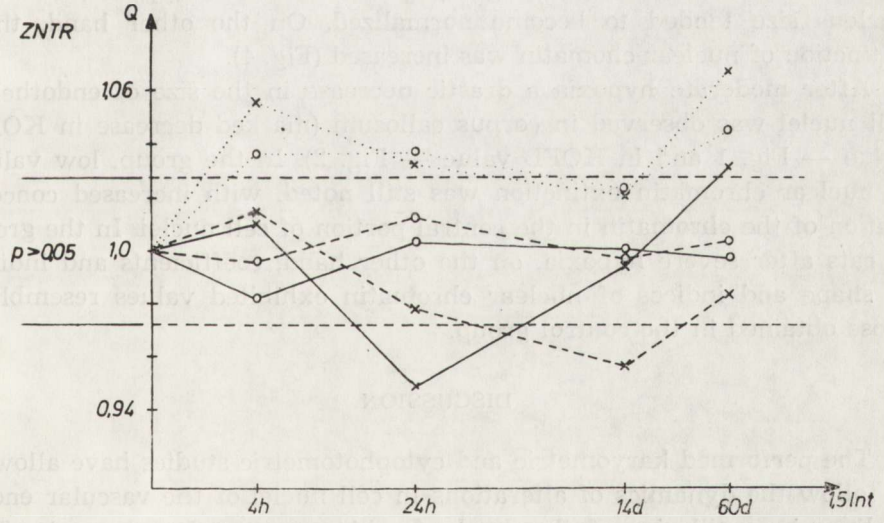

Fig. 5. Q quotient changes of the nuclear chromatin concentration (ZNTR) of capillary endothelial nuclei in various structures of white matter in dependence upon time after hypoxia. For explanation see Fig. 1

Ryc. 5. Zmiany wartości ilorazu Q koncentracji chromatyny jądrowej (ZNTR) jąder śródbłonków włośniczek w strukturach istoty białej w zależności od czasu po niedotlenieniu. Objaśnienia jak do ryc. 1

chromatin decreased slightly as compared with that at earlier times after hypoxia, but remained higher than in the control group (Fig. 5).

Cell nuclei in fimbria hippocampi capillary endothelia were enlarged following moderate hypoxia, as compared with the control group. After severe hypoxia, however, their size and shape did not change, similarly as in the 4th and 24th hours of observation. In each group of hypoxia the nuclear chromatin extinction value remained at the level of the control group (Fig. 4), while the nuclear chromatin concentration increased.

In corpus callosum, the cross-section area of the studied cell nuclei was smaller following moderate hypoxia than in the control group (Figs 1 and 2). In animals subjected to moderate hypoxia, nuclear chromatin extinction exhibited the lowest value (Fig. 4) as compared with the remaining groups. On the other hand, after severe hypoxia it showed the same level as in the control group.

On the 60th day after hypoxia, cell nuclei of capillary endothelia of fornix columns were still spherically transformed and slightly enlarged in each hypoxia group, as compared with the controls (Fig. 1-3). The changes were accompanied by an increased value of the nuclear chromatin extinction index. The value of the nuclear chromatin concentration index was similarly augmented (Fig. 5). After severe hypoxia the endothelial cell nuclei of fimbria hippocampi were smaller and rounder than in the control group (Figs 1 and 3). They showed a decreased nuclear chromatin extinction (Fig. 4). After moderate hypoxia, the cell nucleus size tended to become normalized. On the other hand, their extinction of nuclear chomatin was increased (Fig. 4).

After moderate hypoxia a drastic decrease in the size of endothelial cell nuclei was observed in corpus callosum (marked decrease in KONL value — Fig. 1 and in KOFL value — Fig. 2). In the group, low values of nuclear chromatin extinction was still noted, with increased concentration of the chromatin in the central portion of cell nuclei. In the group of rats after severe hypoxia, on the other hand, coefficients and indices of shape and indices of nuclear chromatin exhibited values resembling those obtained in the control group.

DISCUSSION

The performed karyometric and cytophotometric studies have allowed to follow the dynamics of alterations in cell nuclei of the vascular endothelium in capillaries of the cerebral white matter after hypoxia. The alterations varied, depending upon the degree of hypoxia, time of observation after hypoxia and the studied region of the white matter. The early post-hypoxia period (4th and 24th hour) was manifested by in-

creased cross-section size in the studied cell nuclei of fornix columns, the increase being proportional to the severity of hypoxia. This observation, in association with smoothing out of nuclear membrane folds corresponds to edema. Endothelial cell nuclei of fimbria hippocampi were enlarged more extensively following moderate hypoxia. Different changes were observed in corpus callosum, in which endothelial cell nuclei preserved their size, but became ovally transformed with increased folding of their nuclear membrane what may correspond to an early stage of a degenerative process.

In late stages after hypoxia (14th and 60th day) extensive differences have also been noted in the type of observed karyometric changes between individual structures of cerebral white matter. Edematous changes in endothelial cell nuclei decreased slightly, but their rounded shape remained significantly different as compared with the control group. The alterations were more pronounced after moderate hypoxia. In capillary endothelia of corpus callosum the pattern of karyometric changes reflected the severity of hypoxia. Following severe hypoxia the results of karyometric measurements approached normal ones and most coefficients and indices of shape and of the status of nuclear chromatin showed no differences as compared with the control group. Moderate hypoxia, on the other hand, resulted in progressive pycnotic alterations — a decreased size of cell nucleus cross-section and rounder cross-section. Measurements in fimbria hippocampi, in contrast to what was observed in endothelial cell nuclei of corpus callosum, gave normalized coefficients and indices of karyometry following moderate hypoxia, whereas increasingly intense pycnotic changes following severe hypoxia.

The indices of nuclear chromatin point to a polyploid tendency, particularly evident in endothelial cell nuclei of the fornix columns late after hypoxia of any intensity. Severe hypoxia, both at an early or late stage of observation induced a decreased extinction of nuclear chromatin. Since both, the increase and decrease in values of nuclear chromatin extinction were associated with augmented concentration of nuclear chromatin in the central portions of the cell nuclei, such a change points to a decreased biological activity of the structure and to accelerated aging, as compared with the control group (Krygier-Stojałowska et al. 1980).

In the light of the presented data it seems secure to conclude that moderate hypoxia, but lasting for a longer period, exerts a more pronounced damaging effect on endothelial cell nuclei than severe but short lasting hypoxia. The opinion of some authors on the relative resistance of some cellular elements of blood vessels to injurious effects of hypoxia seems unfounded when confronted with the earlier performed karyometric and cytophotometric studies on oligodendroglia (Szczech 1987) in the same brain structures. In the latter study edema of oligo-

dendroglia was observed, which corresponded in time to the presented alterations in vascular endothelia. In a similar way, the long lasting changes still observed on the 60th day after hypoxia seem to deny the existence of easily reversible histopathological consequences of hypoxia (Kapuściński 1983). The performed measurements indicate a particular sensitivity of cell nuclei in corpus callosum vascular endothelium to degenerative changes resulting from long lasting, even if moderate only, hypoxia. On the other hand, vascular endothelia in fornix columns exhibit a greater tendency to develop edema as a result of acute hypoxia. The relatively least pronounced alterations were noted in endothelial cell nuclei in fimbria hippocampi vessels. Explanation of such differences may involve a different phylogeny of the white matter structures. Corpus callosum, securing interhemispheric connections, is phylogenetically younger structure and may be less resistant to the damaging effect of hypoxia, similarly as the cortex of the brain hemispheres is less resistant to ischemic injury compared to subcortical structures, as demonstrated by clinical observations.

CONCLUSIONS

1. Acute and moderate hypoxia represents a damaging factor for endothelial cell nuclei of capillaries in various structures of rat brain white matter.

2. The type and intensity of karyo- and cytophotometric changes in capillary endothelium cell nuclei depend upon the intensity of hypoxia, time elapsed after hypoxia and white matter region.

3. In capillary endothelium cell nuclei of the corpus callosum severe, even if short lasting, hypoxia induces lesions which are reversible to a significant extent, while moderate but long-lasting hypoxia results in progressive degenerative lesions.

4. In capillary endothelium cell nuclei in the fornix columns both severe and moderate anoxia induce edema, more pronounced at the early stage after acute hypoxia. At later stages independently of hypoxia intensity, extinction of nuclear chromatin is increased.

5. Capillary endothelium cell nuclei in fimbria hippocampi exhibit relative resistance to hypoxia, as compared with other white matter structures.

PORÓWNAWCZA OCENA ŚRÓDBŁONKÓW NACZYŃ KRWIONOŚNYCH STRUKTUR ISTOTY BIAŁEJ MÓZGU SZCZURA PO NIEDOTLENIENIU

Streszczenie

Przeprowadzono kariometryczną i cytofotometryczną ocenę śródbłonków włośniczek spoidła wielkiego mózgu, strzępka hipokampa i kolumn sklepienia u zwierząt

poddanych niedotlenieniu ciężkiemu (3 min w atmosferze zawierającej 2% tlenu) i niedotlenieniu umiarkowanemu (30 min w atmosferze zawierającej 7% tlenu). Badania przeprowadzono po 4 i 24 godzinach oraz w 14 i 60 dniu po niedotlenieniu.

We wczesnym okresie po niedotlenieniu obserwowano powiększenie jąder śródbłonków o intensywności zależnej od stopnia niedotlenienia oraz struktury istoty białej. Były one najsilniej wyrażone w 24 godzinie po niedotlenieniu ciężkim w śródbłonkach kolumn sklepienia. W 60 dniu po niedotlenieniu jądra śródbłonków włośniczek spoidła wielkiego mózgu wykazywały zmiany zwyrodnieniowe o charakterze pyknozy, a w śródbłonkach włośniczek kolumn sklepienia obserwowano znaczny wzrost ekstynkcji chromatyny jądrowej. Jądra śródbłonków włośniczek strzępka hipokampa cechowała względna odporność na niedotlenienie w porównaniu do innych badanych struktur istoty białej.

Stwierdzone po niedotlenieniu zmiany kariometryczne i cytofotometryczne mogą odpowiadać toksycznym zmianom zwyrodnieniowym śródbłonków włośniczek spoidła wielkiego mózgu i przyspieszonym procesom starzenia jąder śródbłonków kolumn sklepienia mózgu.

REFERENCES

1. Brierley J. B.: Cerebral hypoxia. In: Greenfield's Neuropathology. Eds.: W. Blackwood, Corsellis J. A. N. Arnold, London 1977, pp. 43-85.
2. Friede R. L.: The histochemical architecture of the Ammon's horn as related to its selective vulnerability. Acta Neuropathol (Berl), 1966, 6, 1-13.
3. Greń J.: Statystyka matematyczna. Modele i zadania. PWN, Warszawa, 1982.
4. Hassler R.: Zur funktionellen Anatomie des limbischen Systems. Nervenarzt, 1964, 9, 386-396.
5. Kapuściński A.: Ocena wpływu okluzji tętnic szyjnych wspólnych i zmian ciśnienia tętniczego na czynność bioelektryczną mózgu. Neuropatol Pol, 1983, 21, 417-425.
6. Klatzo I.: Neuropathological aspects of brain edema. J Neuropathol Exp Neurol, 1967, 26, 1-14.
7. Krygier-Stojałowska A.: Zasady cytofotometrii. In: Topochemiczne metody badania komórek i tkanek. PWN, Warszawa, 1982.
8. Krygier-Stojałowska A., Kulczycki J., Madej M., Nowacki P., Honczarenko K.: Zmiany ilościowe DNA i białek zasadowych (Histonów) w jądrach komórek nerwowych i glejowych mózgowia szczurów w różnym wieku. Neuropatol Pol, 1980, 18, 97-106.
9. Lindenberg R.: Compression of brain arteries as a pathogenetic factor for tissue necrosis and their areas of predilection. J Neuropathol Exp Neurol, 1955, 14, 223-243.
10. Oktaba W.: Elementy statystyki matematycznej i metodyka doświadczalnictwa. PWN, Warszawa 1966.
11. Scholz W.: Topistic lesion. In: Selective vulnerability of the brain in hypoxaemia. Eds.: J. P. Schade, W. M. McMenemey, Blackwell Scientific, 1963.
12. Spielmeyer W. cit. Brierley pos. 1.
13. Szczech J.: Comparative appraisal of oligodendroglia in various brain structures in rats exposed to hypoxia. Karyometric and cytophotometric studies. Neuropatol Pol, 1987, 25, 473-488.
14. Vogt C., Vogt O.: cit. Hassler R. pos. 4.

15. Voss K., Neumann B., Witsack W.: Universelle Programmsystem für den automatischen Mikroskopbildanalysator Morphoquant. Jenauer Runsch, 1979.
16. Wender M., Kozik M.: Histoenzymology of cerebral white matter in the developing rat brain. J Hirnforsch, 1972, 1, 223-230.

Author's address: Laboratory of Neuropathology, Department of Neurology, School of Medicine, 49 Przybyszewskiego Str., 60-355 Poznań, Poland.

NEUROPAT. POL. 1990, 28, 3-4
PL ISSN 0028-3894

MIECZYSŁAW WENDER, ZOFIA ADAMCZEWSKA-GONCERZEWICZ,
DANUTA TALKOWSKA, JADWIGA PANKRAC

MYELIN PROTEINS OF SENILE RAT BRAIN *

Department of Neurology, School of Medicine, Poznań, Poland

The myelin sheath, a specific assembly of bilayers composed of lipids and proteins, exhibits several abnormalities in aging brain. Morphological studies performed at the ultrastructural level, showed changes both in axons and in myelin sheaths, only in some nervous fibers. However, diffuse abnormality of myelin in aged brain was documented in morphometric studies (Wender et al. 1988).

Chemical studies of cerebral white matter of aged rat brain have shown a highly increased amount of free fatty acids (Wender et al. 1989). This seems to be connected with abnormalities of several aspects in cerebral lipid metabolism in aging, found in many studies (Horrocks et al. 1979; Battistin et al. 1987; Puliti et al. 1987; Alberghino et al. 1988 and many others).

Studies of senile brain have disclosed also profound deviations in the chemistry of myelin, mainly of its lipids (Horrocks 1973; Adamczewska-Goncerzewicz et al. 1988; Wender et al. 1988). Less known is the problem of myelin proteins in aging. The evaluation of myelin proteins is a continuation of our studies on aged myelin.

MATERIAL AND METHODS

The studies were performed on 16 white rats of Wistar strain sacrificed at the age of 2 to 2.5 years. The results were compared with those established in 10 young adult animals (4-6 months old). The animals were sacrificed by decapitation under light halothane anesthesia.

Biochemical methods. The myelin fraction was obtained by fractionation in a discontinuous sucrose density gradient; the technique of

* Investigations supported by the Research Agreement No 06.02.II.3.5. with the Polish Academy of Sciences.

Norton and Poduslo (1973) was used. The Agrawal method (1974) was used for polyacrylamide gel electrophoresis. The separated proteins were then stained with Coomasie Brilliant Blue B-250. The obtained gels (Fig. 1) were scanned by mean of densitometry at 610 nm. A Kipp-Zonen (Holland) microdensitometer with intergrating device was used. The results were expressed as percentage of total proteins. Myelin proteins separated on polyacrylamide gels were identified by using standard proteins of know molecular weight. More details of the method are presented in our previous publication (Wender et al. 1989a).

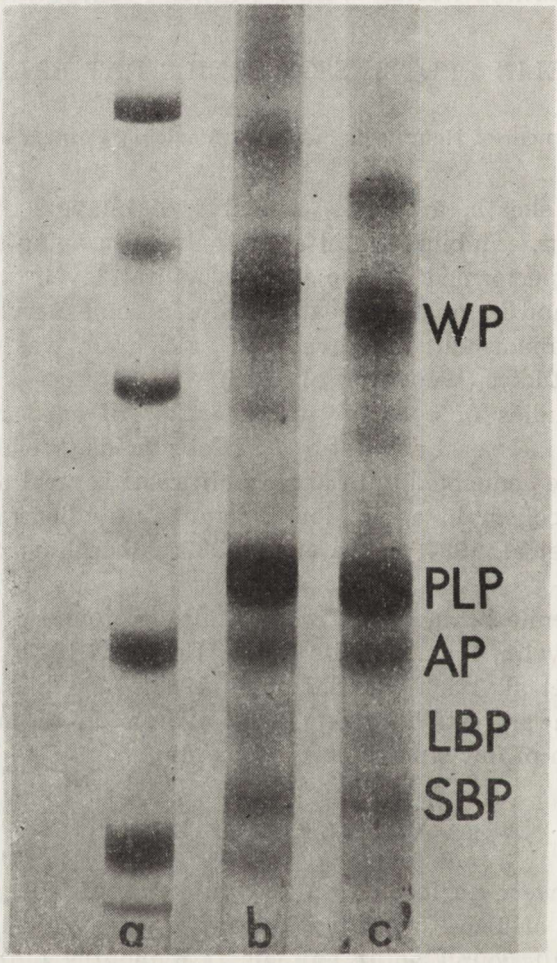

Fig. 1. Brain myelin proteins separated by means of 12% polyacrylamide gel electrophoresis. WP — Wolfgram protein, PLP — Folch-Lees proteolipid, AP — Agrawal protein, LBP — large basic protein, SBP — small basic protein, a — standard proteins, b — young adult (4-month-old), c — aged rat (2.5-year-old)

Ryc. 1. Białka mieliny rozdzielone metodą elektroforezy na 12% żelu poliakrylamidowym. WP — białko Wolfgrama, PLP — proteolipid Folch-Lees, AP — białko Agrawala, LBP — cięższe białko zasadowe, SBP — lżejsze białko zasadowe, a — białka wzorcowe, b — młody dorosły szczur (4-miesięczny), c — stary szczur (2,5 roku)

RESULTS

The results found in electrophoretic studies of myelin proteins in aged rats are presented in Table 1. Folch-Lees proteins and Agrawal proteins were slightly decreased in aged myelin as compared with that of young adult rats. However, both differences are statistically insignificant. The large fraction of basic protein was relatively higher and the ratio of small to large basic proteins lower in aged myelin. The two differences are significant.

Table 1. Resulte of proteins estimation in the cerebral myelin of aged rats (in % of total myelin proteins)

Tabela 1. Wyniki oznaczeń białek mieliny mózgu u starych szczurów (w % całkowitego białka mieliny)

Protein Białko	Young adult rats Młode dorosłe szczury n—10	Aged rats Stare szczury n—16
Wolfgram protein (WP) Białko Wolfgrama	30.1±1.6	32.5±2.0
Folch-Lees proteolipid (PLP) Proteolipid Folch-Lees	40.7±2.1	36.4±2.3
Agrawal protein (AP) Białko Agrawala	12.0±0.9	10.9±0.8
Large basic protein (LBP) Duże białko zasadowe	5.8±0.7	8.8±0.5
Small basic protein (SBP) Małe białko zasadowe	11.4±0.5	11.4±0.7
SBP/LBP ratio Stosunek SBP/LBP	2.0±0.3	1.3±0.3

Results are presented as means ± SEM.
Wyniki przedstawiono jako średnia ± średni błąd średniej.
Statistically significant differences at level $p < 0.01$.
Statystycznie istotne różnice przy poziomie $p < 0{,}01$.

DISCUSSION

The basic problem in studies of the pathomechanism of various kinds of myelinopathies is the question whether the myelin is degraded in a specific way, according to the character of noxious factors or whether the morphological and pathobiochemical reaction of myelin is general and depends mainly on the intensity of the damaging agent. The second question is which molecular part of the myelin bilayers is the weak point in its architecture.

The studies of myelin lipids have shown that the pattern of their degradation is almost identical under various pathological conditions.

In contrast to lipids, more specific are changes in myelin proteins. Pathological processes characterized morphologically by full demyelination show a strong degradation of basic protein evoked by the activation of neutral proteinase (Norton et al. 1978). This is the case in several pathological conditions caused by a neuroallergic reaction. The studies of Matthieu et al. (1974) demonstrated that the myelin breakdown in hexachlorophine intoxication is connected with the greatest loss of myelin-associated glycoprotein (MAG). This also happened at the margin of a developing plaque in multiple sclerosis (Iyoyama et al. 1980). In central Wallerian degeneration the marked loss of basic protein was observed only at the late stage after dissection of the optic nerve (Wender et al. 1983a).

In myelinopathy provoked by triethyltin intoxication characterized by intralaminar vacuolization, the pattern of protein changes is completely different, so that only the Agrawal protein of myelin is considerably reduced (Wender et al. 1983b). The other pattern of changes is produced by moderate or acute hypoxia, which leads to a marked decrease of Wolfgram protein, and in a later period also to a drop in Folch-Lees proteolipid and Agrawal protein (Wender et al. 1989a). In both types of myelinopathy, changes of basic protein are only moderate.

The aging rat brain is characterized by very small deviations in myelin proteins, because the mild decrease of Folch-Lees proteolipid and Agrawal protein is insignificant and the increase of basic proteins seems to be negligible, as being only the result of a concomitant relative shift, without greater significance for the pathomechanism of the aging process.

While comparing the deviations in aging in both main components of the myelin bilayer, i.e. proteins and lipids, it should be stressed that the lipid fraction is more abnormal, showing an increase in lysophosphatidylcholine and decrease in sulfatide and cerebroside content as well as an increase in cholesterol esters. In contrast the myelin proteins seem to be more stable in the course of aging.

CONCLUSIONS

1. Aged rat brain is characterized by small deviations of myelin proteins only.
2. Myelin proteins seem to be more stable than lipids in the course of aging.

BIAŁKA MIELINY STARZEJĄCEGO SIĘ MÓZGU SZCZURA

Streszczenie

Przeprowadzono badania białek mieliny na materiale 16 szczurów rasy Wistar w wieku od 2 do 2,5 lat. Wyniki porównano z uzyskanymi u 10 dorosłych młodych

szczurów (4-6 miesięcznych). Obraz białek określono drogą elektroforezy na żelu poliakrylamidowym.

Wyniki badań doprowadziły do następujących wniosków: 1) starzejący się mózg szczura charakteryzują jedynie niewielkie zmiany białek mieliny, 2) białka mieliny wydają się bardziej stabilne w przebiegu procesu starzenia niż lipidy.

REFERENCES

1. Adamczewska-Goncerzewicz Z., Wender H., Hejduk-Hantke H., Szczech J., Godlewski A.: White matter of the aging brain. Polish-Italian Joint Meeting on Neurology. Faviitalia Carlo Erba, 1988, Abstracts, pp. 17-18.
2. Agrawal H.: Analysis of membrane proteins by sodium dodecyl-sulfate-polyacrylamide gel electrophoresis. In: Fundamentals of lipid chemistry. Eds.: R. Burton, F. Guerra. Science Publ. Div., Webster Groves, Missouri, 1974, pp. 511-543.
3. Alberghino M., Viola M., Insirello L., Stella M.: Age related changes of RNA and lipid synthesis in vitro by retina and optic nerve of the rat. Chem Pathol, 1988, 8, 131-148.
4. Battistin L., Rigo A., Bracco F., Dam M., Pizzolato G.: Metabolic aspects of aging brain and related disorders. Gerontology, 1987, 33, 253-258.
5. Horrocks L.: Composition and metabolism of myelin phosphoglycerides during maturation and aging. In: Neurobiological aspects of maturation and aging. Ed.: D. Ford. Elsevier, Amsterdam, 1973, pp. 383-395.
6. Horrocks L., Sun G., D'Amato R.: Changes in brain lipids during aging. In: Neurobiology of aging. Eds.: J. Ordy, K. K. Brizzue. Plenum Publ. Corp., New York, 1979, pp. 359-367.
7. Iyoyama Y., Sternberger N., de Webster M., Quarles R., Cohen S., Richardson J.: Immunocytochemical observation on the distribution of myelin-associated glycoprotein and myelin basic protein in multiple sclerosis lesions. Ann Neurol, 1980, 7, 167-177.
8. Matthieu J. M., Zimmerman A., de Webster M., Ulsomer A., Brady R., Quarles R.: Hexochlorophine-intoxication, characterization of myelin and myelin related fractions in rats during early postnatal development. Exp Neurol, 1974, 45, 558-574.
9. Norton N., Poduslo S.: Myelination in rat brain: method of myelin isolation. J Neurochem, 1973, 21, 749-758.
10. Norton W., Cammer W., Bloom B., Gordon S.: Neutral proteinase secreted by macrophages degrade basic protein: a possible mechanism of inflammatory demyelination. In: Myelination and demyelination. Ed.: J. Palo. Plenum Publ. Corp., New York, 1978, pp. 361-381.
11. Puliti M., Trovarelli G., De Medio G., Banfi S., Dorigatti L., Gaiti A.: Effect of age and strain on cerebral phospholipid metabolism. Ital J Biochem, 1987, 36, 217-226.
12. Wender M., Adamczewska-Goncerzewicz Z., Szczech J., Godlewski A.: Myelin lipids in human aging brain. Chem Pathol, 1988a, 8, 121-130.
13. Wender M., Adamczewska-Goncerzewicz Z., Talkowska D., Pankrac J., Grochowalska A.: Influence of experimental acute hypoxia on myelin proteins. Neuropatol Pol, 1989a, 27, 169-175.
14. Wender M., Adamczewska-Goncerzewicz Z., Talkowska D., Pankrac J., Grochowalska A.: Pattern of myelin proteins in moderate hypoxia. Exp Pathol, 1989 (in press).
15. Wender M., Hejduk-Hantke H., Goncerzewicz A., Wyglądalska-Jernas H.: Morphometry of myelin in the aging human brain. Neuropatol Pol, 1988b, 26, 9-18.

16. Wender M., Zgorzalewicz B., Śniatała-Kamasa M., Piechowski A.: Myelin proteins in Wallerian degeneration of the optic nerve. Exp Pathol, 1983a, 23, 215-217.
17. Wender M., Zgorzalewicz B., Piechowski A., Spieszalski W., Bucholc M.: The pattern of myelin proteins in triethyltin (TET) intoxication. Exp. Pathol, 1983b, 23, 193-195.

Authors' address: Department of Neurology, School of Medicine, 49 Przybyszewskiego Str., 60-355 Poznań, Poland.

NEUROPAT. POL. 1990, 28, 3-4
PL ISSN 0028-3894

ANTONI GODLEWSKI

KARYO- AND CYTOPHOTOMETRIC STUDIES ON VASCULAR ENDOTHELIA IN THE WHITE MATTER OF THE AGING RAT BRAIN

Laboratory of Neuropathology, Department of Neurology, School of Medicine, Poznań, Poland

Endothelial cell of intracerebral blood vessels represent, in conjunction with the vascular basal membrane and perivascular astroglia, one of the principal morphological and functional elements of the blood--brain barrier (Brightman, Reese 1969; Frederickson, Low 1969; Rascol, Izard 1972). Alterations observed in myelin fibers and in the oligodendroglia of the white matter in aging rats (Godlewski 1989, 1990) suggest that vascular factors, apart from primarily degenerative changes, may participate in the process of aging of the white matter in the central nervous system.

In this study, morphometric analysis of blood vessels endothelia is presented, as examined in the white matter of the aging rat brain. In the accessible, scanty literature on the morphology of the white matter in senescence (Wiśniewski, Terry 1973; Iwanowski 1984; Englund, Brun 1986) no data could be found on the behaviour of endothelium in this process.

MATERIAL AND METHODS

The investigations were conducted on Wistar rats of either sex. Each age group: the control (4-month-old rats), 2- and 2.5-year-old rats consisted of 8 animals. The rats were kept under identical routine laboratory conditions. The animals were sacrificed under ethyl ether anesthesia by means of heart puncture and exsanguination. The brains were fixed in Baker's solution at 4°C. After fixation the brains were embedded in paraffin and then cut into 7 μm thick slices. The sections

thus obtained were deparaffinized and thereafter subjected to acid hydrolysis in 1 N HCl at 37°C for 3.5 hours, followed by staining according to Feulgen (Krygier-Stojałowska 1982).

Karyo- and cytophotometric determinations of the vascular endothelia of the corpus callosum, the fimbria hippocampi and the cerebellar white matter were carried out by means of an automatic scanning microscope — Morphoquant (Zeiss, Jena, GRD) coupled to a KSR 4100 computer (Agadshanian et al. 1977; Voss et al. 1979). Monochromatic light, wave length 560 nm was used. The following parameters of the size, shape and actual state of the nuclear chromatin of the endothelial cell nuclei were evaluated:

KONL — length of nuclear circumference determined by the number of raster points covering the circumference of the examined structure,

KOFL — cross-section area of cell nucleus expressed by the total number of raster points on and inside the circumference of the examined object,

FOFA — shape index of cell nucleus representing the quotient of the squared circumference to the cross-section area,

DMVH — elongation index determined by the quotient of minimal to maximal diagonals. The extent of elongation is inversely proportional to the value of this index,

EXTS — sum of extinction of all points of the examined object, expressed in working units used in cytophotometry,

KOMP — index determining compactness of nuclear chromatin,

ZNTR — index determining rate of chromatin concentration around centre of the nucleus.

Measurements from 300 cell nuclei in each brain structure in each animal were subjected to evaluation. The individual results from each experimental group were summarized and statistically compared by means of the non-parametric test of inter-class incompatibility of Kolmogorov-Smirnov (Greń 1982). An incompatibility of more than 95% between the individual classes under evaluation was accepted as statistically significant (probability level $p \leqslant 0.05$).

RESULTS

Results of karyo- and cytophotometric measurements are presented in Table 1.

Size (KONL — length of circumference, KOFL — cross-section area) of cell nuclei in blood vessels endothelium of the white matter increased in all examined structures in 2- and 2.5-year-old rats as compared with the control-4-month-old rats (Figs 1 and 2). The increase, more pronounced in 2.5-year-old rats, was statistically significant in all three

Table 1. Results of karyo- and cytophotometric investigations of white matter endothelia of the rat brain
Tabela 1. Wyniki badań kario- i cytofotometrycznych śródbłonków naczyń krwionośnych istoty białej mózgu szczura

Brain region/age Okolica/wiek	Value Wartość	KONL	KOFL	FOFA	DMVH	EXTS	KOMP	ZNTR
Corpus callosum Spoidło wielkie								
Control	$\bar{x}\pm SD$	85±15	180±41	210±45	58±10	62±13	68±4	79±8
Kontrola	min.	44	56	127	32	20	54	48
	max.	135	283	378	98	113	87	100
2 years	$\bar{x}\pm SD$	88±13	187±37	210±42	55±8	67±11	69±4	79±8
2 lata	min.	48	29	137	30	20	56	49
	max.	132	282	372	84	123	86	98
	p	0.01	0.01	ns	0.02	0.001	ns	ns
2.5 years	$\bar{x}\pm SD$	91±12	202±37	221±40	51±9	72±11	72±4	79±8
2,5 lat	min.	43	47	150	25	24	60	39
	max.	142	283	388	89	133	89	98
	p	0.001	0.001	0.001	0.001	0.001	0.001	ns
Fimbria hippocampi Strzępek hipokampa								
Control	$\bar{x}\pm SD$	84±15	177±44	201±44	60±10	63±14	68±5	80±9
Kontrola	min.	47	56	127	36	22	54	47
	max.	137	283	378	98	125	87	100
2 years	$\bar{x}\pm SD$	89±13	192±39	207±41	57±9	69±11	68±4	78±8
2 lata	min.	43	47	135	32	22	55	48
	max.	142	283	373	96	113	84	99
	p	0.01	0.001	0.03	0.01	0.001	ns	0.01
2.5 years	$\bar{x}\pm SD$	91±12	196±36	216±42	53±9	71±10	72±4	78±8
2,5 lat	min.	43	47	133	29	22	61	38
	max.	142	283	383	80	113	84	98
	p	0.001	0.001	0.01	0.001	0.001	0.01	0.02
Cerebellar white matter Istota biała móżdżku								
Control	$\bar{x}\pm SD$	86±14	178±39	205±42	58±9	65±12	68±4	79±8
Kontrola	min.	46	66	128	33	30	54	49
	max.	132	282	364	95	129	84	100
2 years	$\bar{x}\pm SD$	88±12	188±36	204±38	56±8	69±11	68±4	78±7
2 lata	min.	58	92	139	32	35	54	49
	max.	127	282	363	81	115	84	99
	p	ns	0.02	ns	ns	0.01	ns	ns
2.5 years	$\bar{x}\pm SD$	93±13	201±37	218±42	52±9	71±11	72±4	78±8
2,5 lat	min.	65	71	138	27	26	58	48
	max.	132	295	388	83	118	85	98
	p	0.01	0.001	0.02	0.001	0.001	0.01	ns

Explanations: $\bar{x}$ — mean, SD — standard deviation of the mean, min. — minimal value, max. — maximal value, p — probability level of significance of differences between control and old aged animals.

Objaśnienia: $\bar{x}$ — wartość średnia, SD — odchylenie standardowe, min. — wartość minimalna, max. — wartość maksymalna, p — poziom istotności statystycznej różnic pomiędzy grupą kontrolną a zwierzętami starymi.

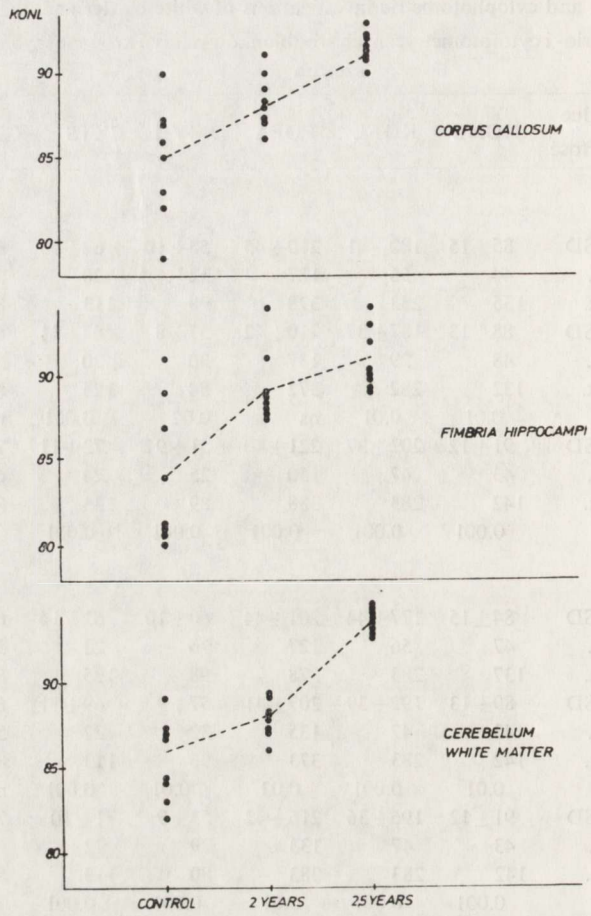

Fig. 1. Length of nuclear contour (KONL). ● — mean of determination from 300 cell nuclei from a single animal, --- — mean of determinations from all animals in a given age group

Ryc. 1. Długość obwodu przekroju jądra komórkowego (KONL). ● — wartość średnia pomiarów 300 jąder komórkowych pojedynczego zwierzęcia, --- — wartość średnia pomiarów wszystkich zwierząt danej grupy wiekowej

structures and in both age groups, except for the cerebellar white matter of 2-year-old animals. In the graphs (Figs 1 and 2) intra-group variability of the cell nucleus size lower than in the control group calls attention in individual aging rats.

The shape coefficient (FOFA) increased significantly in all regions in 2.5-year-old rats and in fimbria hippocampi in 2-year-old animals (Fig. 3). The value of the DMVH coefficient decreased (Fig. 4), cell nuclei of the endothelium became increasingly elongated in the aging rats. The elongation is more pronounced in the oldest, 2.5-year-old rats than in 2-year-old ones.

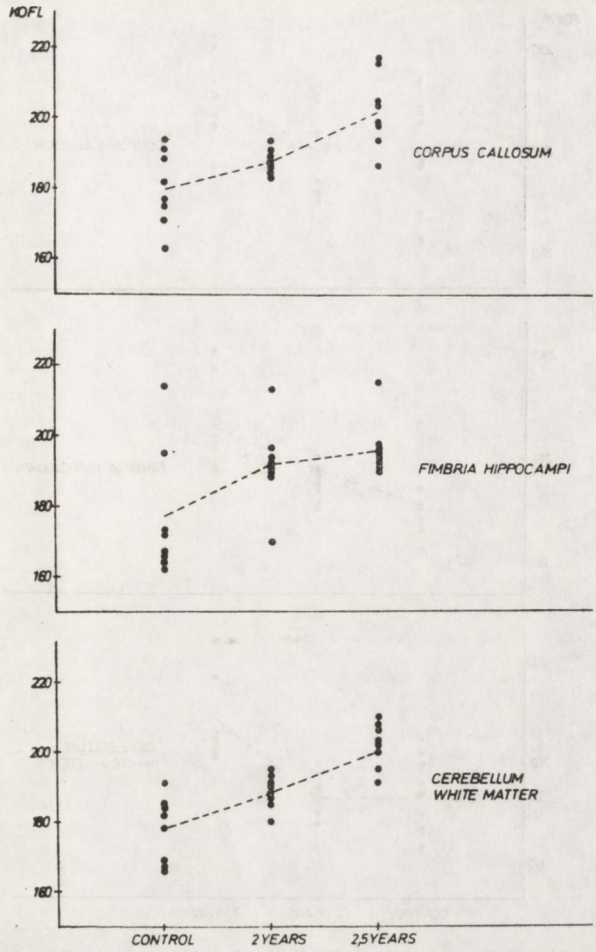

Fig. 2. Area within the nuclear contour (KOFL). Notations as in Fig. 1
Ryc. 2. Pole powierzchni przekroju jądra komórkowego (KOFL). Objaśnienia jak na ryc. 1

In both age groups in all examined structures values of the EXTS coefficient increased (Fig. 5), i.e., the sum of extinction of endothelial cell nuclei was increased, proportionally in the Feulgen technique to DNA content in the cell nucleus. The increase was highly significant ($p \leqslant 0.001$).

The aging process involved also alterations in nuclear chromatin of blood vessel endothelia of the rat brain white matter. The compactness coefficient of nuclear chromatin (KOMP) did not change in 2-year-old animals, but increased in all white matter regions of 2.5-year-old rats, as compared with control (Fig. 6). The coefficient of nuclear chromatin concentration in the central part of the cell nucleus (ZNTR) did

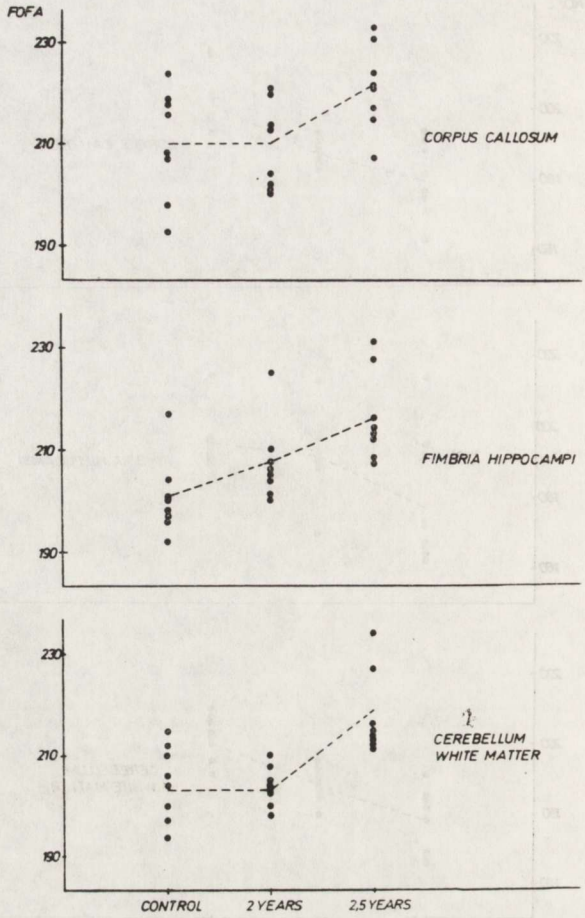

Fig. 3. Shape index (FOFA). Notations as in Fig. 1
Ryc. 3. Współczynnik kształtu (FOFA). Objaśnienia jak na ryc. 1

not change in the white matter of the cerebellum and corpus callosum. On the other hand, this index was increased significantly in the fimbria hippocampi (Fig. 7).

DISCUSSION

The conducted studies revealed a number of morphological alterations in the cell nuclei of blood vesselendothelia in the white matter of old rat brains. Endothelial cell nuclei increased in size became elongated and the compactess of their nuclear chromatin increased. By comparing the above data with those originating from human material, obtained at autopsy (Szczech 1990), one can note a greater similarity of size and shape alteration in rat endothelia and human endothelia from brains of patients deceased with atrophic lesions of Alzheimer type with

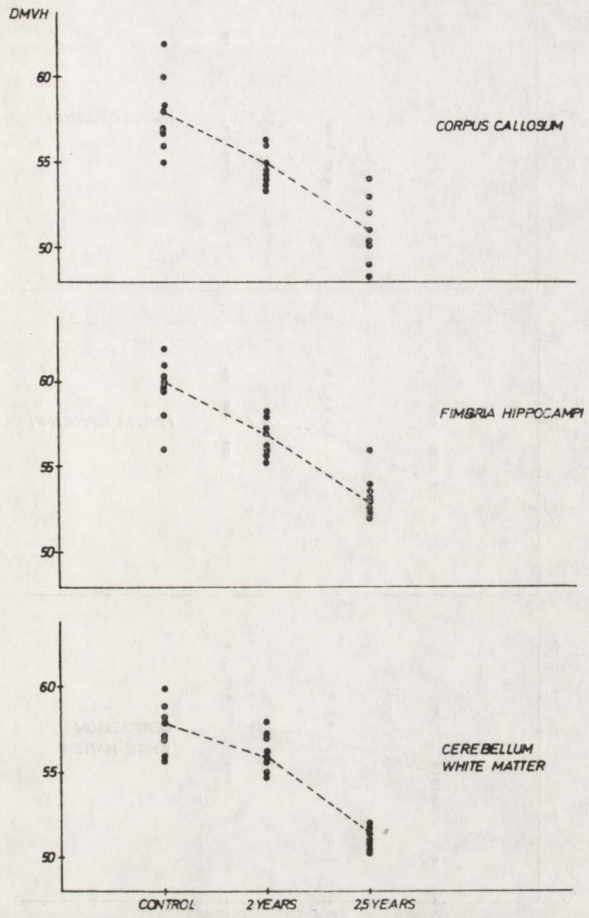

Fig. 4. Cell elongation index (DMVH). Notations as in Fig. 1
Ryc. 4. Współczynnik wydłużenia (DMVH). Objaśnienia jak na ryc. 1

no evident vascular lesions, and a much lower similarity with endothelia of aging humans with vascular lesions exclusively and without brain atrophy of Alzheimer type. Similar studies relating to white matter endothelium of rats subjected to hypoxic hypoxia (Szczech 1989) demonstrate an essential similarity in the pattern of morphological lesions to those noted in humans with vascular alterations.

At this point one should note that enlargement of the cell nuclei in the endothelium of fine blood vessels may itself decrease intracerebral blood flow in individuals of advanced age. Endothelial cell nuclei protrude toward the lumen of blood vessels (Smieško et al., 1985) and, thus the internal diameter of fine blood vessels depends, among other things upon the size of the cell nuclei in the vascular endothelium.

The increase in the sum of extinction (EXTS coefficient) remains in the applied Feulgen technique proportional, with numerous reservations,

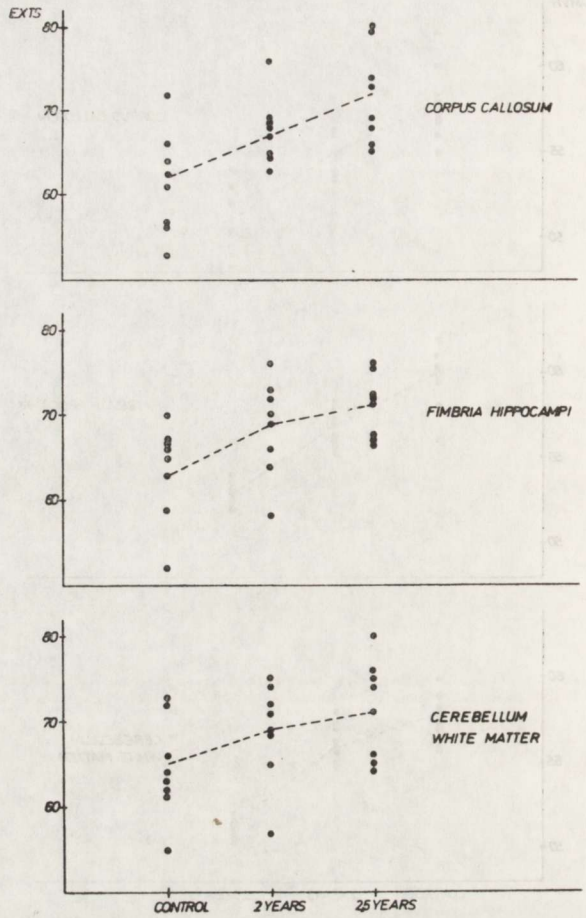

Fig. 5. Extinctionscoefficients (EXTS). Notations as in Fig. 1
Ryc. 5. Suma ekstynkcji (EXTS). Objaśnienia jak na ryc. 1

to the DNA content in the cell nuclei (Krygier-Stojałowska, 1982). Identical changes have been observed in cell nuclei of white matter endothelia of aged humans (Szczech 1990) and in white matter oligodendroglia of aged humans (Wender et al. 1987) and old rats (Godlewski 1989). The phenomenon of increased DNA content in the cell nuclei not only of glia, but also of nerve cells, which represent typical post-mitotic cells, has been observed frequently both in humans and in experimental animals in senescence (Bregnard et al. 1975; Krygier-Stojałowska et al. 1980; Kulczycki et al. 1982). In dependence on localization, the intensity of the observed alterations varies in vascular endothelium cells of the white matter. The data presented heretofore point to a greater sensitivity of blood vessel endothelial cells in fimbria hippocampi to aging process as compared with the white matter of the cerebellum and corpus callosum. Significant changes in the degree of concentration of nuclear chromatin

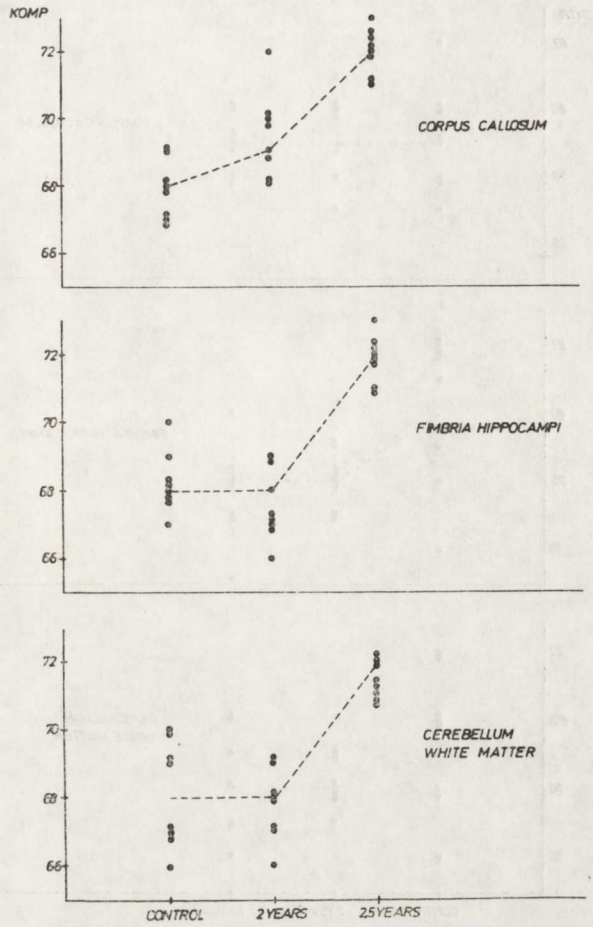

Fig. 6. Nuclear chromatin compactness index (KOMP). Notations as in Fig. 1.
Ryc. 6. Współczynnik zbitości chromatyny jądrowej (KOMP). Objaśnienia jak na ryc. 1

around the center of the nucleus have been noted only in the endothelium of the fimbria hippocampi. The hippocampus structures belong to the most sensitive ones to various noxious endo- and exogenous factors in the central nervous system. In the process of physiological aging of the brain, senescence plaques and neurofibrillary lesions can develop earliest and in greatest number in the hippocampus (Tomlinson et al. 1968; Dayan 1970). The hippocampus is particularly predisposed to lesions due to disturbances in cerebral circulation (Brierley 1976; Ferszt, Cervós-Navarro 1983).

Vascular sclerosis and atheromatosis represent a significant pathophysiological element of aging of the central nervous system. In the absence of these processes, as it usually happens in experimental animals, the role of vascular factors is not clear and opinions on the subject

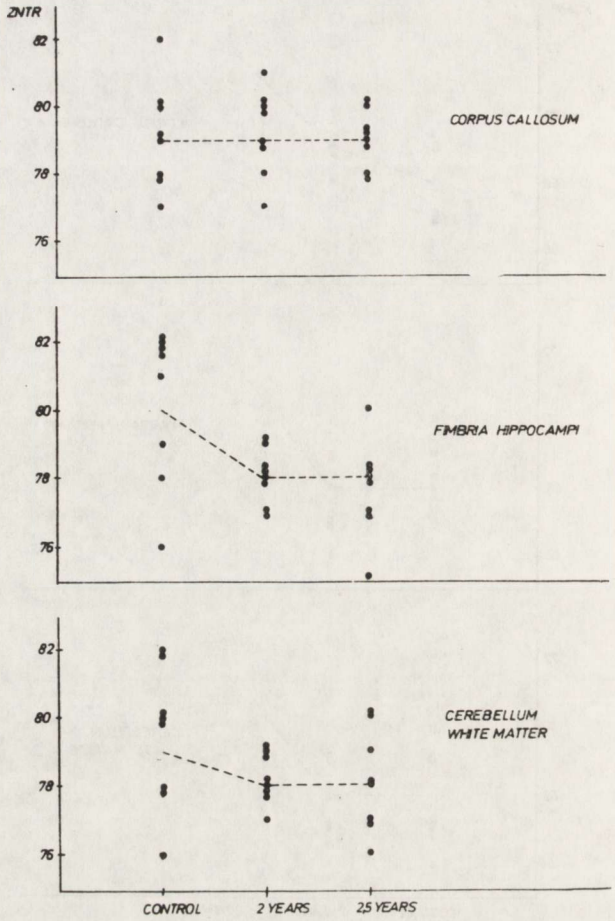

Fig. 7. Index of nuclear chromatin compactness in the geometrical center of the nucleus (ZNTR). Notations as in Fig. 1

Ryc. 7. Współczynnik centryczności ułożenia chromatyny jądrowej (ZNTR). Objaśnienia jak na ryc. 1

vary (Wiśniewski, Terry 1973; Iwanowski, Ostenda 1974; Iwanowski 1984). Some observations indicate an even greater resistance of the aging brain to disturbances in cerebral blood flow. For instance, regional cerebral blood flow is significantly decreased in patients with senile dementia of Alzheimer type (Melamed et al. 1980; Ferszt, Cervós-Navarro 1983), but no clinical or histopathological exponents of cerebral ischemia are available.

Karyometric evaluation of blood vessel endothelia in the white matter may obviously fail to clarify the extent and type of circulatory disturbances in the aging brain. Further studies are needed, particularly those involving evaluation of cerebral microcirculation and of blood-brain barrier permeability. The presented results permit to suggest only that

blood vessel endothelia in the white matter represent another element, along with oligodendroglia (Godlewski 1989) and myelinated fibers (Godlewski 1990) of rat brain white matter which undergoes degenerative changes in the process of aging of the central nervous system.

CONCLUSIONS

1. In the process of aging of the central nervous system morphological changes take place in blood vessel endothelia of the white matter, expressed by enlarged and elongated cell nuclei.

2. Changes in nuclear chromatin, i.e. increase in the sum of extinction (proportional to DNA content) and increased compactness of nuclear chromatin represent elements of aging in endothelia of cerebral blood vessels.

3. The observed alterations are more pronounced in 2.5-year-old than in 2-year-old rats. They reach the greatest intensity in the fimbria hippocampi, lower in corpus callosum and in cerebellar white matter.

BADANIA KARIO- I CYTOFOTOMETRYCZNE ŚRÓDBŁONKÓW NACZYNIOWYCH ISTOTY BIAŁEJ STARZEJĄCEGO SIĘ MÓZGU SZCZURA

Streszczenie

W pracy przedstawiono wyniki badań kario- i cytofotometrycznych jąder komórkowych śródbłonków naczyniowych istoty białej starzejącego się mózgu szczura. Badania przeprowadzono na szczurach rasy Wistar w wieku 2 i 2,5 lat. Pomiary wykonano na preparatach ze spoidła wielkiego, strzępka hipokampa i istoty białej móżdżku, barwionych według metody Feulgena.

Wykazano, że w starzejącym się mózgu szczura dochodzi do powstania wielu zmian morfologicznych w śródbłonkach naczyń krwionośnych istoty białej. Jądra komórkowe śródbłonków powiększają się, stają się bardziej wydłużone, wzrasta stopień zbitości ich chromatyny jądrowej, wzrasta suma ekstynkcji jąder komórkowych (w metodzie Feulgena proporcjonalna do zawartości DNA). Powyższe zmiany są bardziej nasilone u zwierząt 2,5-letnich niż u 2-letnich. Zaobserwowano różnice topograficzne w ich nasileniu. Najwyraźniejsze są w strzępku hipokampa, mniejsze w istocie białej móżdżku i w spoidle wielkim.

REFERENCES

1. Agadshanian S., Döpel P., Gretscher P., Witsack W.: Morphoquant — ein automatischer Mikroskopbildanalysator des VEB Carl Zeiss Jena. Jenauer Rundsch, 1977, 22, 270-274.
2. Bregnard A., Knusel A., Kuenzle C. C.: Are all the neuronal nuclei polyploid? Histochemistry, 1975, 43, 59-61.
3. Brierley J. B.: Cerebral hypoxia. In: Greenfield's neuropathology. Eds.: W. Blackwood, J. A. N. Corsellis. Arnold, London, 1976, pp. 43-85.
4. Brightman M. W., Reese T. J.: Junctions between intimately apposed cell membranes in the vertebrate brain. J Cell Biol, 1969, 40, 648-677.

5. Dayan A. D.: Quantitative histological studies on the aged human brain. I. Senile plaques and neurofibrillary tangles in "normal" patients. Acta Neuropathol (Berl), 1970, 16, 85-94.
6. Englund E., Brun A.: The white matter changes in senile dementia of Alzheimer type: Neuropathological and biochemical correlates. Xth Intern. Congr. Neuropathol., Stockholm, 1986. Abstracts, p. 291.
7. Ferszt R., Cervós-Navarro J.: Cerebrovascular pathology — aging and brain failure. In: Brain aging: neuropathology and neuropharmacology. Eds.: J. Cervós-Navarro, H.-I. Sarkander. Raven Press, New York, 1983, pp. 133-151.
8. Frederickson R. G., Low F. N.: Blood vessels and tissue spaces associated with the brain of the rat. Am J Anat, 1969, 125, 123-145.
9. Godlewski A.: Karyo- and cytophotometric studies on oligodendroglia in the aging brain of rat. Neuropatol Pol, 1989, 27, 477-490.
10. Godlewski A.: Morphometry of myelin fibers in aged rats. J Hirnforsch, 1990 (in press).
11. Greń J.: Statystyka matematyczna. Modele i zadania. PWN, Warszawa, 1982.
12. Iwanowski L.: Myelin in the senile rat brain. Neuropathol Pol, 1984, 22, 219-223.
13. Iwanowski L., Ostenda M.: Ultrastructural changes in the brain capillaries of old rats. Material der 4 Jahrestagung der Gesellschaft für Neuropatologie der DDR: Altersveränderungen des Zentralnervensystems. Mühlhausen (Thür), 1974, pp. 121-122.
14. Krygier-Stojałowska A.: Zasady cytofotometrii. In: Topochemiczne metody badania komórek i tkanek. PWN, Warszawa, 1982, pp. 114-134.
15. Krygier-Stojałowska A., Kulczycki J., Madej M., Nowacki P., Honczarenko K.: Zmiany ilościowe DNA i białek zasadowych (histonów) w jądrach komórek nerwowych i glejowych mózgowia szczurów w różnym wieku. Neuropatol Pol, 1980, 18, 97-106.
16. Kulczycki J., Krygier-Stojałowska A., Jaszczak K., Honczarenko K., Nowacki P., Madej M.: Deoxyribonucleoproteins in neurons and glial cells in the brain of mice at different age. Neuropatol Pol, 1982, 20, 365-376.
17. Rascol M., Izard J.: La disposition des cellules piemeriennes et leurs relations avec les fibres conjonctives. J Zellforsch, 1972, 123, 351-352.
18. Smieško V., Kozik M., Dolezel S.: Role of endothelium in the control of arterial diameter by blood flow. Blood Vessels, 1985, 5, 247-256.
19. Szczech J.: Blood vessels endothelia of the cerebral white matter of rats exposed to hypoxia. Karyometric and cytophotometric evaluation. Exp Pathol, 1989 (in press).
20. Szczech J.: Karyo- and cytophotometric studies on vascular endothelia in the white matter of the aging human brain. Neuropatol Pol, 1990, 28 (in press).
21. Tomslinson B. E., Blessed G., Roth M.: Observations on the brain of non-demented old people. J. Neurol Sci, 1968, 7, 331-356.
22. Voss K., Neumann E., Witsack W.: "Universelles Programmsystem" für den automatischen Mikroskopbildanalysator Morphoquant. Jenauer Rundsch, 1979, 24, 167-169.
23. Wender M., Godlewski A., Szczech J.: Oligodendroglia of the ageing human brain. Karyometric and cytophotometric studies. Neuropatol Pol, 1987, 25, 461-472.
24. Wiśniewski H. M., Terry R. D.: Morphology of the aging brain, human and animal. Prog Brain Res, 1973, 40, 167-186.

Author's address: Laboratory of Neuropathology, Department of Neurology, School of Medicine, 49 Przybyszewskiego Str., 60-355 Poznań, Poland.

SPIS TREŚCI

NEUROPATOLOGIA POLSKA
T. 28, Z. 3–4, 1990

Cena zł 10 600,–

CONTENTS

Indeks 36668